ADDIS ABABA UNIVERSITY

Addis Ababa Institute of Technology

School of Mechanical and Industrial Engineering

‘Investigating the wheel wear of Addis Ababa Light Rail Transit (AALRT)’

by

Dula Fekadu

A Thesis Submitted to the School of Graduate Studies of Addis Ababa University in Partial Fulfillment of the Requirements for the Degree of Masters of Science in Mechanical Engineering (Rolling stock Stream)

Advisor

Dr. Birhanu Beshah

June 2017

ADDIS ABABA UNIVERSITY

Addis Ababa Institute of Technology

School of Mechanical and Industrial Engineering

'Investigating the wheel wear of Addis Ababa Light Rail Transit (AALRT)'

By: Dula Fekadu

APPROVED BY BOARD OF EXAMINERS

Dr. Birhanu Beshah ________	________________	________________
Advisor	Signature	Date
________________	________________	________________
Internal Examiner	Signature	Date
________________	________________	________________
External Examiner	Signature	Date
________________	________________	________________
Railway Center Head	Signature	Date

DECLARATION

I hereby declare that the work, which is undertaken in this thesis entitled "**Investigating the wheel wear of Addis Ababa Light Rail Transit (AALRT)**" is original of my own, one of the problems AALRT is currently facing and has not been presented for a degree of any other university and all the resource materials used for this work have been currently referred.

_________________ ________________

Dula Fekadu Date

This is to certify that the above declared made by the candidate is correct to the best of my knowledge.

________________ ________________

Dr. Birhanu Beshah (Advisor) Date

Acknowledgment

I shall like to express my deep and sincere gratitude to my advisor Dr. Birhanu Beshah and for his supervision, advice, and guidance from the very early stage of this thesis work. I would also like to thank Ato. Muluken Assefa, head of maintenance department at Addis Ababa Light Rail Transit (AALRT), Kaliti depot for his invaluable assistance. Additionally, I want to express my gratitude to Ethiopian Railway Corporation (ERC) staff members, experts and technicians I have come across for assistance in this research work. Their detailed and constructive comments were essential to the completion of this thesis.

I would also like to thank my father, Dr. Fekadu Fufa, my mother Almaz Tadesse and all my siblings for their continuous support through the work of this thesis. My sincere gratitude also goes to my classmates Belayhun Ejiguale and Tesfaye Atalay for their undivided assistance throughout this work.

Abstract

This paper presents a reasonable approach to the causes behind the wheel wear at Addis Ababa Light Rail Transit (AALRT). Factors that led to wheel wear were investigated through site inspections/interviews with experts which gave the general truth of the problem and hinted potential factors that brought about the problem. Based on these findings, combination of issues related to inadequate friction management and poor track infrastructure are key factors which have led to wheel wear. Additionally, analysis of actual wheel data measurements taken from AALRT depots was used to find out the type of wear and from the two lines, North-South and East-West lines, identifying the line that is affected more by comparing vehicles from both lines. The tight curves at AALRT, mainly in the North-South line, contribute to high flange wear as of the wheel data analysis under taken. Then Multi-Body Simulation analysis of AALRT vehicle was carried out using SIMPACK software. AALRT vehicle's performance was simulated in curves and straight tracks, then validated against the standards of the vehicle such as, coefficient of derailment, ride index and lateral force. Then parameters, namely critical speed, coefficient of friction and passenger loading, are identified from literature reviews and their effects on wear index were determined based on existing track infrastructure of AALRT. The simulation results gave longitudinal/lateral creepages and longitudinal/ lateral creep forces which were then used to calculate wear index. Based on the simulation results, critical speed of 40 km/hr led to the highest wear index of 1303.78 while the lowest wear index of 1240.14 is obtained at the critical speed of 20 km/hr, based on existing track infrastructure. In addition, higher coefficient of friction, 0.55 resulted in higher wear index of 3136.33; the lowest coefficient of friction, 0.25, resulted in the lowest wear index of 888.44. It is also evident that based on existing track infrastructure, overload of 20 tons caused higher wear index of 1278.63 compared to empty load obtaining the lowest wear index of 977.07. To minimize the problem of wheel wear at AALRT, suitable lubrication and better method of application, improved wheel/rail material, revised track alignment for easing of sharper curves and improved workshop facilities are recommended in this work.

Keywords: Wheel wear, Addis Ababa Light Rail Transit (AALRT), Multi-Body Simulation, Wear index

Table of Contents

List of Tables

List of Figures

Abbreviations and Notations

AALRT Addis Ababa Light Rail Transit

ERC Ethiopian Railway Corporation

COF coefficient of friction

Q vertical force

Y lateral force

α flange angle

N normal force

μ friction coefficient

W wear Index

F_x longitudinal creep force

ξ longitudinal creepage

F_y lateral creep force

η lateral creepage

CHAPTER ONE

1. Introduction

1.1. Background

1.1.1. Rail Transport

Rail transport is employed to mainly carry passengers and goods (especially cargos), and can run on both single fixed-type and dual-type rails and it essentially covers light rail, heavy rail, and tram as well as funicular and monorail rail means [1]. Rail transport plays key role in the socio-economic and on the environment, which makes this mode of transport the best land transportation option for passengers and goods. It can be considered to be the best option based on several criteria, such as low traffic congestion, high number of passengers and goods carried, less fuel usage and thus reduced emissions, reduced cost, reduced accidents, increased speed, and reduced use of land.

Railroads transformed the world in the 19th century and supported the industrial expansion of the early 20th century, then declined in the face of airline and highway competition. To survive, railroads were forced to rationalize their systems, develop more efficient operations, and introduce new services. At the turn of the twenty-first century, railroads remain dominant for bulk transportation, provide the backbone of rapidly growing intermodal freight services, and compete successfully with airlines in medium distance markets. Highway congestion, limited airport capacity, and environmental concerns guarantee a continued role for rail systems in the twenty-first century [2].

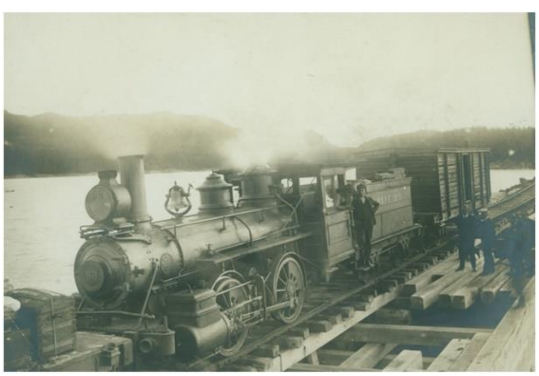
a)


b)

Figure 1.1: a) Steam engine train Quebec, Canada, 1905 [3], b) Japanese Shinkansen 500 series high-speed rail, 2005[4]

1.1.2. Rail Transport in Ethiopia

The idea of constructing a railway to link the Ethiopian capital with the coast appears to have been first conceived by Menelik's Swiss adviser, Alfred Ilg, who had first arrived in Ethiopia in 1877. Having on that occasion taken no less than seven months to make the 700km journey from the coast to the then capital of Ankober he was fully aware of the inconvenience of mule transport, the high costs of which greatly hindered trade in low priced commodities, such as coffee, skins and wax, which constituted the bulk of Ethiopia's exports. Traders at this time often took about six weeks on the journey which was almost inevitably accompanied by considerable stealing as it was very difficult adequately to supervise the muleteers [5].

The Addis Ababa-Djibouti railway parallels meter-gauge Ethio-Djibouti Railways, between Addis Ababa and Djibouti, which began operating between Dire Dawa and Djibouti in 1901, and was later extended to Addis Ababa, though trains have not run on the line since 2008 [6].

Rail transport in Ethiopia currently operates, the Addis Ababa Light Rail which opened in 2015 and, of a one electrified standard gauge rail line, the Addis Ababa-Djibouti Railway, which commenced freight operations in October 2016 [6].

Figure 1.2: AALRT vehicle on route to Kaliti station [7]

The Addis Ababa-Djibouti Railway is the first part of a planned railway network that will link landlocked Ethiopia to its neighbors. The Addis Ababa-Djibouti railway was constructed and is operated by Chinese contractor CREC. It currently carries only freight, with passenger service planned for early 2017 [8]. A 400 km long rail line from Awash to Hara Gebeya is currently under construction by Turkish company Yapi Merkezi with various European subcontractors.

The Ethiopian Railway Corporation has plans for several new lines including links to adjacent countries and further afield. ERC will build these in two phases [9]. A railway from Mek'ele to Awash will link the capital with northern Ethiopia by connecting to the Addis Ababa-Djibouti Railway at Awash, its construction on the railway began in February 2015 and the China Communications Construction Company is the prime contractor for the northern half of the railway, from Mek'ele to Weldiya [10]. Funding for the $1.5 billion northern segment was provided by the Exim Bank of China [11]. Yapı Merkezi is responsible for the southern half of the railway, from Weldiya to Awash. Funding for the $1.7 billion southern segment was provided by a consortium of lenders, including Türk Eximbank, the Swedish National Export Credits Guarantee Board, Denmark's Export Credit Board, and Swiss Export Risk Insurance [12].

A railway from Addis Ababa to Bedele will run westward from the capital to Bedele. The prime contractor is Andrade Gutierrez, and funding was provided by the Brazilian Development Bank; the construction on the project began in May 2015 [12].

A railway from Weldiya to Tadjoura will provide Ethiopia with a second outlet to the sea at the port of Tadjoura in Djibouti. The line will connect to the Mek'ele-Awash railway at Weldiya. The project is being supervised by the Overseas Infrastructure Alliance (India), and the Indian government has committed $300 million so far with the funding coming from the Indian government. However, the project has been delayed five times and has not yet been tendered as of May 2015 [12].

1.1.3. About AALRT

The opening of AALRT, one of the first of its kind in Ethiopia and sub-Saharan countries, has brought about a tremendous development in the transportation sector of the country. Designed to relieve growing road congestion as the city's population passes 5 million inhabitants, the 34km two-line network serving 39 stations has been constructed by China Railway Engineering Corp at an estimated cost of US$475m. The project has been 85% funded by loans from Export-Import Bank of China [13].

The first route to open is the 16.9 km north-south Blue Line linking Menelik Square to Kaliti, serving 22 stations. The second route is the 17.4 km east-west Green Line from Ayat to Tor-Hailoch, serving 22 stations. The two routes share tracks for 2.7 km in the city centre between Lideta and Meskel Square [13]. The network is operated by a vehicle of 70% low-floor trams supplied by CNR Changchun. With trams running at up to 70 km/h, the two routes are designed to carry up to 15,000 passengers/h in each direction. Services are operating between 06.00 and 22.00 each day, and tramway's independent power supply network includes four substations with a total rating of 160 MW [13].

Figure 1.2: Legehar train station [14]

1.1.4. Railway Wheel and Wear discussion

i. Introduction to wheels

Wheels are the most critical part of rolling stock and the most care is given to them as they are the most stressed components of railway vehicles. The main importance of wheels in the rolling stock operation is that they guide the train on the tracks through straight, curves and switches, thus it possible to conclude that wheels are subjected to constant wear process. The following figure shows the different parts of the railway wheel.

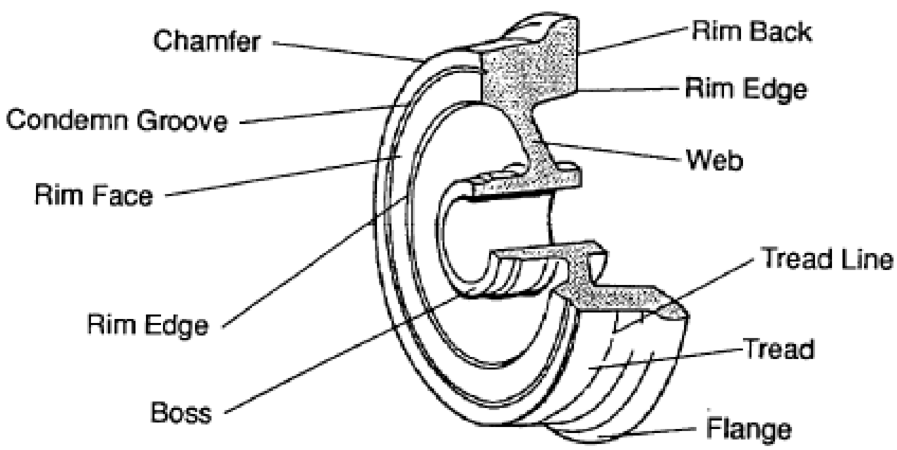

Figure 1.3: Basic wheel components

Railway wheels are usually made of unalloyed or low alloyed steels with a high degree of purity. Standard wheels mainly consist up to 0.6wt% of carbon, up to 8wt% of manganese and up to 0.4wt% silicon.

ii. Wear mechanisms

Wear is the loss or displacement of material from a contacting surface. Material loss may be in the form of debris. Material displacement may occur by transfer of material from one surface to another by adhesion or by local plastic deformation. There are many different wear mechanisms that can occur between contacting bodies each of them producing different wear rates. The simplest classification of the different types of wear that produce different wear rates is “mild wear” and “severe wear”. Mild wear results in a smooth surface that often is smoother than the original surface. On the other hand, severe wear results in a rough surface that often is rougher than the original surface [15]. Mild wear is a form of wear characterized by the removal of materials in very small fragments. Mild wear is favorable in many cases for the wear life of the contact as it causes a smooth run-in of the contacting surfaces. However, in some cases it has been observed that it worsens the contact condition and the mild wear can change the form of the contacting surfaces in an unfavorable way [16]. Another wear process that results in a smooth surface is the oxidative wear processes characterized by the removal of the oxide layer on the contacting surfaces. In this case the contact temperature and asperity level influence the wear rate [17]. Abrasive wear caused by hard particles between the contacting surfaces can also cause significant wear and reduce the life of the contacting bodies [18].

The basic concept for adhesive mechanisms is that actual contact between surfaces occurs at discrete points within the apparent area of contact. At these spots, called junctions, bonding occurs between surface asperities (see Figure 1.5). When the surfaces move relative to each other, these junctions are broken and new ones formed. Usually the tip is plucked off the softer asperity leaving them adhering to the harder surface. This can be via a ductile or brittle fracture. Subsequently the tips become loose and give rise to wear debris. Severe damage can sometimes result in the tearing away of macroscopic chunks of material and this situation is known as *galling*. If adhesive wear results from the breakdown of lubrication in a contact, then the term *scuffing* is used to describe the onset of wear.

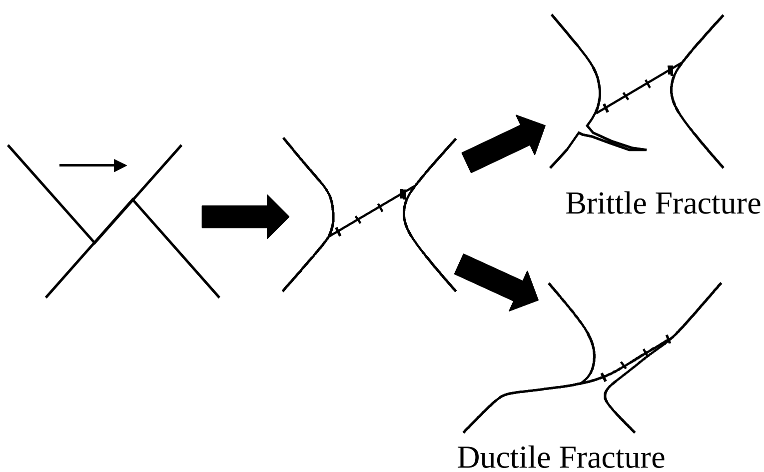

Figure 1.4: Adhesive wear mechanisms [19]

Abrasive wear is damage to a component surface, which arises because of the motion relative to that surface of either harder asperities (*two-body abrasive wear*) or because of hard particles trapped between the surfaces (*three-body abrasive wear*) (see Figure 1.6). Such particles may be introduced between the two softer surfaces as a contaminant from the outside environment, or they may have been formed *in situ* by oxidation or by some other chemical or mechanical process.

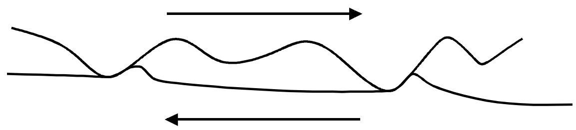

Two-Body Abrasive Wear

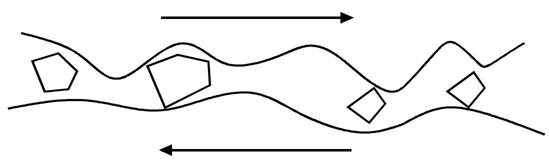

Three-Body Abrasive Wear

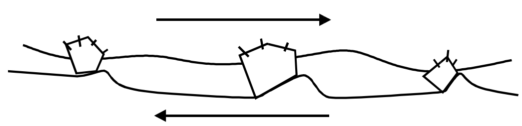

Two-Body Abrasive Wear, with Embedded Particles

Figure 1.5: Abrasive wear mechanisms [19]

The rate of damage is relatively insensitive to the hardness of the particles in a three-body situation, as long as they are at least 20% harder than the surface itself. The most commonly occurring contaminant in industrial machinery is that from quartz or silica (these minerals make up about 60% of the Earth's crust) (silica sand is either used on its own as a friction enhancer in the wheel-rail contact or mixed with water and viscosity enhancer in traction gels such as Sandite or Alleviate) [19].

iii. Review of damages observed in wheels

According to an investigation reported by A. Bevan and his associates [20], the following mechanisms are observed in wheel damages.

a. **Rolling Contact Fatigue (RCF) -** is a type of fatigue which occurs due to rolling contact between the wheel and rail as a result of the repeated cyclic loading and unloading in addition to creep forces from curving, traction and braking.
b. **Thin flange** – is the case in which wear is concentrated on the face of the wheel flange resulting in a reduction in flange thickness (flange wear).
c. **High flange –** is the case in which wear is concentrated across the tread of the wheel resulting in an increase in flange height (tread wear).
d. **Tread damage –** is the combination of damage mechanisms relating to issues associated with the wheel material; such as flat, ovality and cavities. Flats on the wheel surface occur due to *thermal damage* as a result of a wheel spin or slide. The resulting heating and rapidly cooling of the wheel material generates martensite which is very hard and brittle and, following further loading, can spall out of the wheel leaving cavities.
e. **Tread rollover** – deformation of the tread material causing a lip to developing place of the chamfer on the field side of the wheel.
f. **Parity** – turning of the wheels on a wheel lathe to obtain and acceptable diameter on all wheelsets in the vehicle or bogie.
g. **Other –** out of round wheels come due to wheel machining issues or the presence of other tread damage and observations of poor ride or vehicle stability issues.

1.2. Statement of the problem

One of the failure modes in the railway industry is wheel wear. Wheel wear has become a major concern for AALRT. The wheels are promised to serve more than 5 years depending on the track design and operational conditions. The wheel flanges are designed to have a wearing trend of 1mm per 10,000 km unlike the scenario in operation. The wheel wear is also causing all sorts of other problems. To compensate the rapid wear of the flange, the wheel undergoes re-profiling which leads to reduction of the wheel diameter and this causes for the rolling stock gangway to be lowered. Thus, this minimum clearance leads to under floor vehicle equipment damaging the way-side signal equipment, and also causing unwanted contact with the guard rail. Vehicle is only elevated to default position by inserting pads under the secondary suspension of the middle bogie which is carried out routinely every time the wheel diameter is reduced. Wear of the wheels has become a major problem and thus, this research will investigate the causes behind the matter.

1.3. Objectives

1.3.1. General Objective

The main objective of this research will be to identify the causes of wheel wear on AALRT vehicles and to study effects of selected parameters influencing wheel wear on existing track infrastructure of AALRT and then give recommendations on mitigating the problem for reduction of wheel wear on the vehicles.

1.3.2. Specific Objectives

The specific objectives that will attain the general objective are listed down as follows.

i. Determine/define important parameters to be considered in investigating causes of wheel wear through literature review.
ii. By interviewing experts and site inspections of vehicle and depot facilities at AALRT, determining potential causes leading to wheel wear.
iii. Analysis of actual wheel data measurements of AALRT vehicles to determine which route (North-South and East-West) is more affected and determining which type of wear is severe; thus, point out potential factors that led to the current wear.
iv. Using SIMPACK software to assess the dynamic analysis of AALRT vehicle using parameters determined from literature reviews, to determine their effects on wear.

1.4. Significance of the research

This investigative research will be important to address the issues behind the wheel wear and suggesting recommendations to ease the problem facing AALRT. This investigation will identify major causes of the wheel wear and problems in the maintenance shop and technical problems related to the vehicles and track conditions. Knowing the causes will point out the problem focus for solution to wheel wear reduction.

This work will put forward points of focus for future works related to wheel wear which can be instrumental for development of research work and their use in railway industries such as Ethiopian Railway Corporation (ERC).

1.5. Scope of the research

The investigation will be carried out on both roots of the Menilik II Square-Kaliti (North-South), Ayat-Torhayloch (East-West) and vehicles will be looked at and assessed from both stations. The research focuses on operational conditions of AALRT vehicles and the general maintenance activities carried out at the depots. In this work, the data collection is limited to data collected from AALRT staff interviews, inspections and current wheel and vehicle data.

1.6. Research Methodology

A) Through literature review

- Identify the potential factors contributing to rapid wheel wear
- To lay the foundation and identify the knowledge gap

B) In this study, the first duty to be implemented is data collection through interviewing AALRT technicians and site engineers, track inspectors. The respondents will respond to questions as a primary data and then through inspections, the extent of wheel wear is going to be investigated. Based on the inspection and analysis work undertaken for the investigation, possible causes are considered to represent potential factors, and also this gives the general understanding that the staff experts have on the issue of wheel wear and its seriousness.

C) The behavior of the vehicle on straight and curves is assessed using Multi-body simulation software, SIMPACK, and then the wear index is computed thus to identify factors causing the most wear. The vehicle model and standard track gauge of AALRT are used as inputs.

i) Multi-body simulation of operating AALRT vehicle train with real operating conditions on straight and curved track, such as vehicle speed, surface conditions and maximum loading condition. The simulation results should comply with standards of the AALRT vehicle model such as derailment of coefficient, ride index and lateral force.

ii) Multi-body simulation of the vehicle by varying operating conditions and wheel/vehicle parameters and then, wear index is obtained from the simulation for each varying parameter. Then the wear index is compared between them and thus it is possible to determine their effects on wheel wear.

General simulation to be implemented in SIMPACK Software

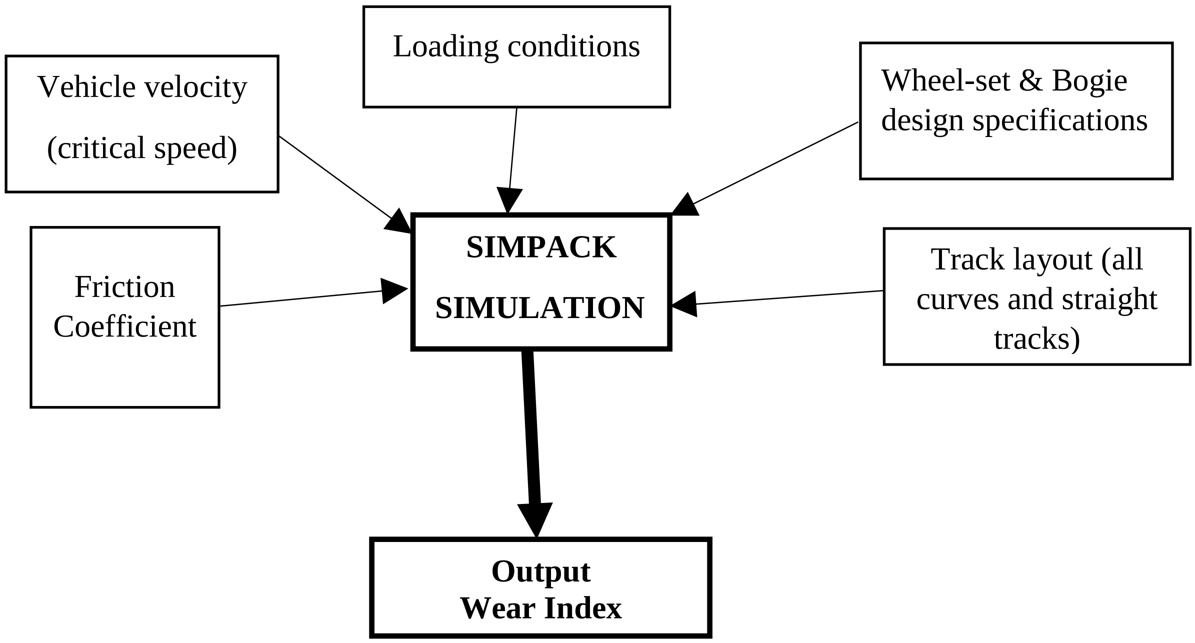

Figure 1.6: Dynamic analysis in SIMPACK

C) Triangulation of results from experts, actual wear and simulation, the root causes will be defined in the following figure manner.

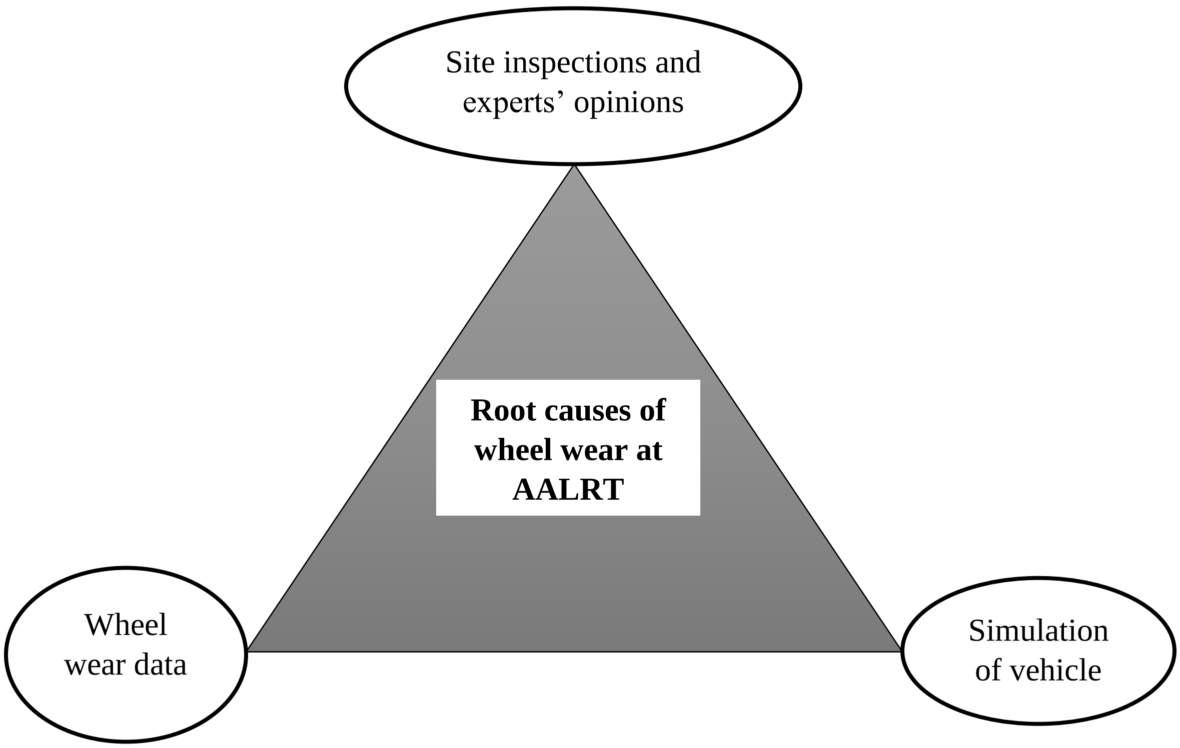

Figure 1.8: Triangulation of results

D) Based on contributors to wheel wear determined from above, recommendations to reduce the problem is put forward and thus, if applied, they would possibly minimize the wear issue.

CHAPTER TWO

2. Literature Review

2.1. Introduction

So many works have been done relating the railway wheel wear with different parameters affecting the wheel. The use of different multi-body simulation software is evident in many of the journals, articles and research works done. These literature reviews are used in this research, in identifying the potential factors that lead to wheel wear at AALRT and to lay down the knowledge gap.

The wheel surface is subjected to high normal and tangential contact stress. The removal of material from the surface by wear is a function of the sliding and contact stresses. These quantities depend on the railway vehicle dynamics that is affected by the change of wheel profile shape: both stability and passenger comfort depend on wheel and rail wear. In railway maintenance practice three indexes, called wear control parameters and denoted by the symbols S_d, S_h and Q_r, are used to quantify the degree or severity of profile wear. The S_d index measures the flange thickness, the S_h index the flange height and the Q_r index the flange steepness (Figure 2.1).

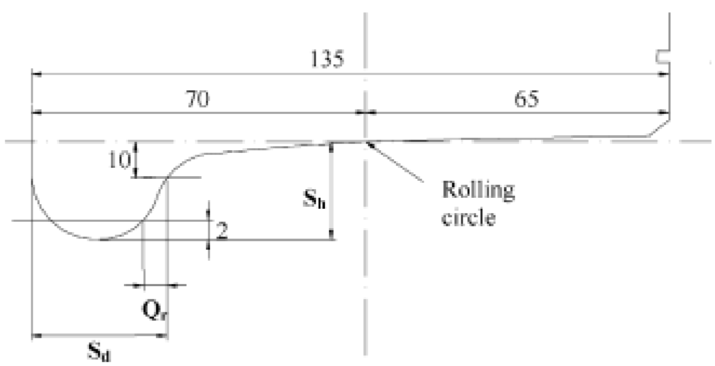

Figure 2.1: Wheel parameters

In railway applications, the estimation of wear at the wheel–rail interface is an important field of study, mainly correlated to the planning of maintenance interventions, vehicle stability and the possibility of carrying out specific strategies for the wheel profile optimization [21].

The wheel wear characterization based on programmed measurements of the geometrical parameters *Sh*, *Sd* and *Qr* is widely used by the railway industry. Such assessment is a relevant criterion to evaluate the wear state of the wheels. This approach consists of monitoring periodically the geometrical parameters of the wheel profiles in order to check if they have reached the safety limit values defined by the technical specifications. When that happens, it means that the wheels have to be re profiled. The measurement of the wear parameters *Sd* and *Qr* allows predicting the influence of the wear state of the wheel profiles on the dynamic behavior of the railway vehicles. For example, the flange thickness *Sd* is very important as it limits the lateral clearance of wheel set with respect to the track, which influences the vehicle stability. The flange slope quota *Qr* is also an important parameter. If it is too small, the wheel flange will be almost vertical, which implies that the transitions (switches crossing) and the flange contacts will occur abruptly. Such a situation originates very high contact forces that damage both vehicle and infrastructure [22].

2.2. Method of optimizing stability and wheel wear in Railway Bogies

L. Mazzola and his associates [23] proposed procedure to optimize bogie suspension parameters in view of minimizing wheel wear produced by curve negotiation, though meeting stability requirements. One of the major causes of maintenance expenditure is associated with the wearing of the wheels and of the rails, requiring periodic wheel re-profiling and rail grinding operations that eventually lead to the replacement of the wheels and of the rails. Unfortunately, the design of a railway represents compromising of curving performances (and hence reduce wear of the wheel/rail couple) and meeting stability requirements. As concluded in this work, the parameters affecting these two targets are bogie wheel base and the stiffness of the primary suspension in the horizontal plane (i.e. the longitudinal and lateral primary stiffness).

In this paper, investigation is carried out for the impact of bogie wheelbase and primary suspension stiffness on the critical speed and on wheel wear for a non-powered high-speed passenger car, having as final aim the definition of an optimal combination of the above parameters, allowing to minimize wheel rates, through ensuring the vehicle stability [23]. The effect of parameters variation has been investigated as well, and the main outcomes compared with the one obtained for the nominal vehicle configuration.

In the minimization process, discrete variations of the bogie wheelbase are taken into account, whereas longitudinal and lateral stiffness parameters of the primary suspension are considered as continuous variables that are allowed to be set to any value within a predefined range. To represent the variation of vehicle critical speed and of wheel wear with primary suspension stiffness, a 3-level full factorial design of experiments (DoE) approach is adopted [23].

The problem is dealt within a form of a constrained minimization problem, in which wheel wear evaluated over a given service scenario is introduced as the cost function to be minimized, and the requirements on vehicle stability are formulated in terms of constraints [23].

2.3. Parametric Analysis of wheel wear in high speed vehicles

According to the work of Na Wu and Jing Weng [24], a dynamic model for a high-speed vehicle was set up, where the wheel set was regarded as flexible body, and the actual measured track irregularities and line conditions were considered, the final goal being to reduce the wheel profile wear of high-speed trains and extend the service life of wheels. In this model, the influence of different parameters is considered which are influence of wheel profile, primary suspension stiffness, track gage, and rail cant on the wear of wheel profile were studied through iterative calculations.

In this work, numerical simulation results show that the type XP55 wheel profile has the smallest cumulative wear depth, and the type LM wheel profile has the largest wear depth. As recommended in this work, to reduce the wheel profile wear, the equivalent conicity of the wheel should not be too large or too small. In addition, a small primary vertical stiffness, track gage around 1,435-1,438mm, and a rail cant around 1:35-1:40 are favorable for dynamic performance alleviation and reduction of wheel wear.

In this work, the following parameters and their influence in the wear evolution of the wheel profile are studied.

2.3.1. Influence of wheel profile on wear

In this study, the wear depth and distribution of four types of wheel profiles (LM, LMA, XP55, and S1002) were compared taking the line conditions for the same operating mileage. Figure 2.2 shows the equivalent conicity and Figure 2.3 shows the wear depth changes for the four wheel profiles.

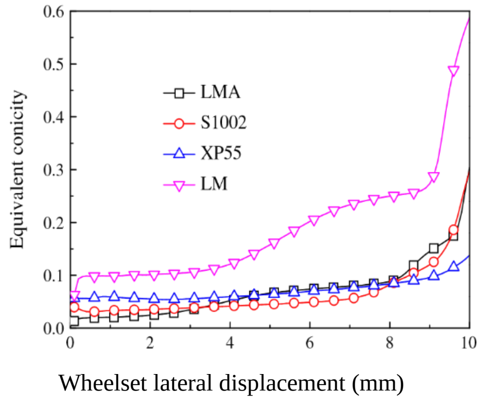

Figure 2.2: Equivalent conicities for different types of wheel profiles [24]

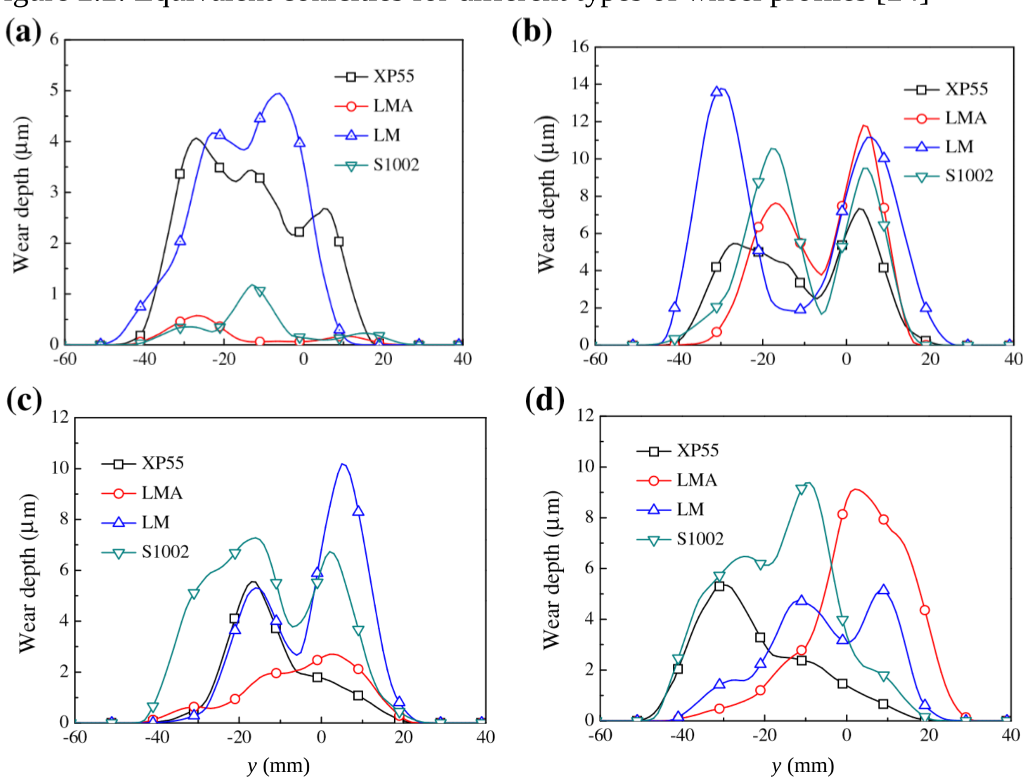

Figure 2.3:wear comparisons for different types of wheel profiles. a) Wear stage 1, b) Wear stage 2. c) Wear stage 3. d) Wear stage 4. [24]

As shown in figure 2.3, the wear depth initially increased rapidly and then sowed with the increase in running mileage, and the wear range slowly broadened. The table below shows the distribution of different types of wheel profiles for the four wear stages. In stage 1, because the type LM profile had the largest equivalent conicity, the wheel wear was close to the flange: the S1002 profile had the smallest equivalent conicity, and the wheel wear was near the outside of the wheel. For the later wear stages, the wear volume for LM was the greatest and the wear ranges the widest, and the wear volume for XP55 the smallest [24]. This shows that the equivalent conicity shouldn't be too large or too small because this will only intensify the wear.

Table 2.1: Wear distribution zone for different wheel profiles (mm) [24]

No.	XP55	LMA	LM	S1002
1	-47-+18	-44-+24	-52-+16	-46-+29
2	-44-+24	-43-+24	-45-+26	-51-+24
3	-44-+26	-45-+26	-44-+25	-47-+27
4	-51-+26	-45-+32	-43-+31	-51-+31

2.3.2. Influence of primary vertical stiffness on wear

To compare the influence of primary vertical stiffness on the wear depth and range, the primary vertical stiffness on the wear depth and range, the primary vertical stiffness with values 0.8, 1.0, 1.2 and 1.4 MN/m was adopted for the calculation [24].

In figure 2.4, it is shown that the primary vertical stiffness has little influence on the wear range. In the wear stage 3, the primary stiffness has little effect on the wear depth but further in the wear stages, 1.0 MN/m will cause greater wear than the others, and the least wear brought by the stiffness 0.8 MN/m. With the increasing of running mileage, the wear depth increases rapidly in the early stages and slowly in the later stages [24].

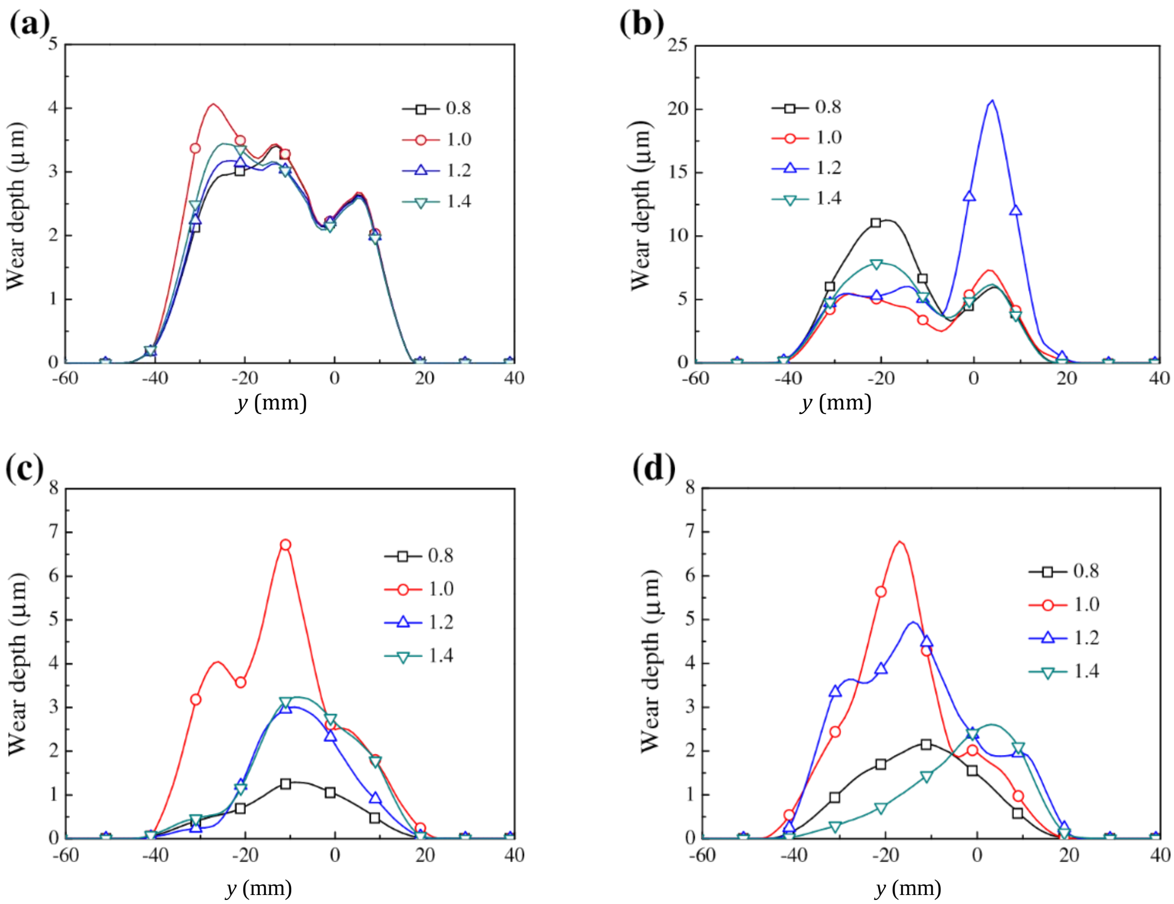

Figure 2.4: Wear comparison for different primary vertical stiffness. a) Wear stage 1, b) Wear stage 2. c) Wear stage 3. d) Wear stage 4. [24]

2.3.3. Influence of track gage on wear

The computed track gages were 1,432, 1435, 1438 and 1,441 mm, and their influences on the wear depth and distribution of the wheel profiles were compared in figure 2.5. As shown in the figure, wear depth reduces and wear range gradually moves away from the flange with the increase in track gage in the first stage. In the lateral stages, track gages 1,435 and 1,438mm have the least wheel wear depth. It can be concluded that slightly widening the wheel gages, can result in reduced wheel wear [24].

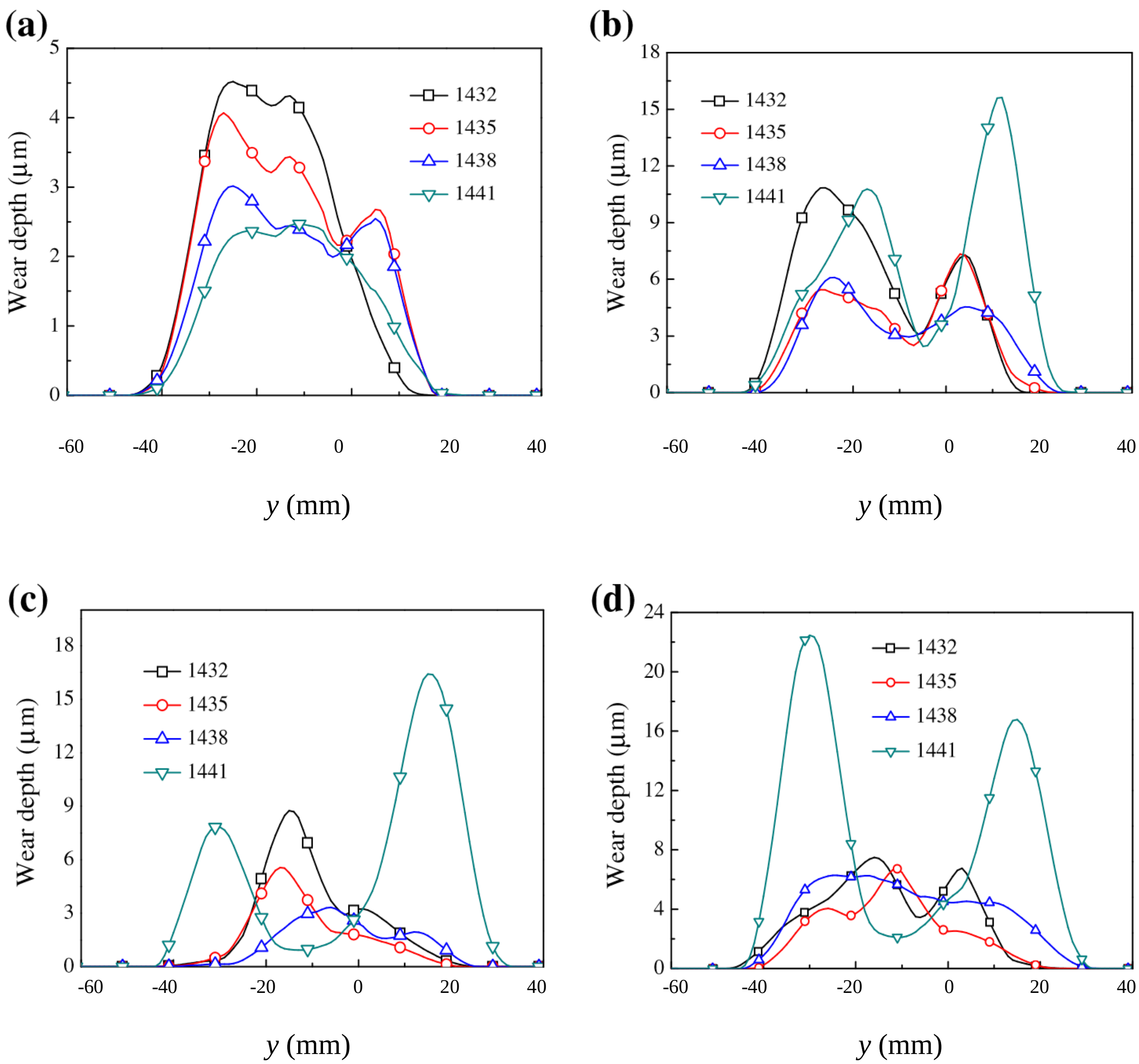

Figure 2.5: Wear comparison for different track gages. a) Wear stage 1, b) Wear stage 2. c) Wear stage 3. d) Wear stage 4. [24]

2.3.4. Influence of rail cant on wear

In this study, rail cants of 1:25, 1:30, and 1:40 were selected for the wheel wear calculation. As shown below in figure 2.6, the wear depth was small when the rail cant angles were 1:35 and 1:40, and the wear distribution was near the flange. Therefore, as recommended in this work, the rail cant should be 1:35 and 1:40 to reduce wheel wear [24].

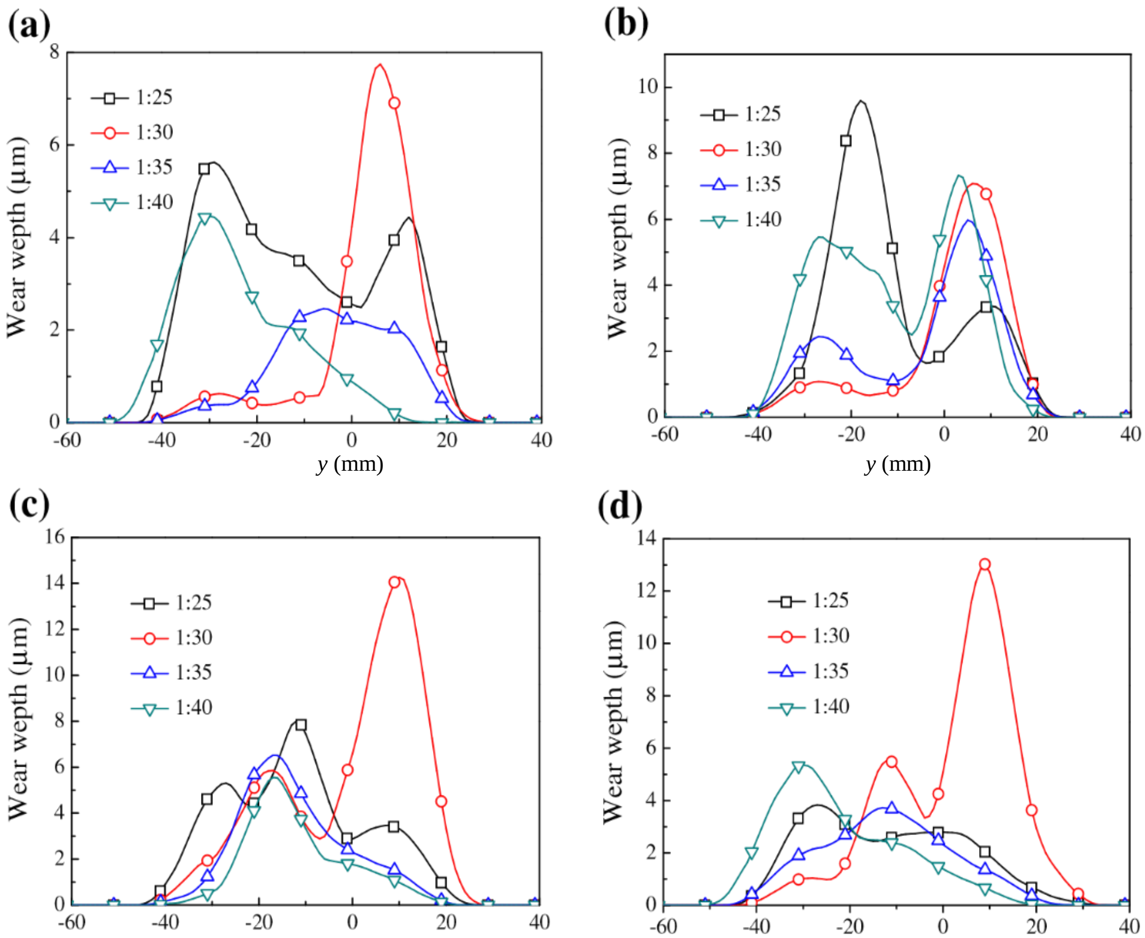

Figure 2.6: Wear comparison for different rail cants. a) Wear stage 1. b) Wear stage 2. c) Wear stage 3. d) Wear stage 4. [24]

As of the work done by Na Wu and Jing Zeng [24], a vehicle dynamic model and wheel profile wear model were established and the following conclusions are obtained based on analysis parameters that possibly influence the wear of wheels.

- Type of wheel profile can significantly influence the wear rate. Among the four types of wheel profiles, the type XP55 wheel had the smallest cumulative wear depth, and LM had the largest wear. To reduce the wear of the wheel profile, an appropriate wheel equivalent conicity needs to be designed, and must not be too large or too small.
- Using a small primary vertical stiffness can have a better dynamic performance and reduce wheel wear.
- The track gage should be between 1,435 and 1,438 mm, a too large or too small gage will aggravate the wheel wear, and rail cant should be between 1:35 to 1:40.

2.4. Study on influence of effective parameters on wear behavior of wheel and rails through ADAMS-RAIL Software

The work by Majid Elyasi and his associates [25] presents a study of parameters such as lateral force, wagon weight, rail path curvature, train speed and path slope those have greatest effects on wear mechanism of wheel and rail. In this work, ADAMS-RAIL Software is used for the dynamical modelling of train while moving via railway. Some experimental tests were made to evaluate wear loss obtained by the parameters.

When simulating the wear behavior using the software ADAMS-RAIL, the main inputs for modelling of wear are geometric model of train, mechanical behavior parameters such as springs and dampers, properties of rigid bodies, and shape characteristics of wheels and rails in contact places [25].

Table 2.2: Input parameters for simulation [25]

Input parameters	**Value**
Modulus of elasticity (GPa)	210
Radius of path curvature (m)	250
rolling radius (m)	0.46
Wheelset base (m)	2.56
Wagon length (m)	24
Poisson’s ratio	0.3
Cant (rad)	0
Wagon total weight (ton)	42
Axle length (m)	2
Wagon height (m)	3

During the work, through experimental results, it was decided that lateral force, velocity, slip distance and surface roughness to be taken as the main parameters. The simulation was carried out under three velocities to obtain the lateral force and then the forces are applied in pin-on-disk test experiments under dry lubricant condition. The following table shows the forces obtained under various velocities from simulation [25].

Table 2.3: Input velocity and force for pin-on-disk machine test [25]

Test No.	Force (N)	Velocity (m/s)
1	46	0.6
2	55	0.6
3	64	0.6
4	46	0.9
5	55	0.9
6	64	0.9

During the test, the surface roughness of both pin and disk were equally polished to be 3μm. The chemical composition of the wheel and the rail used in this research is shown in the table as follows.

Table 2.4: Chemical composition of wheel and rail used in the research [25]

Material	Tensile strength (MPa)	Hardness (HV)	%C	%Si	%Mn	%Cr
Wheel	880	260	0.55	0.4	0.8	0.3
Rail	950	267	0.7	0.3	1	0.3

Figure 2.7: Type of wheel and rail used in the research [25]

Figure 2.8: prepared pin and disc for test [25]

Figure 2.9: The Pin-on-disk wear machine test [25]

The pin-on-disk test is a standard test to analyze wear strength or wear rate of contacts. The tests were carried out with in a disk and different pins. After performing experiments, the specimens were weighed by means of a digital balance with 0.0001 g resolution. Then their mass reductions were recorded to calculate the wear rate using Equation below [25].

$$(W1-W2)/S = \text{Wear rate}$$

Where, *W1* is the specimen's weight before experiment and *W2* is the specimen's weight after experiment. Also, *S* is the slip distance. The S is equal to 1500 m in all experiments. Then the effect of slip distance and surface roughness are carried out [25].

Results from this work are shown as follows:

- The effect of curve shape during the movement of the train

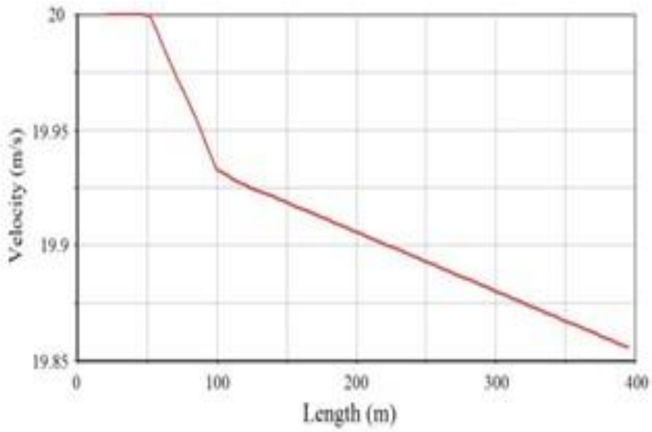

Figure 2.10: Effect of curve shape during moving of train [25]

- Effect of lateral force on wheelset in curvature path

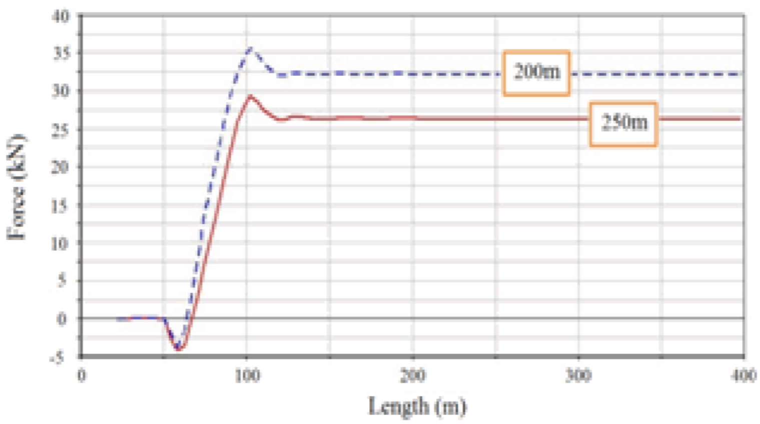

Figure 2.11: Comparison of lateral force in two different curves [25]

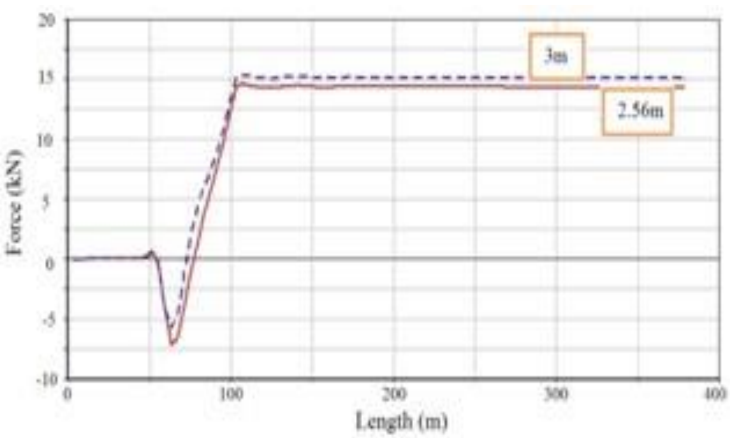

Figure 2.12: Comparison of lateral force in two different wheelbases [25].

- Effect of increasing wagon weight on lateral force

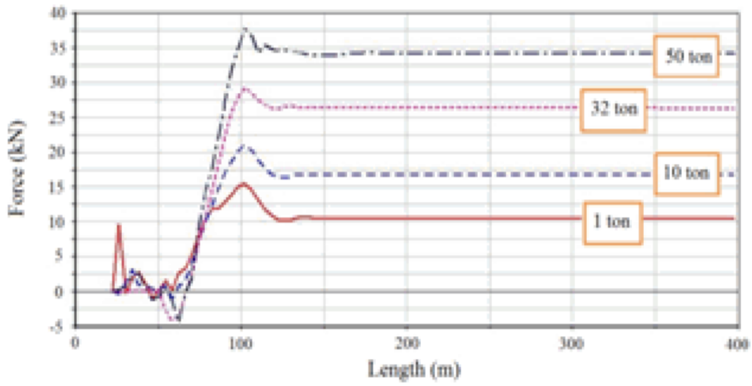

Figure 2.13: Comparison of lateral force between four loads [25]

- Effects of lateral force on wear

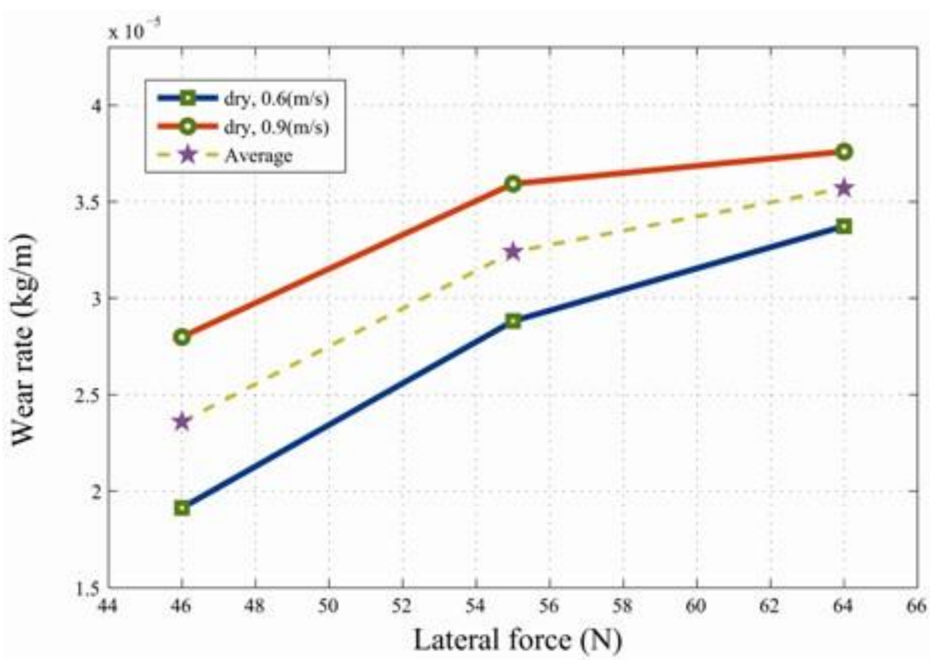

Figure 2.14: Variation of wear rate according to lateral force [25]

- Effect of Slide velocity on wear rate

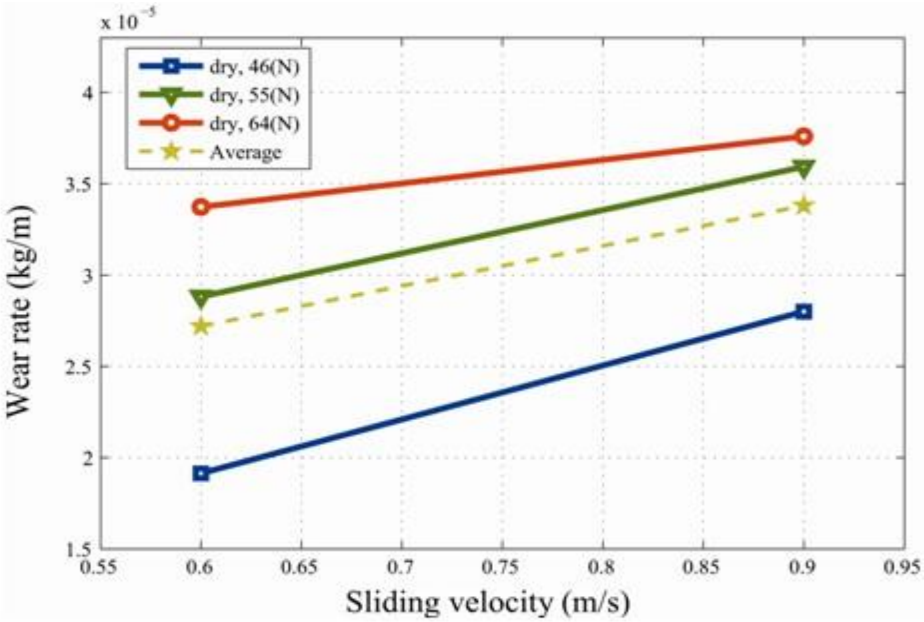

Figure 2.15: Variation of wear rate according to sliding velocity [25]

In the work, the effects of parameters such as lateral force, wagon weight, velocity, path curvature and cant were studied on wear behavior of wheel and rail. Majid Elyasi and his associates [25] have concluded the following from the results obtained.

- Higher curvature radius leads to higher lateral force and resulting higher wear between wheel and rail
- By increasing train velocity, the derailing probability increases accordingly
- Cant has a great influence on critical rates such as derailing rate and it may also lead to decreasing of wear between wheel and rail
- Lower curvature radius or higher curvature angle leads to higher lateral force.
- The wear, under dry condition, increases lateral force from 46N to 64N, the wear rate increases by about 66%
- Increase in slip velocity leads to increased wear rate. But effect of the velocity wasn't as significant as lateral force

2.5. Other literatures on wheel wear

So many literatures, journals and articles have been published related to wheel wear. In this investigative research, literature reviews will be used to identify the potential factors that lead to wheel wear thus gives important parameters to be considered in wheel wear. The following literatures are related with works done on wear of wheel and in some rail wear. The effect of different parameters on wheel wear and ways wear occurs are discussed in the literature. In others, effect of wheel and rail profile on stability of railway vehicles and discuss damages occurred to wheels and other structures of the vehicle/track.

The work reported by Nielsen *et al.* [26] focuses on the train-track interaction and mechanisms of irregular wear. These authors discuss the causes, consequences and suggest solutions to minimize the problems for several types of wheel and rail wear.

Hur and co-workers [27] use a 1/5 scaled roller rig bogie prototype to analyze the influence of the wheel profile wear on the running stability (critical speed) of railway vehicles. Fröhling [28] addresses the asymmetric wheel profile wear and analyses the consequential damages to the wheels, rails, turnouts and bogie components.

Wu [29] discusses the effects of wheel and rail profiles on vehicle curving and lateral stability through the evaluation of the North American freight railways wheel profile. Fergusson and co-workers [30] tackle the wheel wear problem in another perspective. They present a methodology to minimize the wheel wear by optimizing the primary suspension stiffness and the center plate friction of a self-steering three-piece bogie without compromising the vehicle stability.

2.6. Research gap

In this investigation of rapid wheel wear of AALRT vehicles, the general causes of wheel wear are going to be presented through interviews with experts and technicians at AALRT depot in which they address the general problems leading to the current wheel wear. Actual wheel data measured at AALRT depots is analyzed to identify which line of operation is more affected between Kaliti and Ayat line vehicles and to study the severity of the wheel wear problem. Then using multi-body simulation software SIMPACK, the vehicle dynamics performance will be simulated by using vehicle parameters and operating conditions and as a result determine which parameters should be dealt with under short and long-term plans, to eventually minimize the problem. The parameters used in the simulation are identified through literature reviews discussed above. Track curvature, critical speed, coefficient of friction (track condition) and vehicle load are taken as potential parameters which lead to wheel wear in railway.

CHAPTER THREE

3. AALRT network and operational characteristics

3.1. Infrastructure Network and Environment Conditions

At AALRT, the vehicles give transportation service in two main lines, one being the East-west and the other North-South lines. The total length of the lines is 31.025km, where the East-West main line is around 16.99km long; the North-South main line is around 16.689km long. Both lines share a section of 2.662km. AALRT uses double track dedicated for the service of passengers for both lines with a track gauge of 1435mm. The minimum radius of horizontal curve for mainlines between sections is 50m and for yard line the radius goes down to 30m. The minimum radius of vertical curve for the lines is 1000m while maximum gradient is 55%. The type of rails for main lines and depot is 50kg/m, the maximum super-elevation being 120mm and inclination at rail bottom 1/40. The axle load is ≤11（1+3%）t.

Table 3.1: Natural environment in Addis Ababa region

Altitude	≤2500m
Ambient temperature	0℃ ~ +29.7℃
Average daily highest temperature in years	25.5℃
Average daily lowest temperature in years	6.1℃
Average relative humidity in years	95%
Average annual rainfall	1000-1600mm
Maximum daily rainfall	47mm

In the East-West line (Ayat-Torhayloch), there are 21 trains allocated for operation, standby and maintenance, which are green in line. In the North-South line (Kaliti- Menilik II Square), there are 20 trains allocated in the same way. It should be noted that all the trains that are in operation are of the same vehicle type and specifications. The trains operating in each route are identified by their vehicle number; trains operating in the East-West line start by vehicle number 2XX and trains operating in the North-South line start by vehicle number 1XX. In the East-West line, there are 22 stations and in the North-South line, there are 22 stations. These routes share stations at four locations with shared track, which are stations at Stadium, Legehar, Mexico, Tegbaret and St. Lideta.

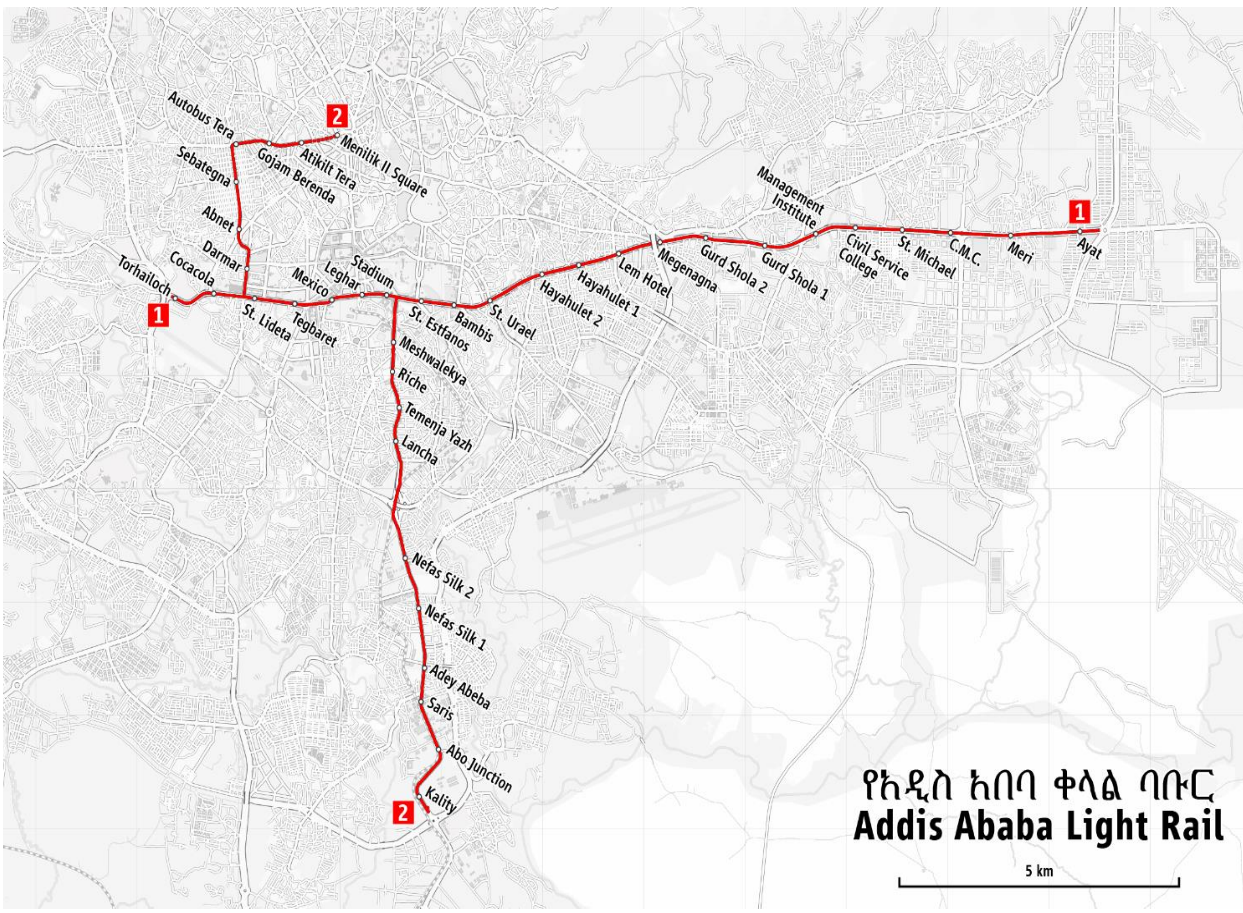

Figure 3.1: Map of AALRT line showing respective stations in each route

Table 3.2: Stations of AALRT through East-West and North-South routes

East-West line stations (Ayat-Torhayloch)	**North-South line stations (Menilik II Square-Kaliti)**
Ayat	Kaliti
Meri	Abo Junction
CMC	Saris
St. Michael Church	Adey Abeba
Civil Service College	Nifas Silk 1
Management Institute	Nifas Silk 2
Gurd Shola 1	Lancha
Gurd Shola 2	Temenja Yazh
Megenagna	Riche
Lem Hotel	Meshwalekiya
Hayahulet 1	Stadium
Hayahulet 2	Legahar
St. Urael	Mexico
Bambis	Tegbaret
St. Estifanos	St Lideta
Stadium	Darmar
Legahar	Abinet
Mexico	Sebategna
Tegbaret	Autobus Tera
St Lideta	Gojam Berenda
Cocacola	Atikilt Tera
Torhayloch	Menilik II Square

3.2. AALRT Rolling Stock Characteristics

The vehicles are 70% low-floor articulated 6-axle modern trams with two tramcars that are able to operate with double heading.

Train formation: -Mc+Tp+Mc-

Mc module: motor car with driver's cab

Tp module: trailer without driver's cab and with pantograph

+: articulation device

-: hidden folding coupler

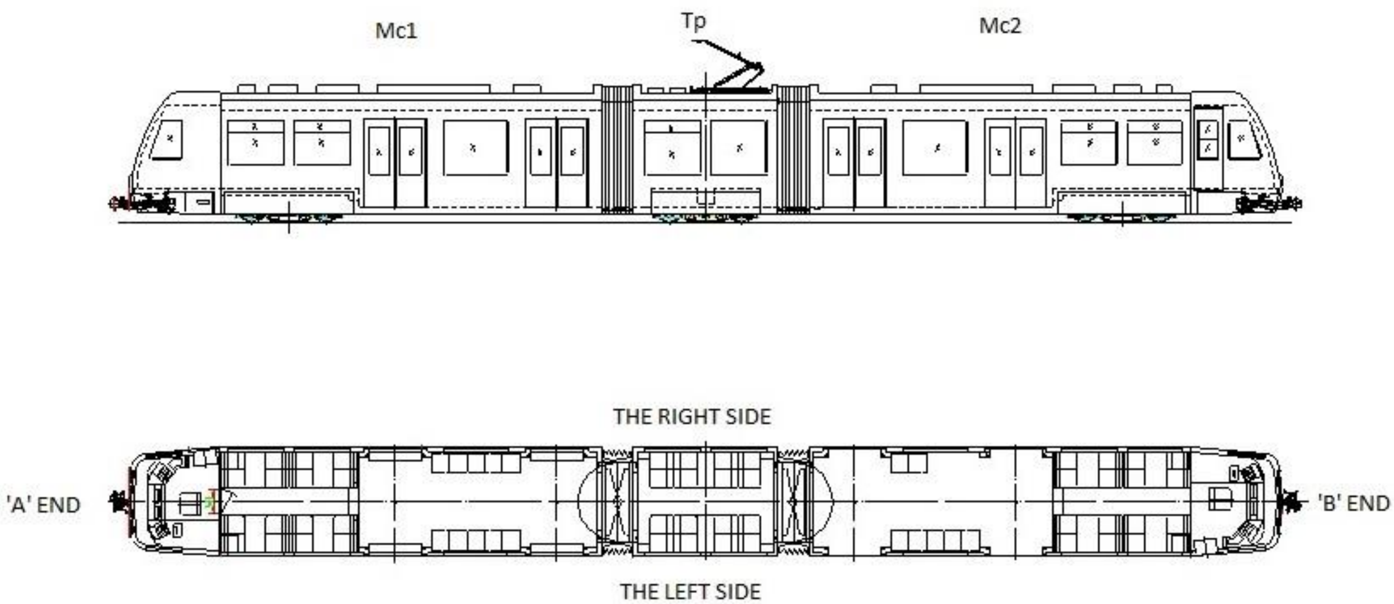

Figure 3.2: Train formation of AALRT vehicle

3.2.1. Main dimensions of vehicle

The following table shows the basic vehicle dimensions that AALRT vehicles have.

Table 3.3: Main dimensions of AALRT vehicle

Length of car body	≤ 30000 mm
Height of vehicle roof from top of rail (excluding pantograph)	≤ 3700 mm
Maximum width of car body	2650mm
Height of vehicle floor from top of rail (low floor area, new wheels and empty load)	≤380 mm
Height of vehicle floor from top of rail (exit and entry areas, new wheels and empty load)	≤350 mm
Height of vehicle floor from top of rail (raised floor area, new wheels and empty load)	≤900 mm
Wheelbase (power bogie)	1900 mm
Wheelbase (unpowered bogie)	1800 mm
Clear height of passenger compartment	≥ 1980 mm
Wheel diameter (new wheel)	≤ 660 mm
Wheel diameter (Max wear)	≤ 580 mm
Side doors of passengers' compartment	four pairs per side
Clear opening of passenger compartment door (width x height)	≥1300×1860 mm

3.2.2. Seating capacity of vehicles

The vehicle is designed to hold many passengers at a time thus it is spacious and designed for more people to stand to use space for servicing more people at once.

Table 3.4: Seating capacity of AALRT vehicle

Number of passengers (persons)	Seated	Standing	Total
Seats (AW_1)	65	0	65
Seating capacity (AW_2) (standing: 6 persons/m^2)	65	189	254
Overload capacity (AW_3) (standing: 8 persons/m^2)	65	252	317

3.2.3. Vehicle weight

Weights of vehicles are given in following table with vehicle axle load of ≤11（1+3%）t and taking 60 kg as average weight of each passenger

Table 3.5: Vehicle weight of AALRT vehicle

Loads	Car body weight	Passenger weight	Total weight
Empty vehicle (t)	44	0	44
Seating capacity (t)	44	15.24	59.24
Overload capacity (t)	44	19.02	63.02

3.2.4. Main Technical Parameters of the Vehicle

The maximum operation speed of the vehicle is 80 km/hr with average travelling speed of 20 km/hr average dwelling time of 30 seconds at each station. The average acceleration of the vehicle under rated load and rated voltage on straight and dry track, with half-worn wheels is given as follows.

- For speed from 0km/h to 40 km/h ≥1 m/s^2
- For speed from 0km/h to 80 km/h ≥0.5 m/s^2

The average braking acceleration under rated load on straight and dry track, with half-worn wheels from maximum vehicle operation speed of 80 km/h is as below:

- Maximum service brake deceleration: ≥1.1 m/ s^2
- Emergency brake deceleration: ≥ 2.0 m/ s^2

The ride quality of vehicle is ≤ 2.5, coefficient of derailment of the vehicle is ≤ 0.8. The longitudinal vehicle jerk rate is ≤ 1.0 m/s^3.

3.2.5. Vehicle bogie

The vehicle bogie is made up of cast steel frame of high strength which under normal conditions, it should have a lifetime of not less than 30 years in operation. The bogie has two suspension systems which are, primary suspension of rubber spring and secondary suspension of steel spring. The bogie's damping action is implemented by the secondary lateral oil damper and secondary vertical oil damper. The following table shows additional technical parameters of the vehicle bogie that AALRT is using.

Table 3.6: Bogie specifications of AALRT vehicle

Maximum operation speed	70 km/hr
Maximum test speed	80 km/hr
Axle load	≤ 11 (1+3%) t
Track gauge	1435mm
Fixed wheelbase	1900mm
Wheel diameter	Φ660mm(New wheel), Φ580mm(Fully worn wear)
Axle box bearing	Tapper roller bearing unit
Motor car drive mode	Double reduction gear
Brake rigging brake	Disk brake + Magnetic track brake

The vehicle consists of two types of bogie which are powered and unpowered (trailer) bogies.

i) Powered bogie

This bogie is mounted at both end of the car, underneath module Mc. The structure of this bogie is of bolster, full side bearing, outer-side axle box and fixed axle wheelset. This bogie mainly consists of frame, wheelset, primary/secondary suspension, traction assembly, driving unit, brake unit and auxiliary devices. The details of the structure of the bogie is shown in figure 3.3 as follows.

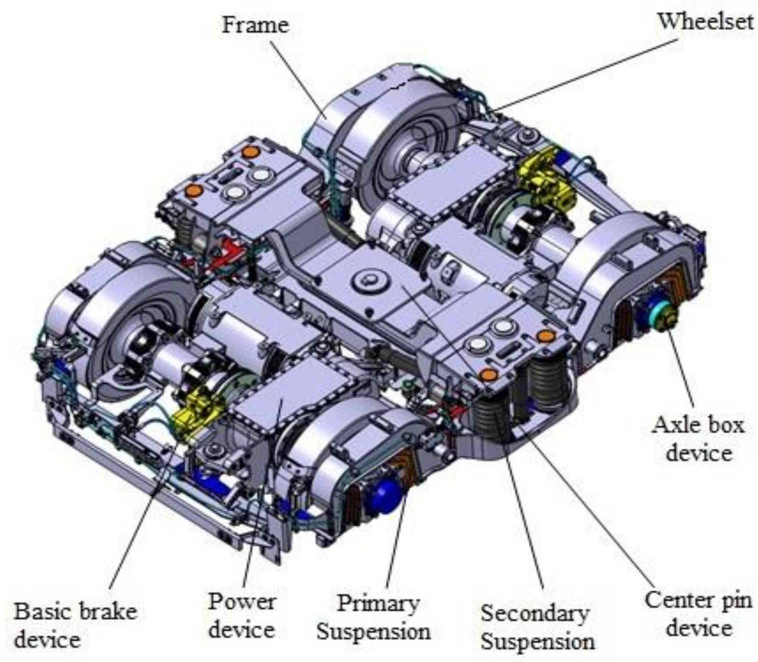

Figure 3.3: Power bogie

a. Frame and wheel set

The powered bogie has welded structure which includes steel plates and cast steel parts. These parts are side sill, cross beam and end sill. This bogie is designed to have improved frame strength and reduced welds through monobloc casting of the critical bearing area. This frame is designed according to UIC615-4, EN13749 and VDV152. The bogie wheelset consists of resilient wheel, axle, axle box and bearing unit.

b. Primary and secondary suspension

The primary suspension is of chevron metal rubber spring and is mounted between frame and axle box, with primary hanger link that enables the wheelset to be lifted up along with bogie. The secondary suspension is located at side bearing so that it handles weight of car body and it includes bolster, secondary spring, vertical damper, lateral damper, side bearing, lateral rubber stop, secondary hanger link and load sensor.

c. Traction assembly

This assembly transfers longitudinal force and lateral force between bogie and car body

d. Driving and Brake unit

The driving unit includes traction motor, gear box, hollow shaft and star coupling. The gear box is of two gears which are double reduction and parallel-axe gears. The traction motor is incorporated with gear box on one side and suspended on cross beam of bogie frame. The other end is suspended on end sill. The brake unit consists of hydraulic disk brake and magnetic track brake.

e. Auxiliary devices

There are all sorts other devices which are of significant importance. These include flange lubrication unit, rail cleaner, fender, hydraulic pipe, sanding and others. Flange lubrication, which is dry type, is of great importance because it is used to reduce flange wear and extend wheel reprofiling interval. It is located on each one axle of end bogies.

ii) Unpowered (trailer) bogie

This bogie is mounted underneath Tp module in middle of car. Similar to the powered bogie, the trailer bogie also consists of frame, independently rotated wheelset, primary suspension, secondary suspension, traction assembly, brake unit and auxiliary devices. The figure below shows the structure of the unpowered bogie.

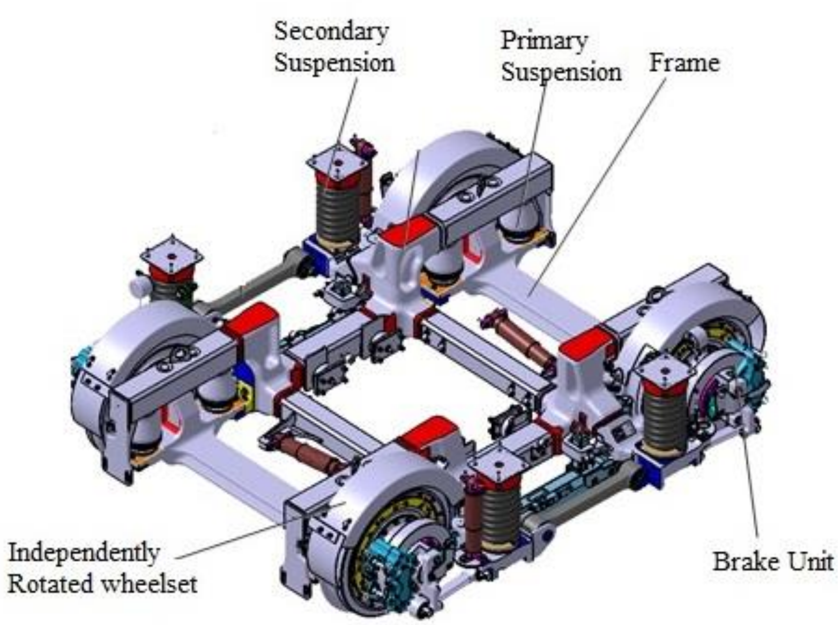

Figure 3.4: Unpowered (trailer) bogie

a. Frame

The frame of this bogie is an H shaped welded structure, and is welded of casting and square boxes. Like the powered bogie, same calculation and criterion is used for the design and weld of this bogie.

b. Secondary Suspension and traction assembly

The secondary spring supports the car body having similar structure as the suspension of the powered bogie. Similar with the powered bogie, the traction assembly consists of double traction bars arranged at both sides of bogie.

c. Brake unit and auxiliary devices

The brake unit mainly consists of the hydraulic brake and magnetic track brake like the powered bogie. While the auxiliary devices include the wheel fender, ground device and speed sensor.

CHAPTER FOUR

4. Data Collection and Analysis

4.1. Introduction

For the most part, ERC is serving the transportation sector and the economy in general, and thus doing a great deal of work for the country. But the risk in terms of wheel wear of train vehicles is a concern. Wheel/rail contact is very important factor for the movement of the train and at the same time, wear is taking place in the process. It is impossible to stop wear completely but it can be minimized to some extent. Nevertheless, the life of railway wheels is usually limited by wear.

AALRT is still in the beginnings of its services and thus there are challenges that come with it. Generally, in the initial stages of a new factory or industry operations, the probability of failure is high, but by dealing with the problems timely, eventually a low failure and optimum operation condition is met. In identifying factors that led to wheel wear at AALRT, wide range of combined causes are possible and to identify these causes, data collection is carried out through oral interviews with maintenance personnel, visual inspections of track and vehicle components. In addition, actual wheel data of vehicles measured after some mileage travel, before and after wheel profiling which includes vehicles from both routes. As of this research, it is purpose is to lay down the factors that led to rapid wheel wear of the wheels. The research findings will be very instrumental to determine the factors that brought about the problem and based on them, it is possible to find solution to minimize the problem of wheel wear.

For the case of AALRT, the wheels are worn on the flange side with reduced flange thickness including worn tread section. The surfaces of the wheels are evenly worn. The wheels are of 660mm diameter with minimum 580mm diameter allowed.

Figure 4.1: Wheel of a vehicle at AALRT

As of the problem of rapid wheel wear at AALRT, there is no definite reason why the problem occurred but technicians and experts give different technical points. Some say that the rapid wear occurred due to poor construction of the tracks with irregularities. Others say that small curves constructed inside and outside the depots led to high frictional contact, thus contributed to the rapid wheel wear. Others agree that the wheel material is of a low standard and thus sensitive to wear.

4.2. Site Inspections and Interview discussions

Interview and inspections are carried out in this investigation to identify the potential causes that led to wheel wear from the point of view of operational and technical problems observed at AALRT. The factors that are considered to be potential causes are identified based on interviews and inspections carried out with technicians/experts in the field. Interviews were undertaken with four personnel at Kaliti depot namely the head maintenance department who holds Masters in railway engineering, two rolling stock maintenance experts of whom are Bachelor degree graduates in Mechanical Engineering and a technician who manually operates/works on AALRT vehicles. They have all taken necessary trainings in China in their respective positions, on rolling stock maintenance including wheel and rail interaction. Interview questions are shown in Appendix A.

Table 4.1: Interviewed personnel at AALRT

Personnel position	No.
Head of maintenance department	1
Rollin stock expert	2
Technician on rolling stock maintenance	1

The following challenges are pointed out during interviews with the head maintenance personnel, and technicians at AALRT depots. The general technical problems observed are related to friction management, lack of maintenance facilities, and track system. These are some of the challenges that potentially aggravate the wear problem.

a) Lack of testing of vehicles

Basic tests on AALRT vehicles are carried out at both depots of which are daily inspection of vehicles before the trains start operations like lighting checking, checking appearance of entire bogie (painting damage, mechanical damage, etc.), and whether the components are loose or missing. Additionally, annual, quarter and monthly maintenance are carried out. Overhaul maintenance of vehicles and load testing take place at overhaul maintenance workshop which contains load tester and fixed/movable lifting jack. Wheel re-profiling activities are carried using under floor wheel lathe machine at the wheel re-profiling workshops.

a.

b.

c.

d.

Figure 4.2: a. Daily inspection workshop, b. Monthly inspection workshop, c. Overall maintenance workshop, d. Wheel re-profiling workshop

It is said that other than these routine tests, other important tests like dynamic testing of vehicles is not carried out at both depots. It is understandable that dynamic testing is costly as it demands space and facilities, however it is very important to monitor the dynamic performance of vehicles on periodic basis because vehicle's dynamic performance is directly related to the interactions between wheel and rail. This could well mean that lack of dynamic performance monitoring has direct effect on the wear of the wheels.

b) Limited application of required lubrication on wheel and rail

It is said that lubrication system is applied for vehicle components periodically. When the vehicles are running, there is a lubricating system attached in front of the wheels that releases lubricating oil during curvature of the vehicle called flange lubricator; however, the device had run out of oil for most vehicles and as of what it is gathered from the interview, this device has been abandoned and it is not refilled with oil due inaccessibility of the right type of oil in the country. Routine maintenances that are taken on the track are lubricating the rail fasteners with grease and making sure they are fastened well. Some portions of the rails at curves are manually lubricated but due to severe conditions like direct sun ray, the lubricating oil is not doing its intended job.

c) Track layout challenges

AALRT uses double track layout and the vehicles use two-way cabin system. It can be observed that during service of the vehicles, one side of the vehicle is always exiting first and the other cabin is always entering first. Thus, one side of the wheel always runs on one side of the track which increases greater irregularity of wheels and rail heads. Therefore, it is understandable that wear of wheels and rails became rapid due to this. High noise and squeal are also observed in operation especially vehicles in the North-South route. Track irregularity has direct influence both from the point of view of vehicle dynamic performance and wheel/rail interaction. During the interview, it is said that there is limited use of instruments that check track irregularity as part of maintenance plan and we can infer that the track, possibly, may have some mishap with daily operational loading. Common maintenance activities carried out on the tracks are periodic checkups for loose components of the rails and lubricating the fasteners using grease carried out by technicians on daily basis. The conditions of the rails are checked by detecting cracks using UV device.

At AALRT, the track layouts have elevations with concrete bridges, and track curves of radius as low as 30m in the depot and 50m on the mainline are seen. The 30m radius curves are observed both at Kaliti and Ayat depots, and these adverse conditions worsen wheel wear at AALRT. Machine supported maintenance operations are scarce at AALRT, there is no device that grinds the rails on routine basis. Grinding the rails is an important procedure that must be taken to help smoothen the contact between a wheel and a rail, thus reduced wear between them.

Critical curves of North-South line: Kaliti R150m, Abo Junction R150m, Stadium R50m, St. Lideta R50, Darmar R100m_ left turn, Darmar R100m_right turn, Autobistera R50m, Menilik II Square underground R65m
Critical curves of East-West line: Torhayloch R65m, after Coca Cola station R190m

4.1.1. Summary of results from site inspections and interviewing technicians

a. Lack of dynamic testing to monitor dynamic performance of the vehicles may lead to unseen problems, in the interaction between wheel and rail.
b. There is a lubricating system attached in front of the wheels that release lubricating oil during curvature of the vehicle called flange lubricator runs out often which leads to vehicles running on curves without lubrication and thus risking wheel wear.
c. Dry condition of the tracks greatly affects the wheel/rail interactions. No grinding of the rails is being carried out at AALRT and thus this leaves the rails being unsmoothed increasing friction between wheel and rail.
d. Tracks are affected by inhibitors like dirt and small stones on the tracks which increase adhesion between the wheel and rail and thus increased risk of wear. In addition, high noise and squeal of wheel and rail interaction are observed in the North-South route (Kaliti) during curving and uphill travel of the vehicles.
e. In wheel machining lathe, it is observed that in order to compensate the severe wear of the flanges of wheels, material from the tread is lathed to increase the flange thickness and thus leads to decrease in the overall size of the wheels.
f. The wear resistance characteristics of the material currently used for wheels is of a low grade compared to other grades available.
g. At 8 locations, sharper curves of less than R150m and as lows as 50m curve radiuses are observed in the North-South line which are critical to rapid wear taking place.

4.3. Actual wheel data measurements

Actual wheel data measurements were undertaken at both depots of Kaliti and Ayat by AALRT technicians and availability of data records from February 2016 to December 2016 are found to be helpful for this investigation. The inspection of vehicles and track is carried out for the purpose of examining and measuring vehicle wheel and rail conditions.

4.3.1. Wheel Inspection of AALRT vehicles

Inspections of AALRT vehicles were undertaken at both depots from February 2016 to December 2016 by AALRT personnel. Most of the vehicles' measurement were taken before they were about to be machined using lathe. From the data records, some vehicles were about to be machined for the first time while some were being machined for the second and third time. Therefore, full measurements of wheel flange thickness and tread diameter were taken before and after machining of the wheels. A total of 24 vehicles operating from both depots, were inspected between the time frame mentioned; 9 vehicles inspected at Ayat depot while 15 vehicles inspected at Kaliti. Table 4.2 shows the summary of vehicles that were inspected at the depots. Full measurements of wheel parameters for the vehicles inspected is provided in Appendix B.

Table 4.2: AALRT Vehicles inspected between February 2016 and December 2016

Vehicle Number	Depot Location
104, 107, 108, 109, 110, 111, 114, 115, 119	Ayat wheel re-profiling workshop
205, 206, 207, 208, 209, 210, 211, 212, 213, 215, 216, 217, 218, 219, 220	Kaliti wheel re-profiling workshop

4.3.2. Comparison between AALRT vehicles of East-West and North-South

In this investigation, wheel data measurements of AALRT vehicles from both routes, which were recorded by AALRT workshop personnel, are shown in Appendix B. Vehicles of similar mileage are compared with measurements taken before wheel-lathe machining at their respective depots. The purpose of the analysis is to find out which route is affected more and also to determine which type of wheel wear is critical for case of AALRT. Table 4.3 shows vehicles from both routes, used for comparison of flange thickness and tread diameter which are selected based on total average mileage run similarity. **New wheel diameter 660mm, worn limit 580mm*

**New flange thickness 21.21mm, worn limit of 15 mm*

Table 4.3: Vehicles selected for comparison from the two routes

East-West Vehicle No.	Mileage run, km	North-South Vehicle No.	Mileage run, km
115	45540	*212*	44026
114	45551	*205*	49030
108	40415	*215*	47312
111	45551	*208*	43452
110	54807	*218*	54471
109	76430	*206*	75028
115	69044	*216*	66522
108	52732	*210*	51662
Average run, km	**53758.75**	Average run, km	**53937.88**

The following two tables 4.4 & 4.5 show flange thicknesses of vehicles from both routes summarized from Appendix B. The average flange thickness per wheel and per bogie are computed for vehicles of each route.

Table 4.4: East-West (Ayat) vehicles Flange thickness (Sd)

Vehicle No.	**Flange thickness (Sd) in mm for respective wheels**											
	1	**2**	**3**	**4**	**5**	**6**	**7**	**8**	**9**	**10**	**11**	**12**
115	20.62	19.75	20.39	20.28	19.2	15.13	19.77	14.08	20.71	20.59	20.45	19.91
114	19.6	20.48	20.29	20.47	18.52	19.71	18.4	19.63	19.68	20.34	21.11	19.99
108	20.44	20.4	19.94	19.66	18.59	17.81	17.9	16.94	19.64	19.67	20.05	20.08
111	18.52	18.79	18.05	18.59	17.14	13.11	17.26	13.04	19.68	20.34	21.11	19.99
110	18.71	19.11	18.86	18.64	17.13	14.58	17.02	13.09	19.71	18.67	18.97	18.06
109	18.71	18.59	19.16	18.28	12.45	17.42	13.68	16.42	18.65	18.27	19.18	18.24
115	21.41	19.37	21.15	19.99	19.34	15.24	18.52	14.09	21.45	20.51	20.98	19.82
108	21.29	20.63	20.87	19.87	18.78	18.65	18.6	18.04	20.71	19.97	20.98	20.43
Average Sd/wheel	**19.91**	**19.64**	**19.84**	**19.47**	**17.64**	**16.46**	**17.64**	**15.67**	**20.03**	**19.80**	**20.35**	**19.57**
Average Sd/ bogie	**19.72**				**16.85**				**19.94**			

Table 4.5: North-South (Kaliti) vehicles Flange thickness (Sd)

Vehicle No.	Flange thickness (Sd) in mm for respective wheels											
	1	**2**	**3**	**4**	**5**	**6**	**7**	**8**	**9**	**10**	**11**	**12**
212	16.06	17.5	17.02	13.66	16.49	17.69	17.48	17.62	16.63	19.38	16.41	16.93
205	16.71	16.54	17.48	13.48	17.38	18.24	16.38	17.37	16.48	16.59	17.59	18.51
215	17.07	17.93	15.46	13.46	18.05	16.75	17.09	15.45	16.54	16.65	16.17	16.03
208	16.34	17.53	13.45	18.34	17.05	15.44	17.28	14.47	18.68	16.96	17.09	15.99
218	13.7	16.65	14.16	13.86	17.08	16.14	14.11	12.83	18.38	18.06	16.02	15.26
206	17.08	16.77	16.57	15.74	15.41	15.38	14.6	14.34	16.52	16.09	16.07	15.47
216	16.52	16.1	15.96	15.02	17.86	16.84	18.15	17.53	18.47	16.75	16.6	14.75
210	16.12	16.36	16.3	14.39	15.52	14.21	17.51	17.45	16.4	16.93	16.38	14.98
Average Sd/wheel	**16.20**	**16.92**	**15.80**	**14.74**	**16.86**	**16.34**	**16.58**	**15.88**	**17.26**	**17.18**	**16.54**	**15.99**
Average Sd/bogie	**15.92**				**16.41**				**16.74**			

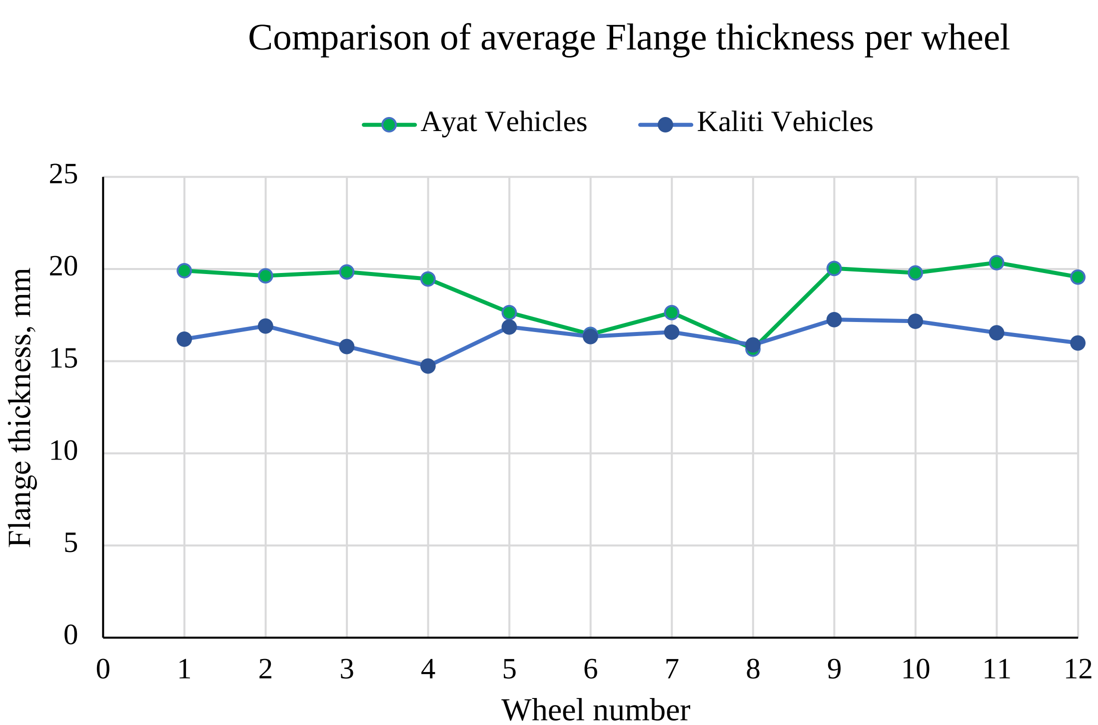

Figure 4.3: Comparison of Ayat and Kaliti vehicles in average Flange thickness (Sd) per wheel

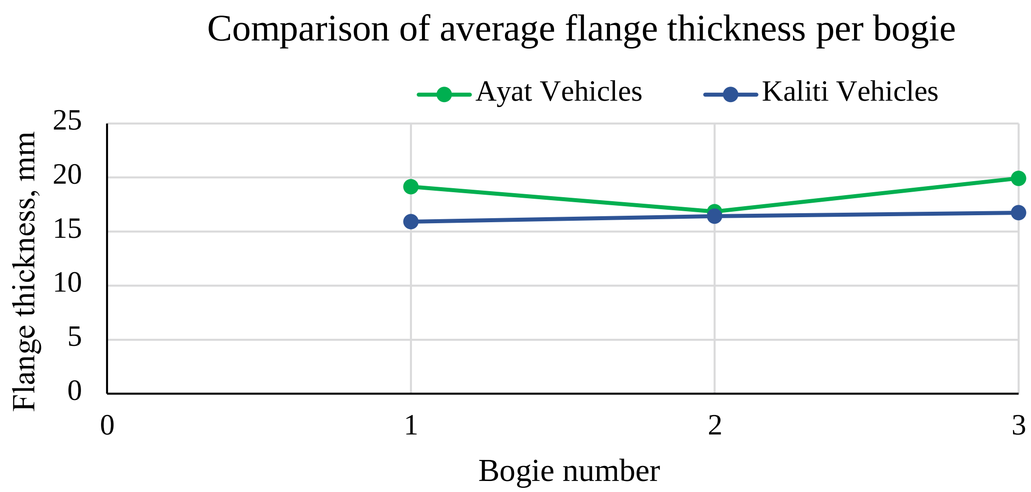

Figure 4.4: Comparison of Ayat and Kaliti vehicles in average Flange thickness (Sd) per bogie

****Total average flange thickness of Ayat vehicles*** = 18.83 mm

Total loss = New wheel – Worn wheel = 21.21- 18.83 = 2.38 mm, Percentage loss = 11.2 %

Total average flange thickness of Kaliti vehicles = 16.36 mm

Total loss = New wheel – Worn wheel = 21.21- 16.36 = 4.85mm, Percentage loss = 22.9 %

The above figures 4.3 and 4.4 show comparison of average flange thickness between selected Ayat and Kaliti vehicles. As shown in figure 4.4, the average flange thickness per wheel of Kaliti vehicles is greatly worn than that of Ayat's vehicle. Kaliti vehicles, with average flange thickness of 16.36 mm, show a total percentage loss of 22.9 % in flange thickness as compared to Ayat vehicles'18.83 mm average flange thickness with percentage loss of 11.2%. It can be observed that trailer (bogie 2) bogies' flange thicknesses are worn greatly compared to other two motor bogies. One of the characteristics of trailer bogies is that these types of bogies do not promote self-steering through curves, increasing flange forces and angle of attack which lead to flange wear and noise and thus the wheel life of trailer bogies is less than that of motored bogies [31]. This is especially the reason for wheel flange wear for Kaliti vehicles due to adverse conditions of sharper curves in the route.

The following two tables 4.6 & 4.7 show tread diameters of vehicles from both routes summarized from Appendix B. The average tread diameter per wheel and per bogie are computed for vehicles of each route.

Table 4.6: East-West (Ayat) vehicles Tread diameter (Td)

Vehicle No.	**Tread diameter (Td) in mm for respective wheels**											
	1	*2*	*3*	*4*	*5*	*6*	*7*	*8*	*9*	*10*	*11*	*12*
115	659.7	659.5	659.8	659.7	659.9	660.3	659.9	660.3	659.9	659.7	659.6	659.4
114	659.9	659.7	659.9	660.0	660.3	660.1	660.3	660.0	659.9	659.8	659.8	659.7
108	659.9	659.5	659.7	659.6	660.5	660.3	660.2	660.3	659.9	659.6	659.9	659.5
111	659.2	658.7	658.9	658.7	659.8	660.4	659.7	660.3	659.9	659.8	659.8	659.7
110	659.3	659.1	659.4	659.2	660.0	660.3	659.8	660.4	659.8	659.3	659.2	659.0
109	658.8	658.7	658.9	658.8	660.4	659.9	660.2	659.9	659.2	659.0	658.9	658.8
115	659.1	658.8	659.1	659.1	635.1	635.9	634.9	635.4	659.3	659.0	658.8	658.7
108	659.7	659.2	659.3	659.3	654.4	655.1	653.7	654.0	659.5	659.2	659.5	659.2
Average Td/wheel	**659.4**	**659.2**	**659.4**	**659.3**	**656.3**	**656.5**	**656.1**	**656.3**	**659.7**	**659.4**	**659.4**	**659.2**
Average Td/bogie	**659.3**				**656.3**				**659.4**			

Table 4.7: North-South (Kaliti) vehicles Tread diameter (Td)

Vehicle No.	**Tread diameter (Td) in mm for respective wheels**											
	1	*2*	*3*	*4*	*5*	*6*	*7*	*8*	*9*	*10*	*11*	*12*
212	659.7	659.6	659.7	659.4	660.1	660.1	660.1	660.2	659.3	659.9	659.6	659.5
205	659.4	659.5	659.6	659.6	660.2	660.2	660.0	660.0	659.6	659.6	659.6	659.7
215	659.6	660.0	659.8	659.7	660.3	660.4	660.1	660.3	659.8	659.8	659.8	659.6
208	659.4	659.5	659.6	659.8	660.1	660.3	660.2	660.1	659.7	659.6	659.4	659.6
218	659.3	659.6	659.3	659.4	660.2	660.2	660.1	659.9	659.1	659.7	658.9	659.3
206	648.5	648.5	647.4	647.5	638.8	638.9	637.3	637.6	652.6	652.7	652.4	652.6
216	648.9	649.1	645.6	645.5	660.0	660.0	660.0	659.8	647.3	647.2	647.2	647.3
210	659.0	659.3	659.4	659.2	660.1	660.3	650.7	650.9	659.3	659.5	659.2	659.2
Average Td/wheel	**656.7**	**656.9**	**656.3**	**656.3**	**657.5**	**657.6**	**656.1**	**656.1**	**657.1**	**657.2**	**657.0**	**657.1**
Average Td/bogie	**656.5**				**656.8**				**657.1**			

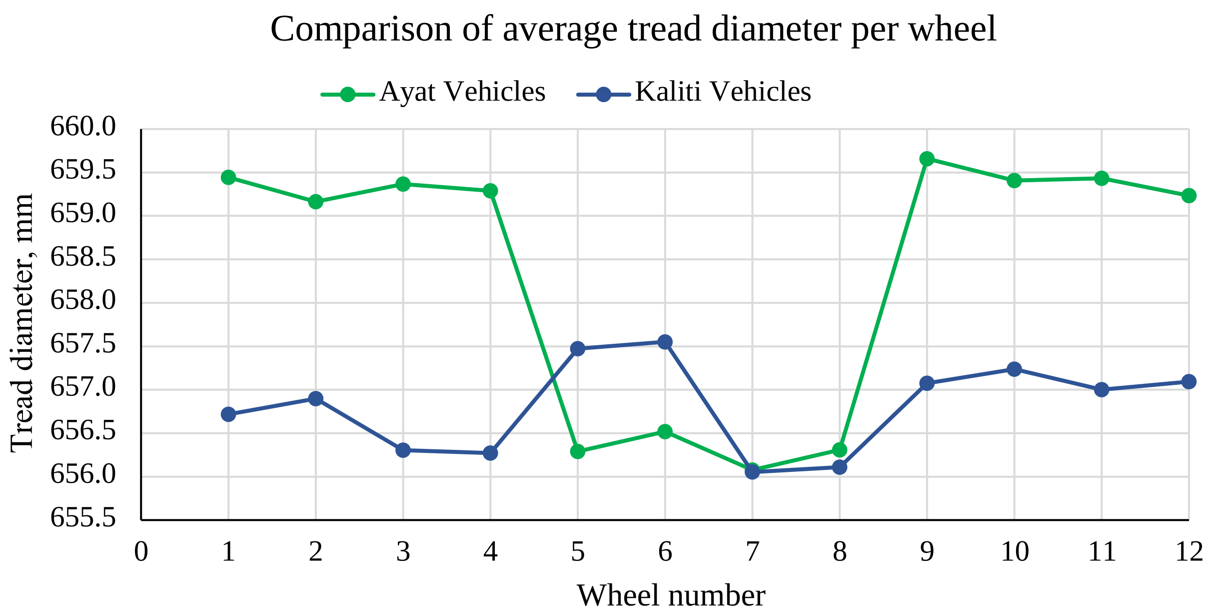

Figure 4.5: Comparison of Ayat and Kaliti vehicles in average tread diameter (Td) per wheel

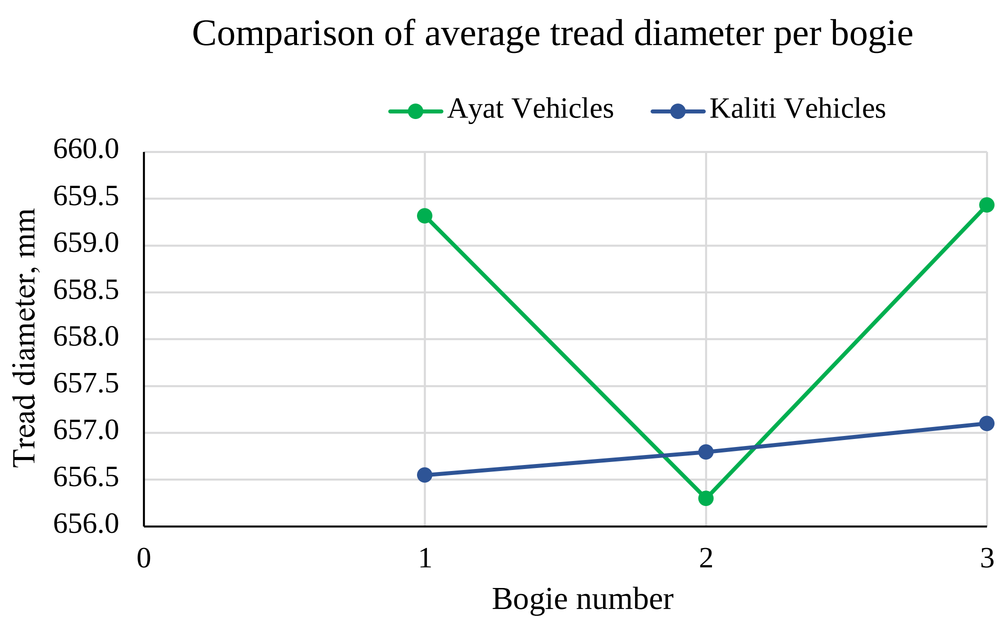

Figure 4.6: Comparison of Ayat and Kaliti vehicles in Tread diameter (Td) per bogie

Total average tread diameter of Ayat vehicles = 658.3 mm

Total loss = New wheel – Worn wheel = 660 – 658.3 = 1.7 mm, Percentage loss = 0.25 %

***Total average tread diameter of Kaliti vehicles** = 656.82 mm

Total loss = New wheel – Worn wheel = 660 – 656.82 = 3.19 mm, Percentage loss = 0.48 %

The above figures 4.5 and 4.6 show comparison of average tread between selected Ayat and Kaliti vehicles. As shown in figure 4.6, the average tread diameter per wheel of Kaliti vehicles is greatly worn than that of Ayat's vehicle. Kaliti vehicles, with average tread diameter of 656.2 mm, show a total percentage loss of 0.48 % in tread diameter as compared to Ayat vehicles' 658.3 mm average flange thickness with percentage loss of 0.25 %. Average tread diameter of the trailer bogies for Ayat vehicles is much more worn than the other two bogies which is because trailer bogies tend to wear at a greater rate than the rest due to increased forces at contact since these bogies don't allow self-steering. Under normal conditions, trailer bogies do wear faster than motorized bogies.

4.3.3. Summary of results from actual wheel data of AALRT vehicles

a. Vehicles having similar travel mileages, from the two lines, are compared and the results showed that the wheels of vehicles operating in the North-South line are more worn than vehicles operating in the East-West line. This is due to vehicles operating in relatively sharper curves in the North-South route. Both the flange and tread wear of wheels in the route are much more worn. The tread is mainly worn due to machining in order to increase thickness of worn flanges.
b. The flanges of the wheels are greatly worn for vehicles in the North-South route due to operation in sharper curves. Some wheels have surpassed their worn limit of flange thickness.
c. It is also observed that trailer bogies of AALRT vehicles are much more worn than the motorized bogies due to behaviors of trailer bogies of not allowing self-steering motion while curving and higher lateral forces on straight track also which make it even more difficult when vehicles operate on irregularly constructed tracks and sharp curves.

CHAPTER FIVE

5. Dynamic modelling, simulation and analysis of AALRT vehicle

5.1. Railway vehicle dynamics

Dynamic analysis of a railway vehicle combines the interaction of different components put together to create optimized vehicle which can run safely and within design boundary. A railway vehicle consists of wheelsets, bogies, and a body, where the wheelsets and bogies are connected through primary suspension systems while the bogies are connected to the carbody through the secondary suspension systems. Figure 5.1 shows a typical railway vehicle consisting of the mentioned components.

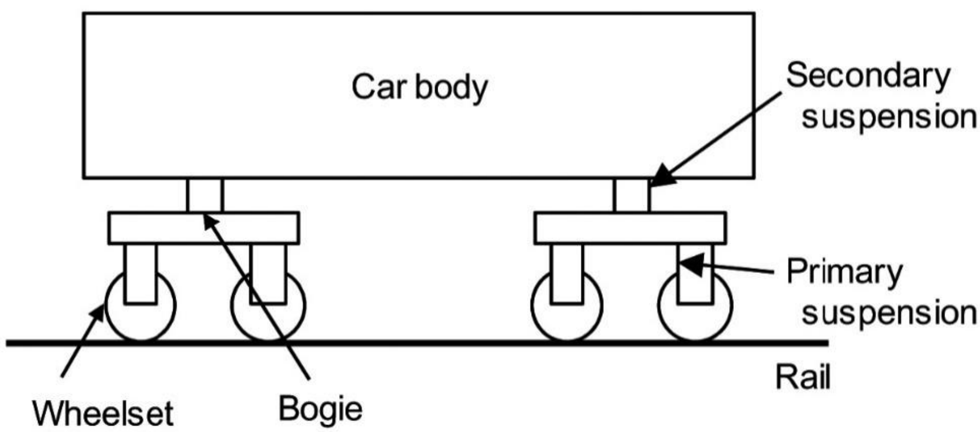

Figure 5.1: Components of railway vehicle [32]

As in the case of common motion dynamic analysis, to analyze the kinematic performance of a railway vehicle, each of the components given in Figure 5.1 is expressed as a rigid body, and equations of motions in the vertical, lateral, and longitudinal directions are formulated in consideration of the spring rigidity and damping properties of the suspension systems. Then, according to track and running conditions separately given, the kinematic behavior of a railway vehicle is analyzed through simulation based on multibody dynamics [32].

5.2. Wheel/Rail contact

Vehicle dynamic performance is influenced strongly by interacting wheel and rail forces. There are two planes considered in contact forces as shown below in figure 5.2.

- Plane 1 (Normal plane)

This plane involves constraint forces namely the normal force and geometry forces. 'Q' denotes the vertical force acting on the contacting point, while 'N' is the normal force and 'Fy' denotes the lateral force.

- Plane 2 (Tangential plane)

Tangent forces or creep forces such as Tx, Ty friction forces in x, y direction, which depend on longitudinal (Sx) and lateral (Sy) creepages.

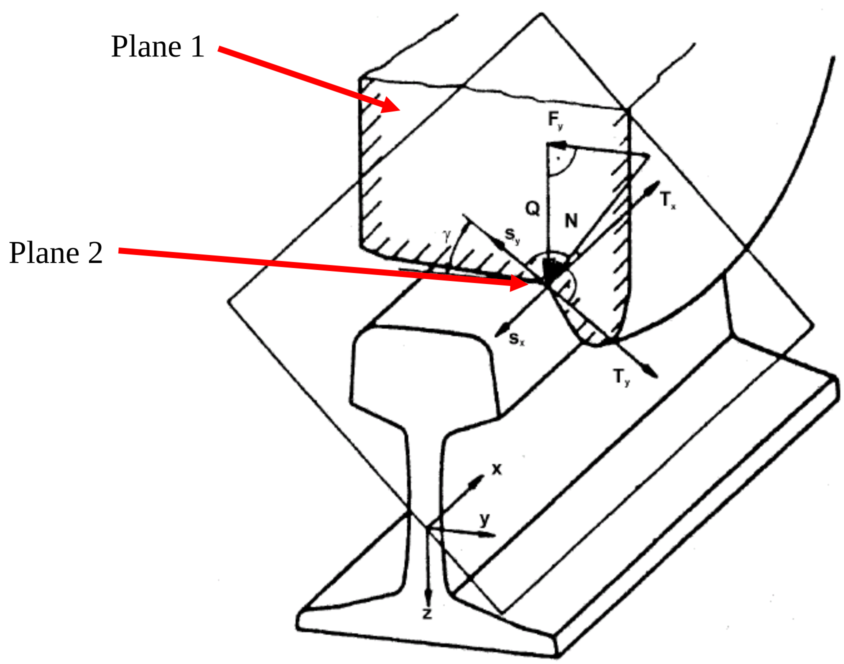

Figure 5.2: Wheel/rail contact forces

<u>Derailment Coefficient</u>

The derailment ratio *Y/Q* is used as a measure of the running safety of a railway vehicle. Several theories have been developed to establish the *Y/Q* ratio. One of the most widely used is the Nadal [1908] derailment criterion which describes the conditions necessary to sustain equilibrium of the forces in flange contact. Description of the Nadal theory can be found in Dukkipati [2000]. Nadal's formula takes into account the influence of the wheel flange angle, the wheel/rail friction coefficient, and wheel/rail forces on the possibility of wheel climb derailment [33]. This principle is expressed in Nadal's formula:

$$\frac{Y}{Q} = \frac{tan\alpha - \mu}{1 + \mu tan\alpha} \quad \text{……………………………………eq. 1}$$

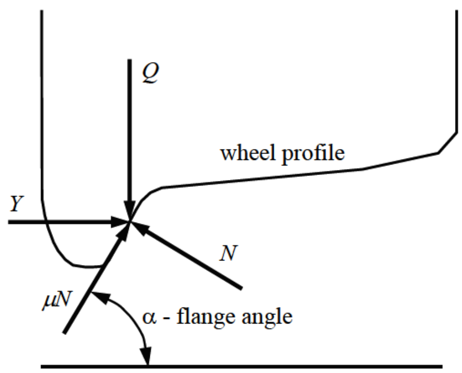

Q vertical force;

Y lateral force;

α flange angle

μ friction coefficient

Figure 5.3: Flange angle and flange forces

5.4 Wheel/Rail wear

The level of wear at the wheel and rail surface is indicated by the energy dissipated in the contact patch; this is calculated by taking the product of creepage and creep force. Wheel wear is estimated using the wear index *W* taken from the English Normative (British Rail) that reads [33]:

$$W = F_x \cdot \xi + F_y \cdot \eta \quad \text{…………………………………………eq. 2}$$

where $\boldsymbol{F_x}$ is the longitudinal creep force; $\boldsymbol{\xi}$ is the longitudinal creepage; $\boldsymbol{F_y}$ is the lateral creep force; $\boldsymbol{\eta}$ is the lateral creepage.

5.3. About SIMPACK Simulation Software

SIMPACK is a multi-body simulation package that is used to simulate and model complex mechanical systems. The software allows the user to make use of different electrical, hydraulic and pneumatic elements in the process of modelling and simulation. This software allows modelling of multi-body systems for the purpose improving the design process involved. The following points are the common requirements that is expected from the software.

- Optimization of design parameters
- Calculation of dynamically interacting forces within critical components
- Effect of varying design parameters
- Determining major design parameters affecting dynamic behavior
- Analyzing weak points of the mechanical design

From the initial concept stage to the point where SIMPACK has presented the results, there are six steps. The first three steps are performed outside SIMPACK. They are as follows:

1. Problem definition
2. Development of a mechanical model
3. Provision of the physical parameters for the model

The first three steps may appear obvious, but should be completed before entering SIMPACK

Steps 4 to 6 are performed within SIMPACK

4. Pre-processing: Input the data set, obtained from steps 1-3, with the help of the SIMPACK user interface
5. Problem Solution: Generation and solution of the motion governing differential equations
6. Post-processing: Presentation of the results

5.4. Modelling of AALRT vehicle in SIMPACK

The railway vehicle on which this investigation has been performed is the current AALRT train, 70% low-floor tram of Chinese brand. Specifications of the vehicle dimensions and bogie are used for the modelling of the train. This vehicle is made up of three coaches and three bogies with two wheel-sets each; the external bogies are motorized and the one in the middle is a trailer one. The vehicle is modelled in SIMPACK 8.904 as shown in figure 5.4.

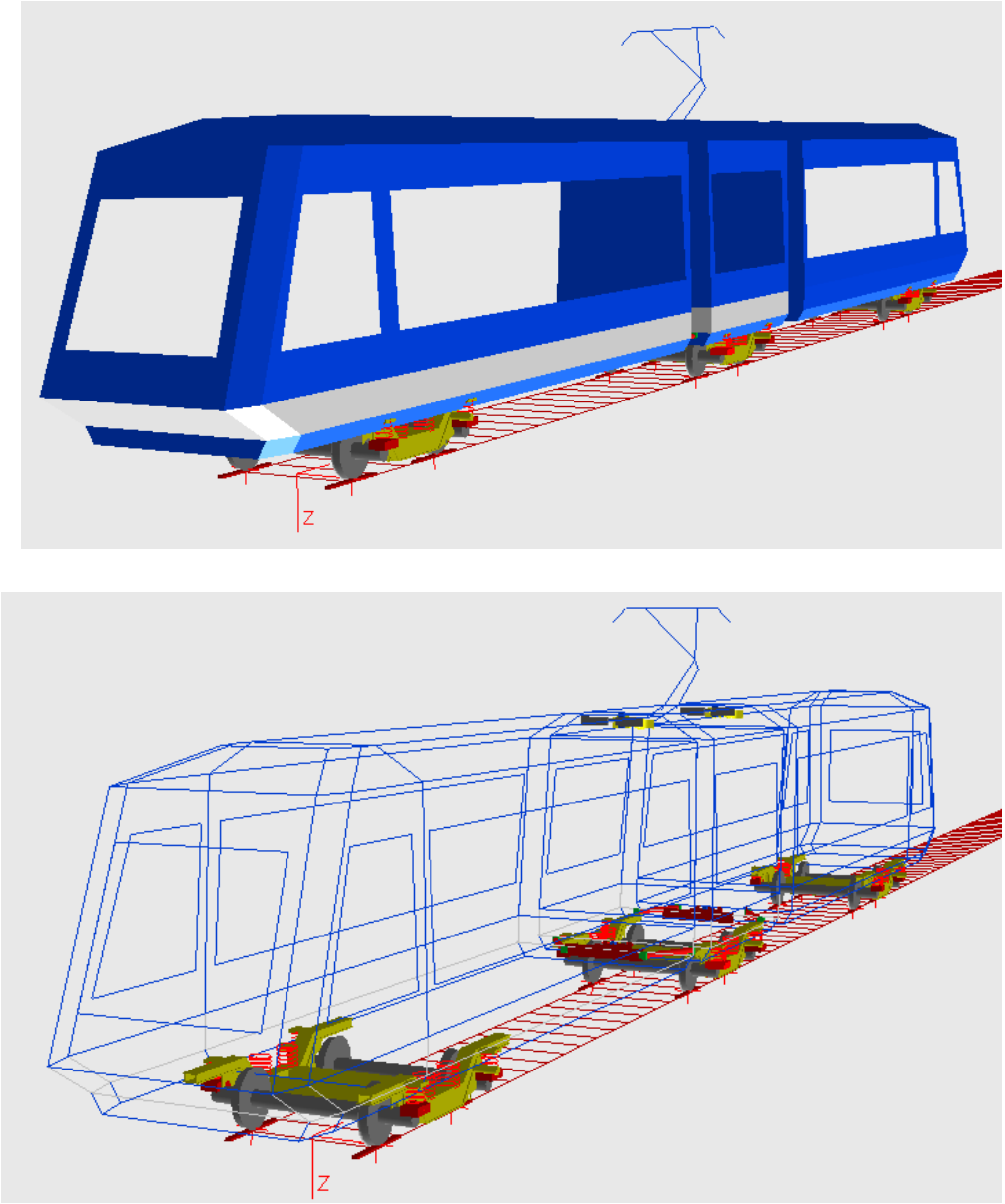

Figure 5.4: AALRT vehicle model represented in solid and wireframe

In the modelling of the vehicle, the standard selected for the wheel type is S1002 and for rail type, UIC 60 is selected. The standard track gauge 1435mm that AALRT uses is selected.

- Wheel Type: S1002 with flange angle of 70^0 and flange thickness (S_d) 21.21mm
- Rail Type: UIC 60
- Track Gauge: 1435 mm

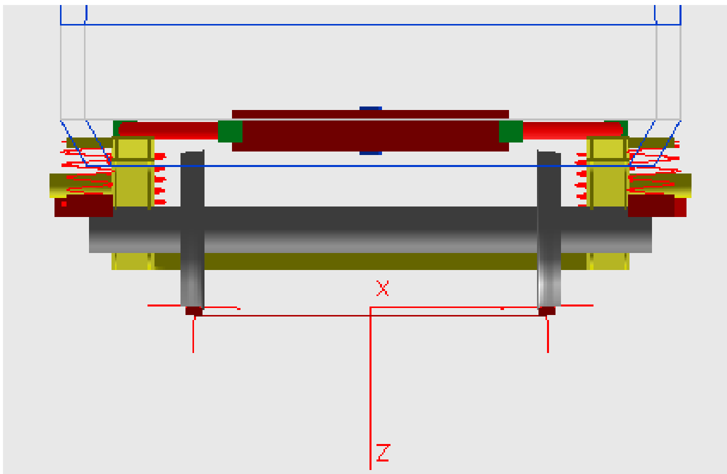

Figure 5.5: Wheel/Rail configuration

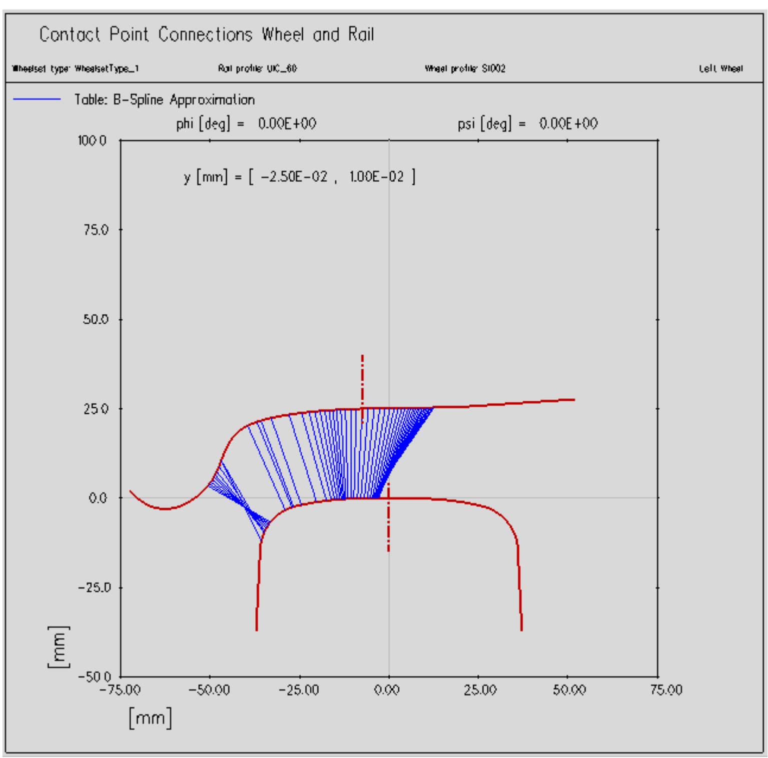

Figure 5.6: Wheel/Rail contact view

The bogie frame is important part of railway vehicle which holds the car body firmly sitting between the wheelsets and the car body. It connects the secondary suspension to the car-body and the frame itself is connected to the wheel set using the primary suspension.

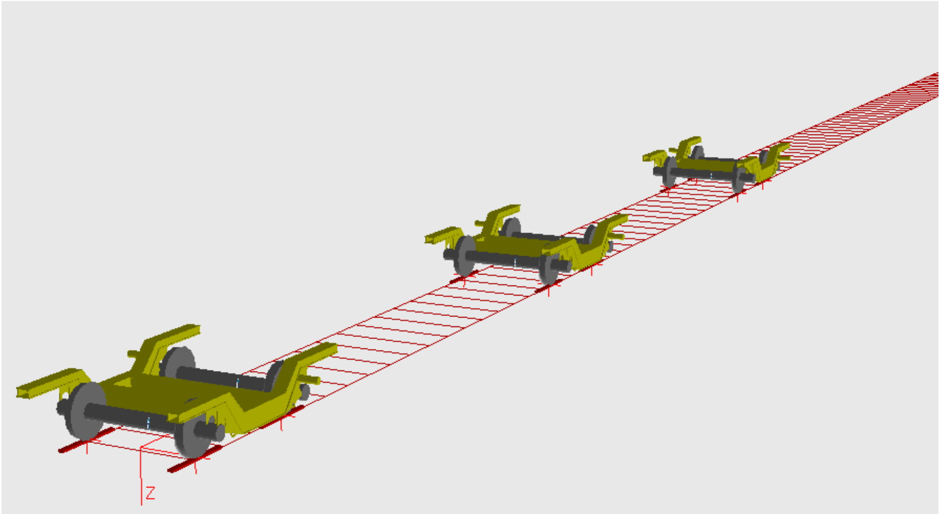

Figure 5.7: Bogie frame formation

The bogies are provided with two stages of suspensions. The primary suspensions are of two coaxial springs, which mainly provide the vertical stiffness linking the axle-boxes with the bogie frame. The secondary suspension stage comprises two springs for the vertical, longitudinal and lateral stiffness.

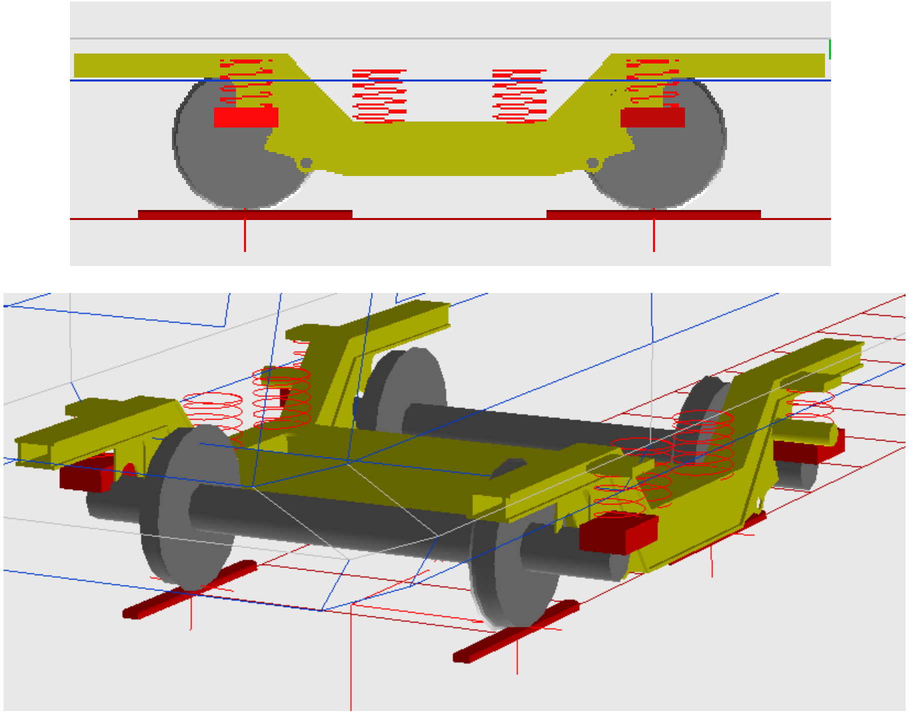

Figure 5.8: Bogie suspension of primary and secondary stages

In the modelling of the vehicle, articulation components play a big role in connecting the car bodies so that the bodies are able to move together on a straight track and during curving of the vehicle. The linking components are composed of lower fixed articulations, upper fixed components and fixed articulation dampers. The components are all modelled using CATIA V5 software and the models are saved as (.igs) format files, then exported to Solid Work to be saved as Pro engineer format, then exporting them to Pro Engineer to change to (.slp) format of SIMPACK software. The following figures show the articulation components.

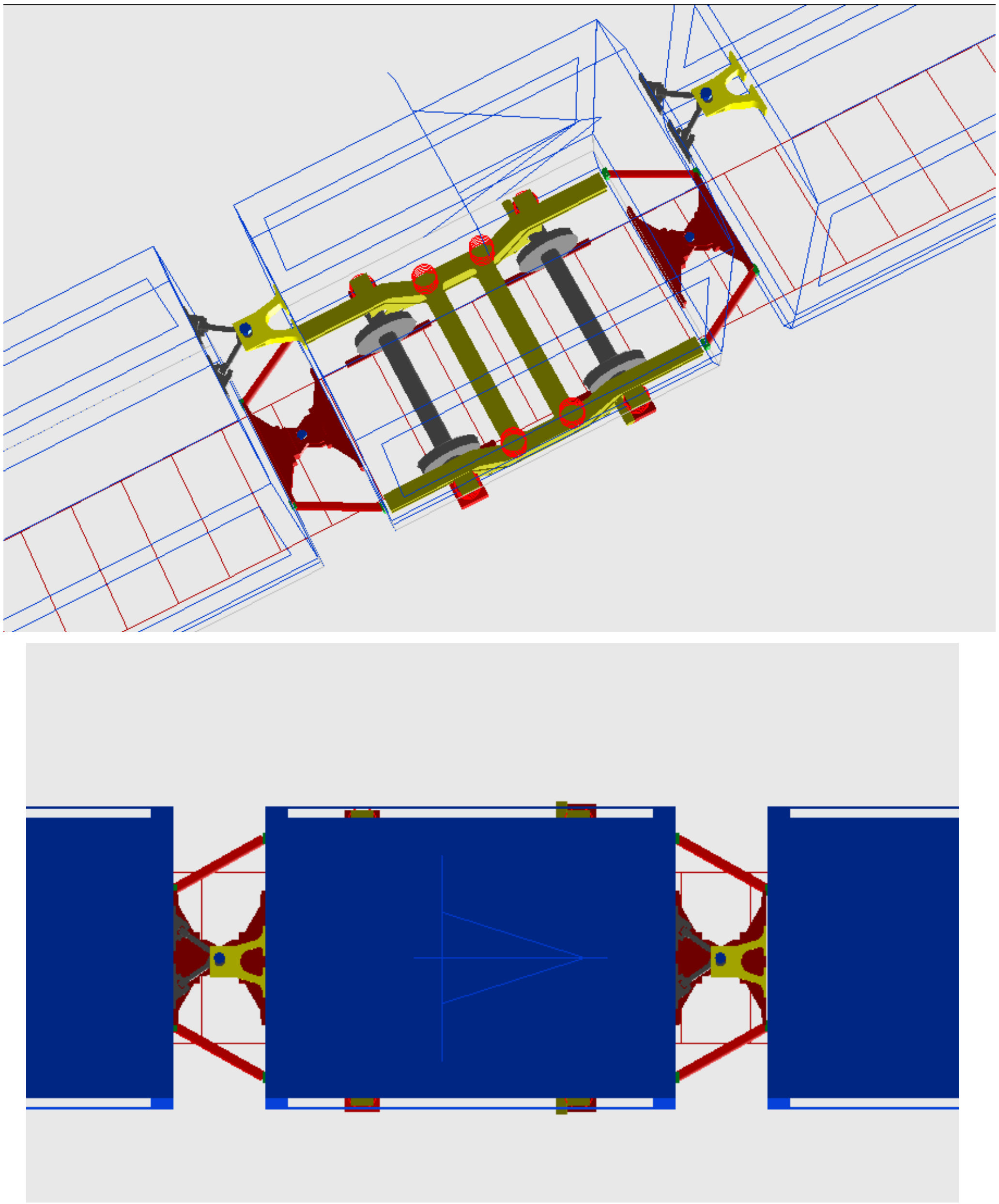

Figure 5.9: Articulation components

The resultant whole SIMPACK multibody includes 3 coaches, 3 bogies, 6 wheel sets and 12 axle-boxes; all of these components are considered as rigid bodies. The total degree of freedom is 72 DOFs. The degree of freedom (DOF) of the vehicle model considering these rigid bodies are as follows in details. DOF= quantity x number of DOF

- DOF of 6 Wheelsets = 6 x 6 = 36 DOFs
- DOF of 3 Bogie frames = 3 x 6 = 18 DOFs
- DOF of 3 car bodies (coaches) = 3 x 6 = 18 DOFs
- Articulation component =2 x 6 = 12 DOFs
- Total Degree of Freedoms = 36 + 18 + 18+18 = 84 DOFs

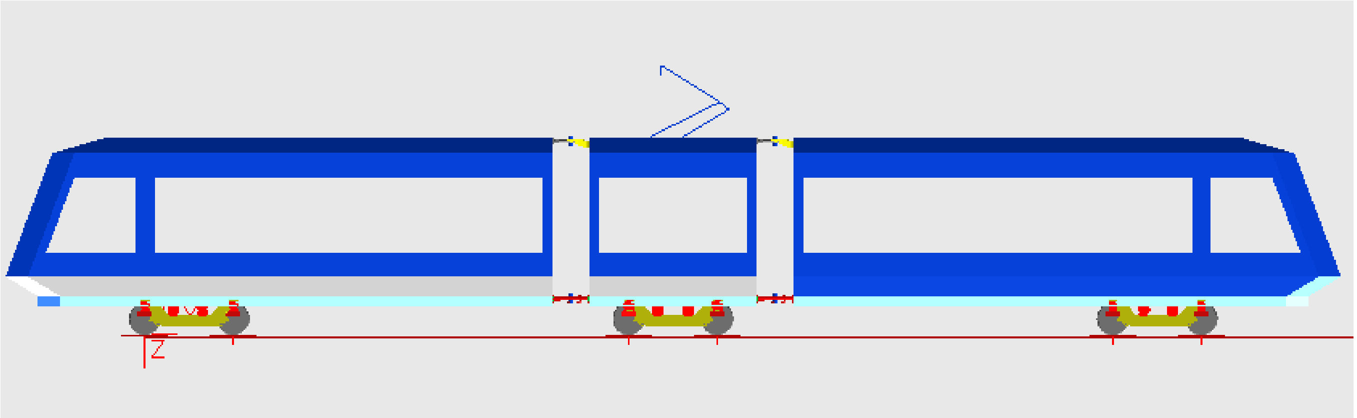

Figure 5.10: Side View of vehicle showing all components

The most significant inertial properties of the model bodies are summarized in Table 5.1 and the main linear characteristics of the suspensions are summarized in Table 5.2.

Table 5.1: The AALRT vehicle train main inertial properties (Overload condition)

Body Component	Mass kg	I_{xx} kgm^2	I_{yy} kgm^2	I_{zz} kgm^2
Car body A	17500	4375	8750	8750
Car body B	12325	3081.25	6162.5	6162.5
Car body C	17500	4375	8750	8750
Bogie frame	4200	1215	1875	2182
Wheelset	880	176	76	176

Table 5.2: Main linear stiffness properties of the AALRT vehicle

	Kx(N/m)	Ky (N/m)	Kz (N/m)
Primary Suspension	613,000	613,000	1,415,000
Primary Damping	-	-	80,000
Secondary Suspension	150,000	150,000	500,000
Secondary Damping	-	200,000	400,000

5.5. Conditions of simulation

The following conditions are considered in the simulation of AALRT vehicle

- All simulations carried out at maximum loading condition of around 63000 kg mass
- Simulation is carried out in dry condition with 0.36 coefficient of friction and results are validated against standard derailment coefficient, vehicle ride index and lateral force.
  - coefficient of derailment of the vehicle is $Y/Q \leq 0.8$
  - the ride quality of vehicle is ≤ 2.5
  - lateral force Y < 60 KN, UIC 518
- Operating vehicle speed of AALRT is used for simulation
  - Max speed of 80 km/hr on straight track
  - Speed of 15 to 20 km/hr for curving 50 m track radius
  - Speed of 20 km/hr for curving 100 m track radius
- Track irregularity is not included so regular standard track is considered
- Wheel profile of the wheels are considered identical

5.6. Validating dynamic analysis of AALRT vehicle on straight track

The modelled AALRT vehicle is simulated on a straight track with a running speed of 80 km/hr. The results are validated against the specifications of the vehicle, such as derailment of coefficient, ride index and maximum lateral force. It can be observed from figure 5.11 (a) that derailment of coefficient satisfies the standard ($Y/Q \leq 0.8$). The simulated ride quality of the vehicle also complies with the standard (≤ 2.5) of the vehicle as seen in figure 5.11 (b). In the same way as shown in figure 5.12, lateral force also fulfills the standard $Y < 60$ KN according to UIC 518, 2005.

a.

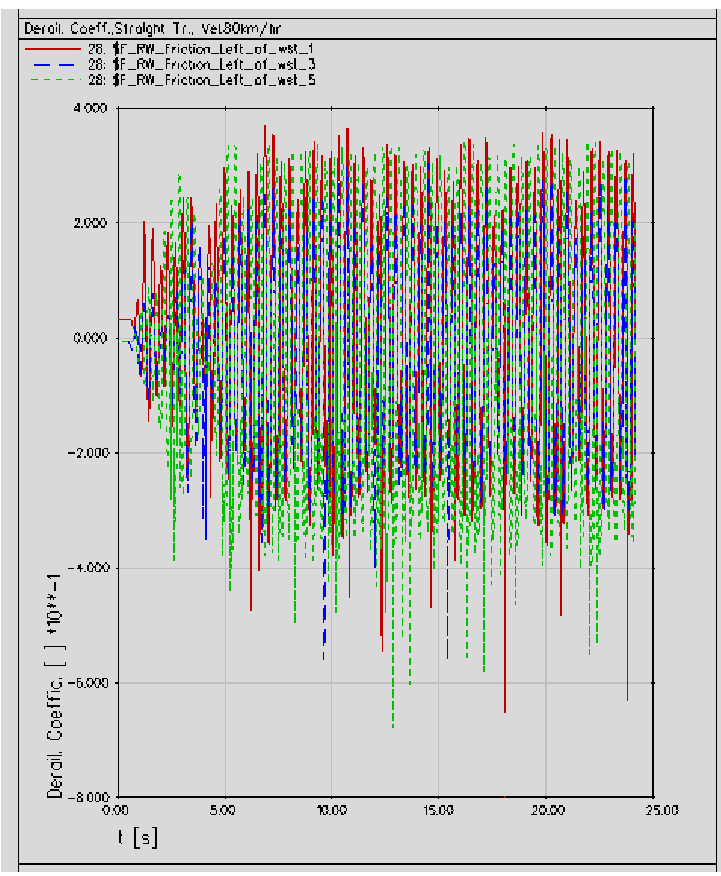

b.

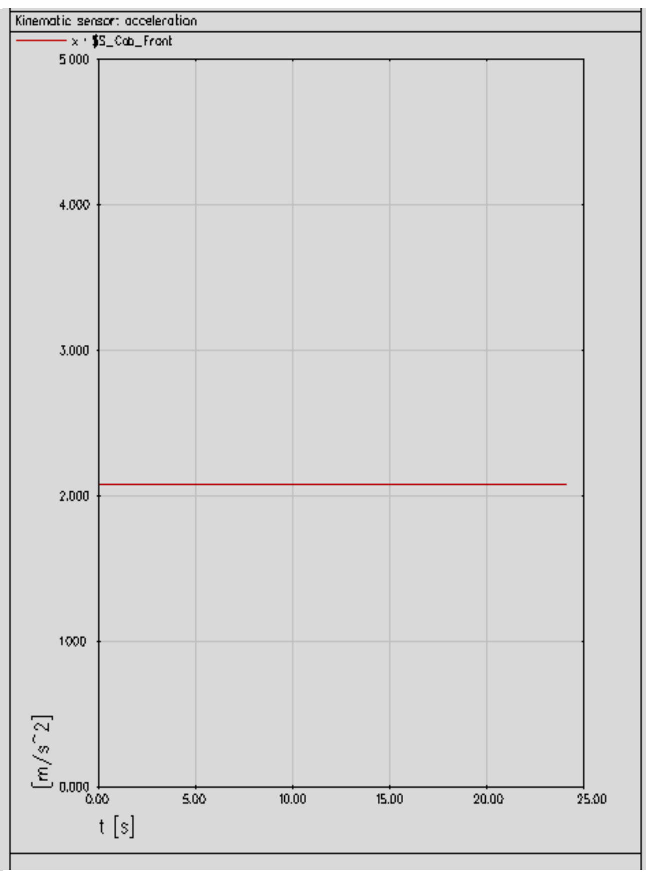

Figure 5.11: a. Derailment coefficient of wheelset 1, 3, 5 on straight track, b. Ride index of front cab on straight track

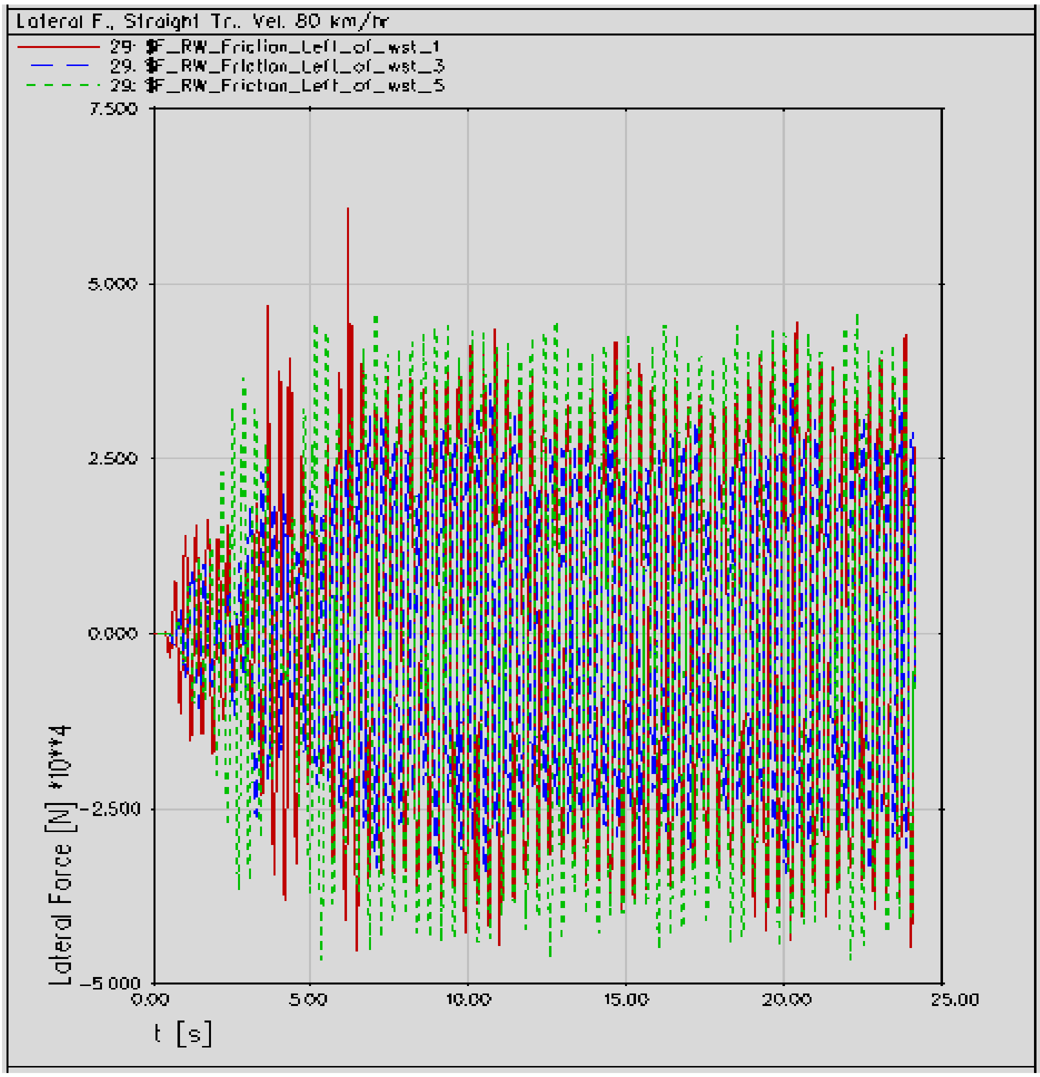

Figure 5.12: Later force on a straight track wheelset 1, 3, 5 on straight track

5.7. Validating dynamic analysis of AALRT vehicle on curved track

The modelled AALRT vehicle is simulated on curved track of radius 50m and 100m, with a running speed of 20 km/hr. The results are validated against the specifications of the vehicle, such as derailment of coefficient, and maximum lateral force. The results of simulation are shown as follows for both curves. It is evident from the results that curve radius of 50 resulted in greater lateral force compared to others, and thus, it can be concluded that small curves increase the risk of flange wear with increased lateral force.

5.7.1. Simulation of vehicle on minimum curve radius 50 m

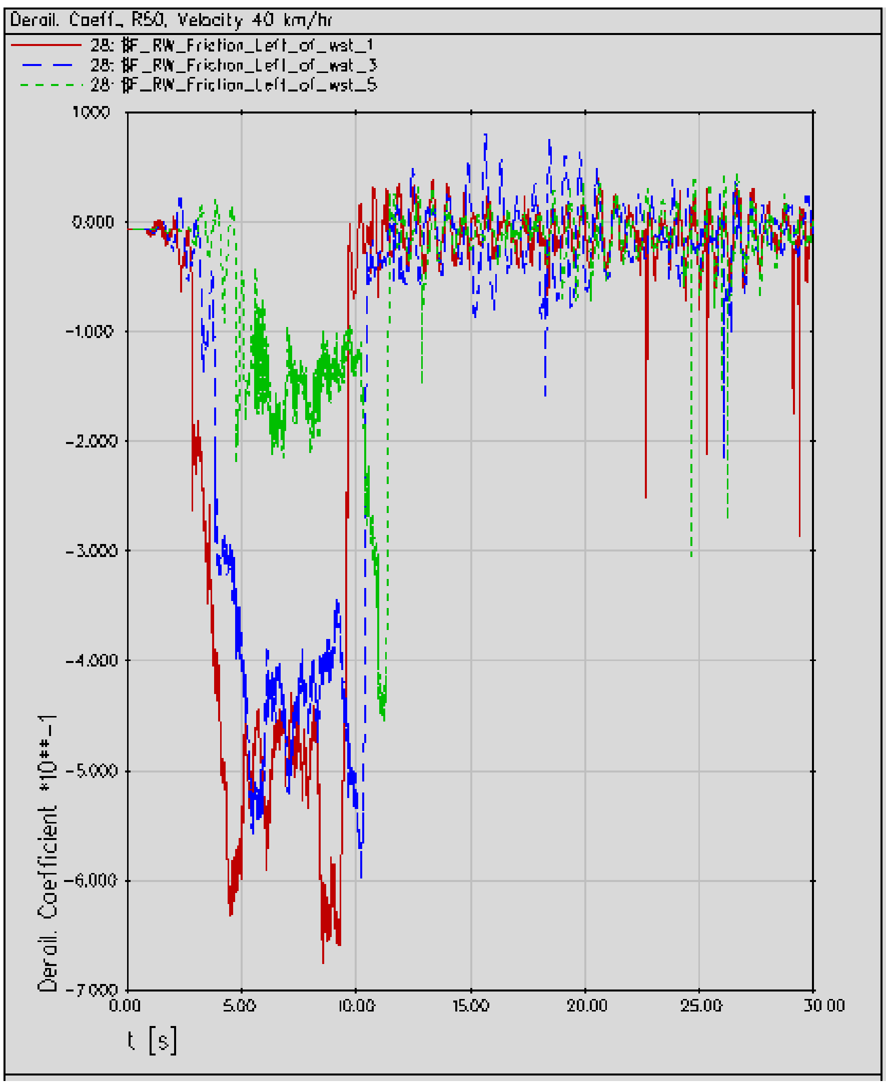

Figure 5.13: Derailment Coefficient of wheelset 1, 3, 5 on curve radius 50 m

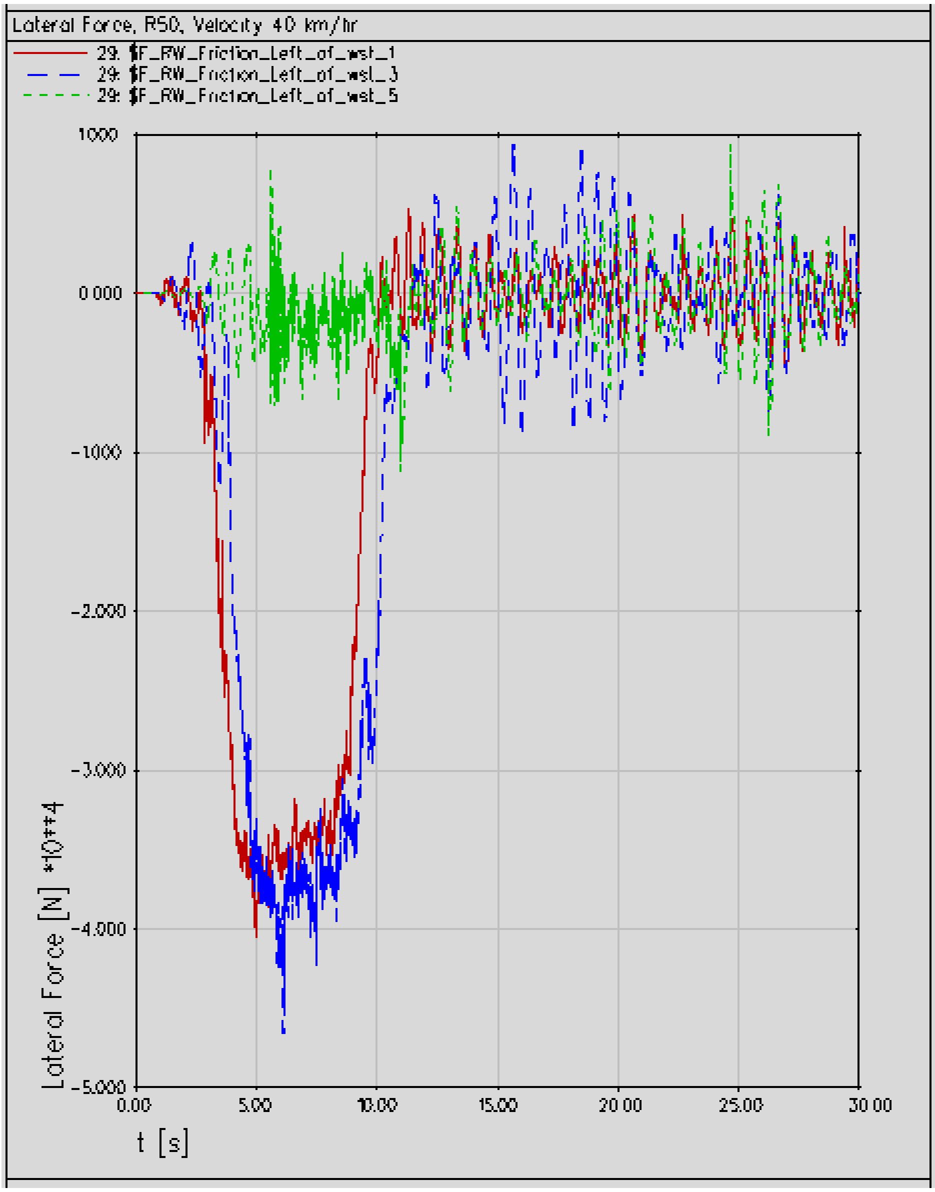

Figure 5.14: Later force on wheelset 1, 3, 5 on curve radius 50 m

5.7.2. Simulation of vehicle on curve radius 100 m

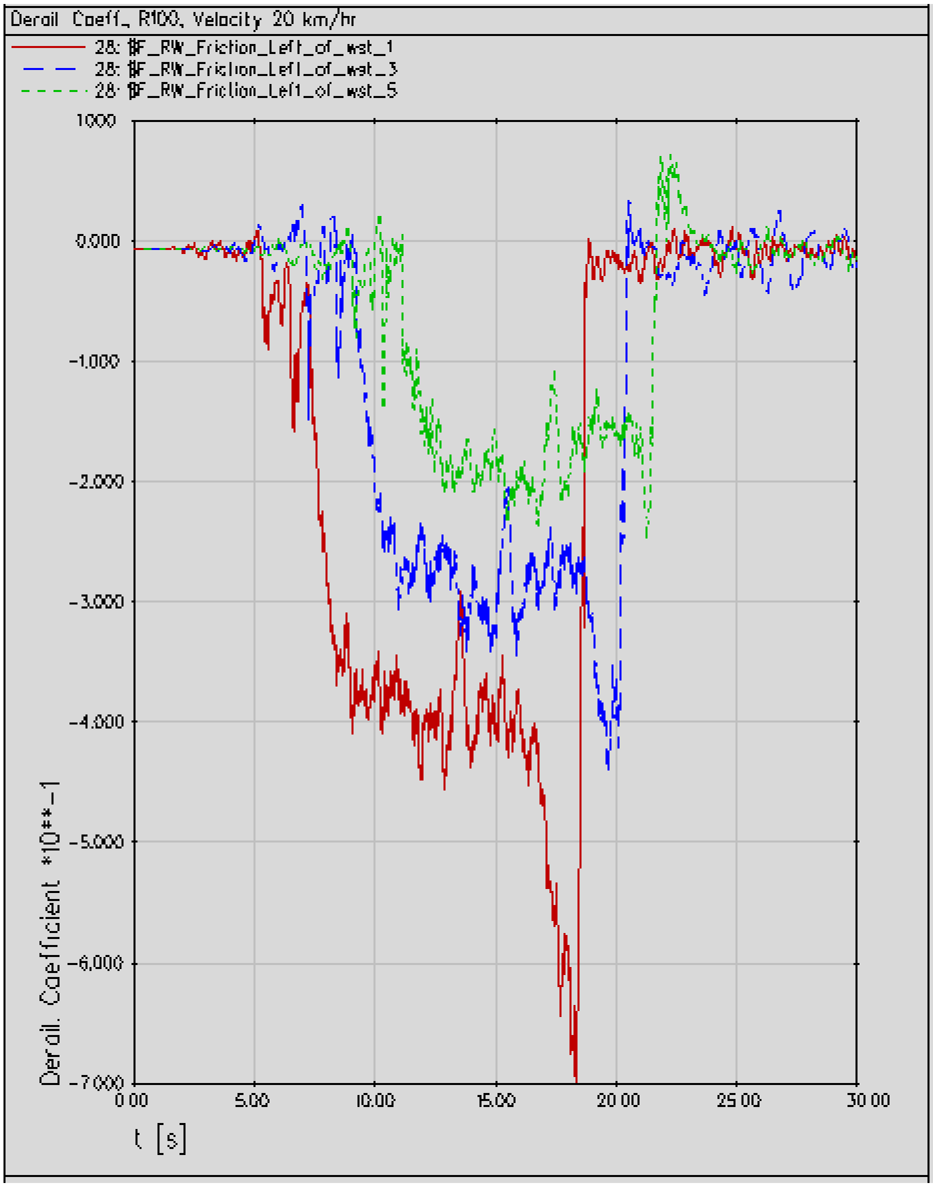

Figure 5.15: Derailment Coefficient of wheelset 1, 3, 5 on curve 100 m

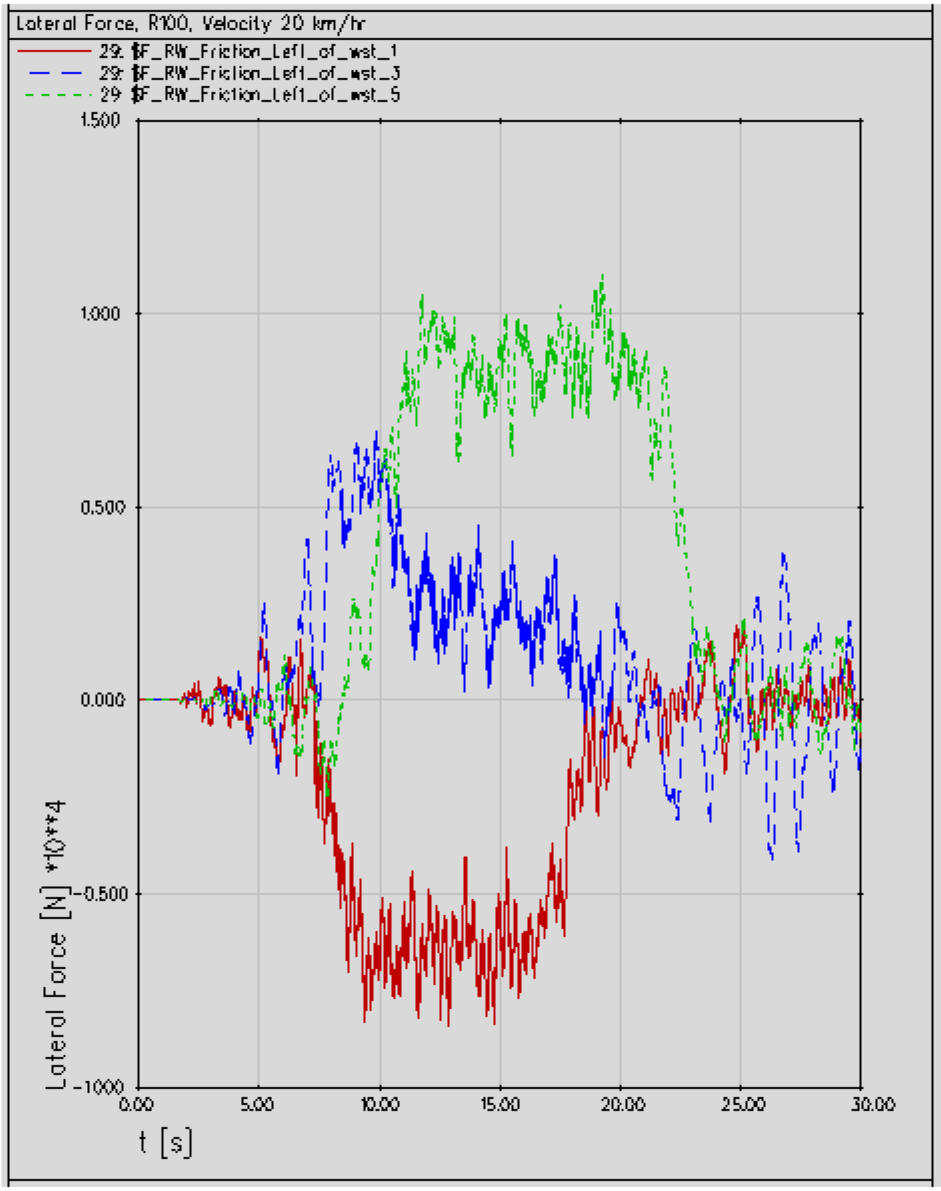

Figure 5.16: Later force on wheelset 1, 3, 5 on curve 100 m

5.8. Dynamic analysis of AALRT vehicle using parameter variation

5.8.1. Introduction

The effects of parameters such as critical speed, coefficient of friction and passenger load are studied in SIMPACK ParVariation option. The mentioned parameters are identified though literature review in Chapter 2, as potential factors that lead to wheel wear. By varying the values of the mentioned parameters, the following variables such as longitudinal creepage, lateral creepage, longitudinal creep force and lateral creep force are calculated in SIMPACK by performing time integration of the parameter variation. The wear of the wheels is greater on curves of small radius as it is validated from the data analysis of the wheel measurements in Chapter 4, in which vehicles from Kaliti line showed greater wear due to operation through small curve radiuses compared to Ayat line. Therefore, for this case, the simulation is done on minimum curved radius R50 m track of AALRT line with transition track of 15 m. After attaining the results of the simulation, the results are exported into excel and wear index is calculated for each parameter according to British Rail; $W = F_x \cdot \xi + F_y \cdot \eta$ where $\boldsymbol{F_x}$ is the longitudinal creep force; ξ is the longitudinal creepage; $\boldsymbol{F_y}$ is the lateral creep force; $\boldsymbol{\eta}$ is the lateral creepage.

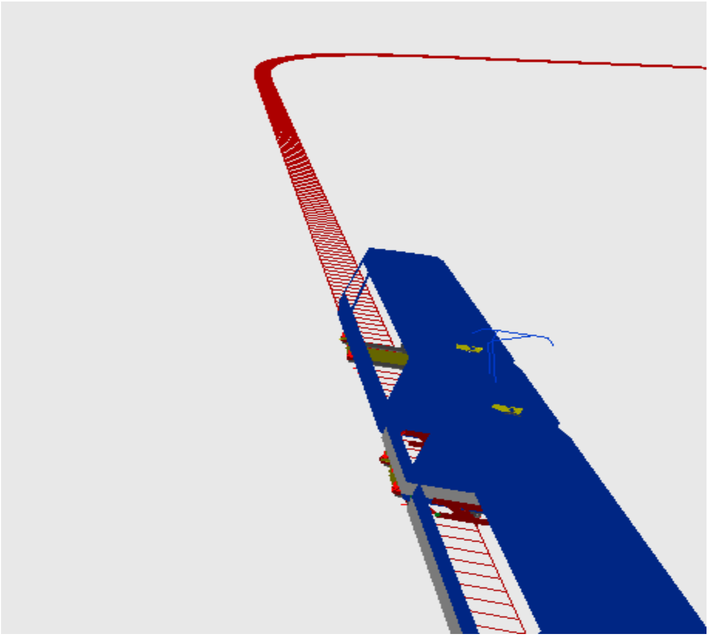

Figure 5.17: AALRT vehicle model curving R50 m track

5.8.2. Effect of critical speed on wear

The effect of critical speed is simulated by varying the critical speed from 10 km/ hr to 40 km/hr with 4 variations of speeds and COF of 0.36. For each speed, the longitudinal creepage, lateral creepage, longitudinal creep force and lateral creep force are obtained from the simulation as shown in Appendix C and then wear index is calculated by exporting the data into excel summarized below in Table 5.3. The following figures 5.18 and 5.19 show the comparison between the parameters of wear index by varying critical speeds. It can be observed that longitudinal creepages are higher at lower critical speeds during curving of the vehicle. In the same way, lateral creepages are also greater at lower critical speeds during curving of the vehicle. It can be said that at lower speeds, higher friction between wheel and rail is evident and thus higher longitudinal creepage and lateral creepage when curving. Higher longitudinal and lateral creep forces are resulted at higher critical speeds and thus this can foretell increased wear risk.

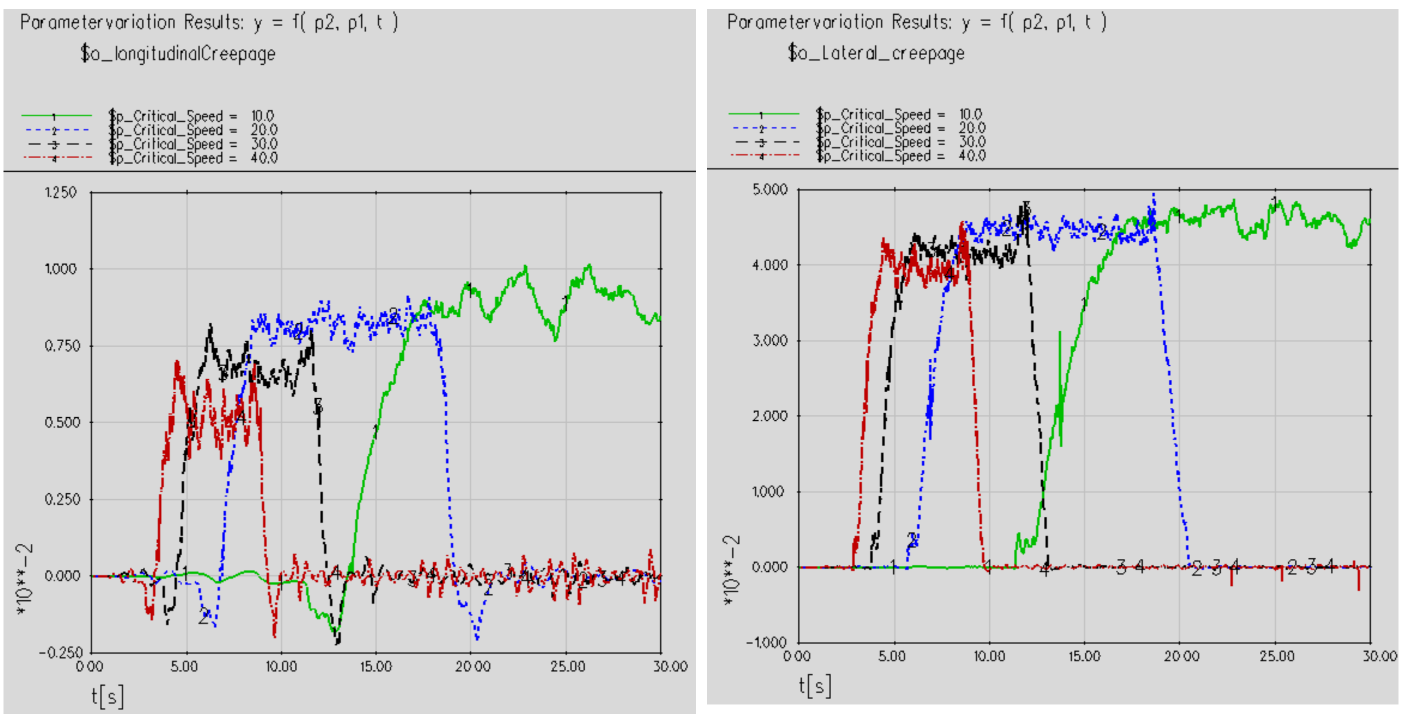

Figure 5.18: Longitudinal and lateral creepages for different critical speeds

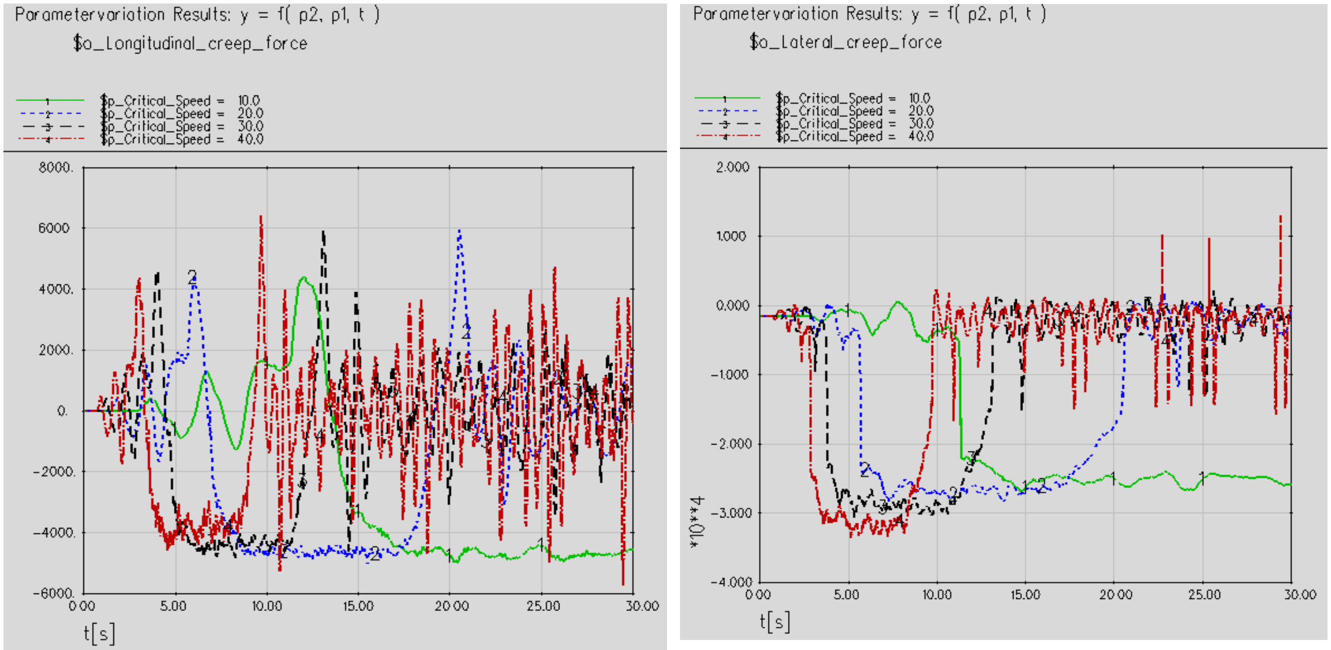

Figure 5.19: Longitudinal and lateral creep forces for different critical speeds

Table 5.3: Wear index for varying critical speeds

Time (s)	**Wear Index**			
	For V_10 km/hr	*For V_20 km/hr*	*For V_30 km/hr*	*For V_40 km/hr*
0	0.00	0.00	0.00	0.00
3	0.01	0.028	0.28	77.76
6	0.15	89.84	1267.20	1303.78
9	0.15	1240.14	1281.33	840.71
12	74.90	1234.31	1021.50	0.12
15	938.53	1232.72	1.48	1.13
18	1182.44	1048.48	0.024	0.05
21	1223.42	0.80	0.03	0.66
24	1246.80	0.45	0.31	0.05
27	1170.62	0.03	0.30	0.83
30	1233.69	0.19	0.05	0.02

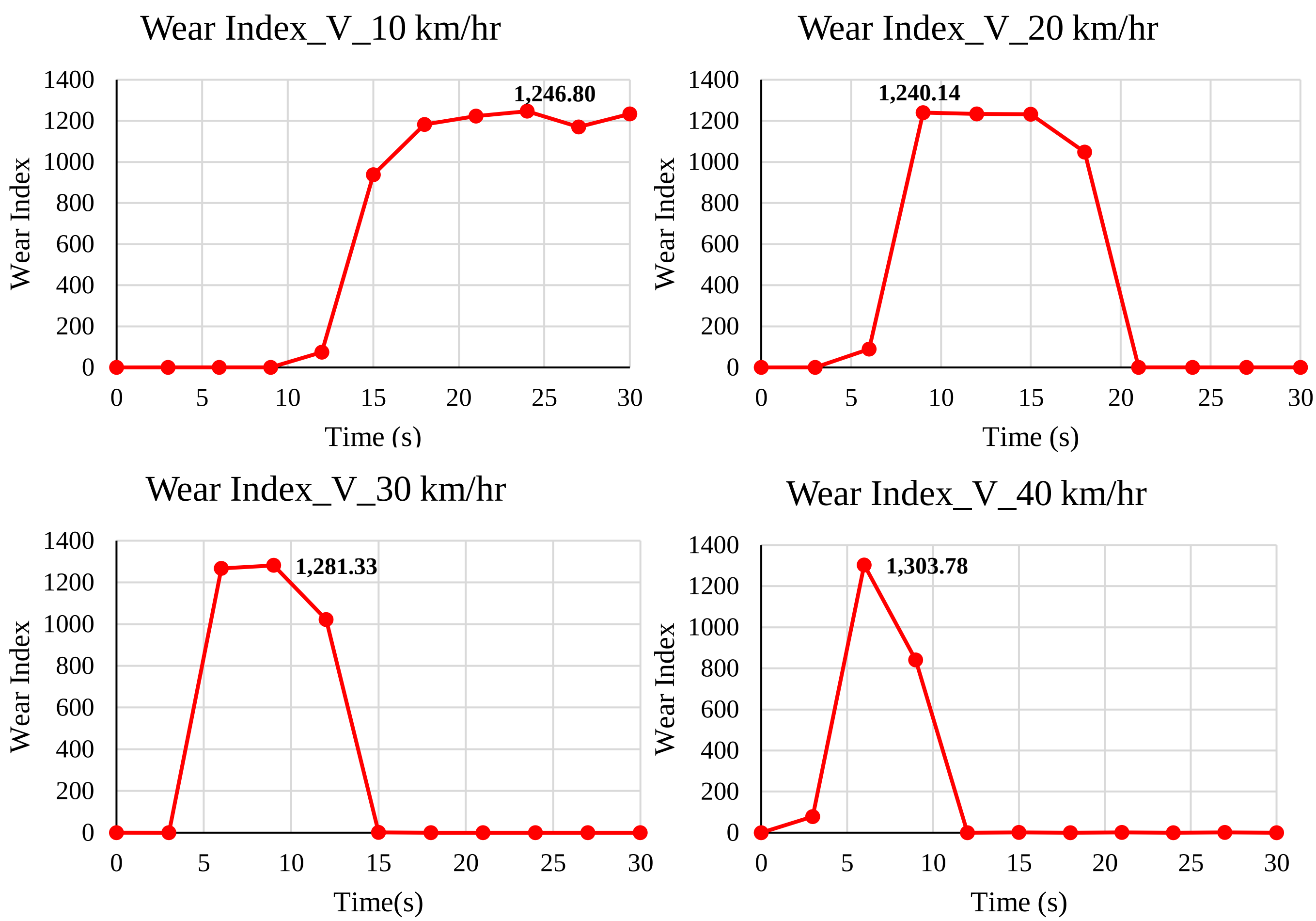

Figure 5.20: Wear index comparison for different critical speeds

The wear index is calculated as shown in Table 5.3 for the different critical speeds simulated in curving of 50 m track radius. The above figure 5.20 shows the wear index calculated for the different critical speeds. The highest wear index of 1303.78 is resulted for critical speed of 40 km/hr and the lowest wear index of 1240.14 is obtained at the critical speed of 20 km/hr. It can be generalized that critical speed has a great influence on the wear of wheels when curving and it can be considered as one of the critical factor in influencing wheel wear based on existing track infrastructure.

5.8.3. Effect of coefficient of friction on wear

The effect of coefficient of friction is simulated by varying coefficient of friction from 0.25 to 0.55 with variations 0.25, 0.35, 0.40 and 0.45. For each coefficient frictions, the longitudinal creepage, lateral creepage, longitudinal creep force and lateral creep force are obtained from the simulation and can be seen in Appendix D. The wear index is calculated by exporting the data into excel as summarized below in Table 5.4 using results of simulation. The following figures 5.21 and 5.22 show the comparison between the parameters of wear index by varying coefficient of frictions. Higher longitudinal and lateral creepages are evident at higher coefficient of friction during curving of the vehicle. It can be said that at lower coefficient of frictions, lower friction between wheel and rail is evident and thus lower longitudinal and lateral creepages when the vehicle is curving as shown in Figure 5.21. Figure 5.22 shows higher longitudinal and lateral creep forces are resulted at higher coefficient of friction during curving of vehicle.

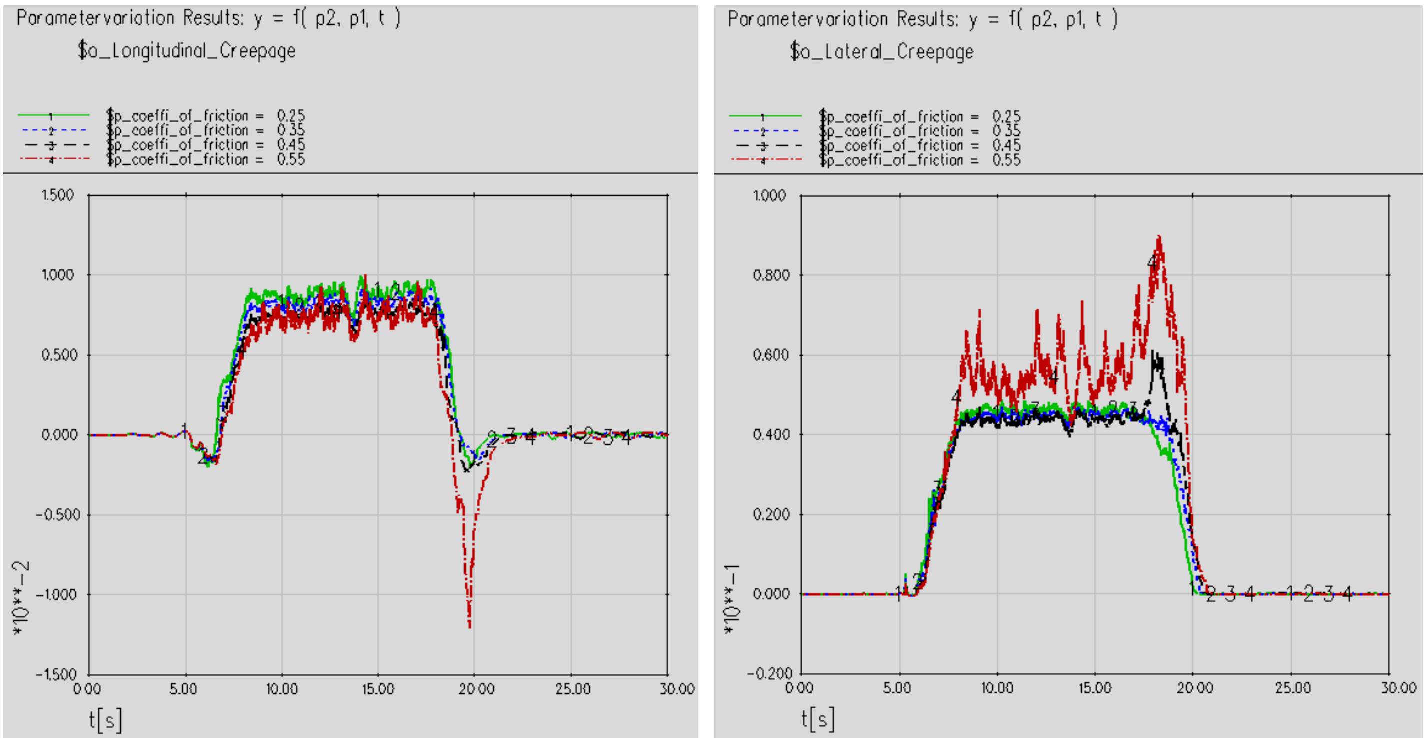

Figure 5.21: Longitudinal and lateral creepage for different coefficient of frictions (COFs)

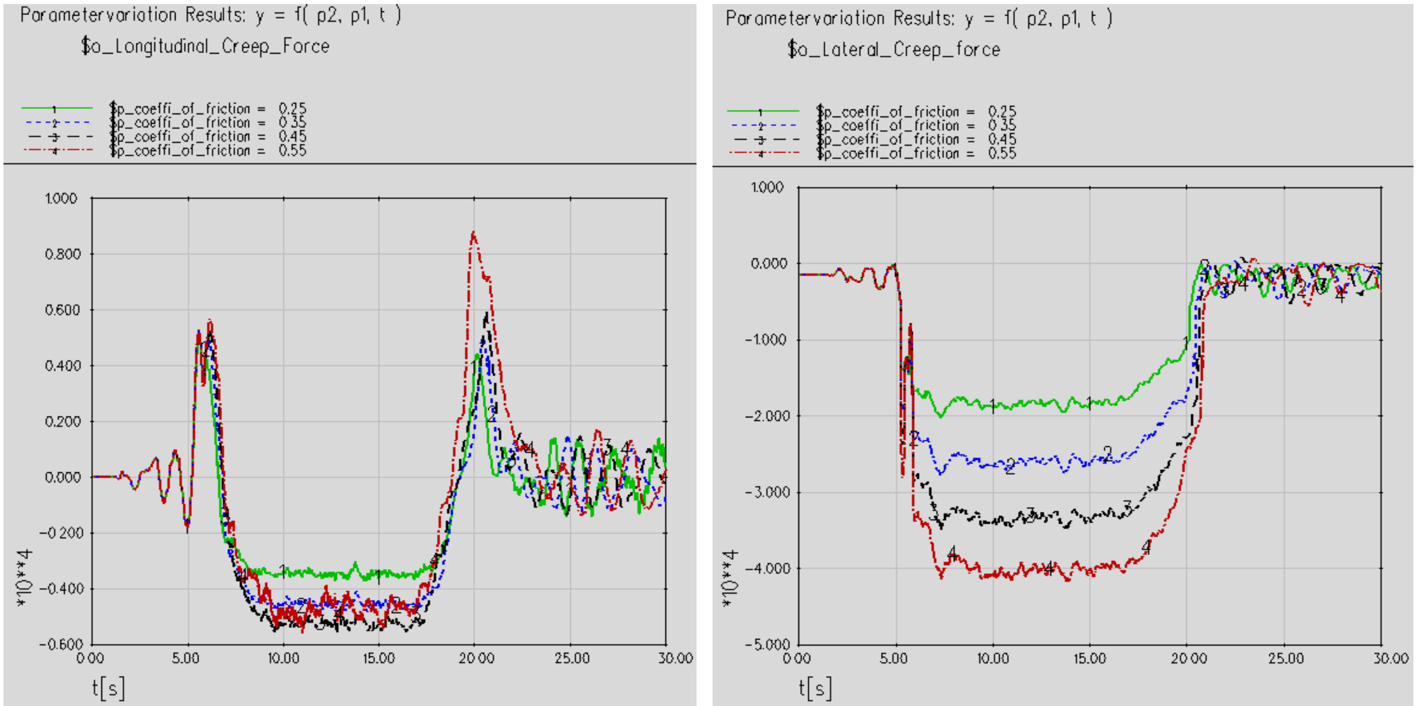

Figure 5.22: Longitudinal and lateral creep forces for different coefficient of frictions (COFs)

Table 5.4: Wear index for varying coefficient of friction

Time (s)	**Wear Index**			
	For COF_0.25	*For COF_0.35*	*For COF_0.45*	*For COF_0.55*
0.00	0.00	0.00	0.00	0.00
3.00	0.04	0.04	0.05	0.05
6.00	75.67	78.01	77.36	73.24
9.00	864.04	1173.63	1512.67	2599.52
12.00	868.48	1195.54	1545.93	2914.90
15.00	888.44	1233.78	1526.19	2094.17
18.00	660.22	1028.63	1710.32	3136.33
21.00	0.10	0.67	2.02	5.37
24.00	0.92	0.20	0.10	0.03
27.00	0.27	0.19	0.23	0.06
30.00	0.02	0.18	0.01	0.31

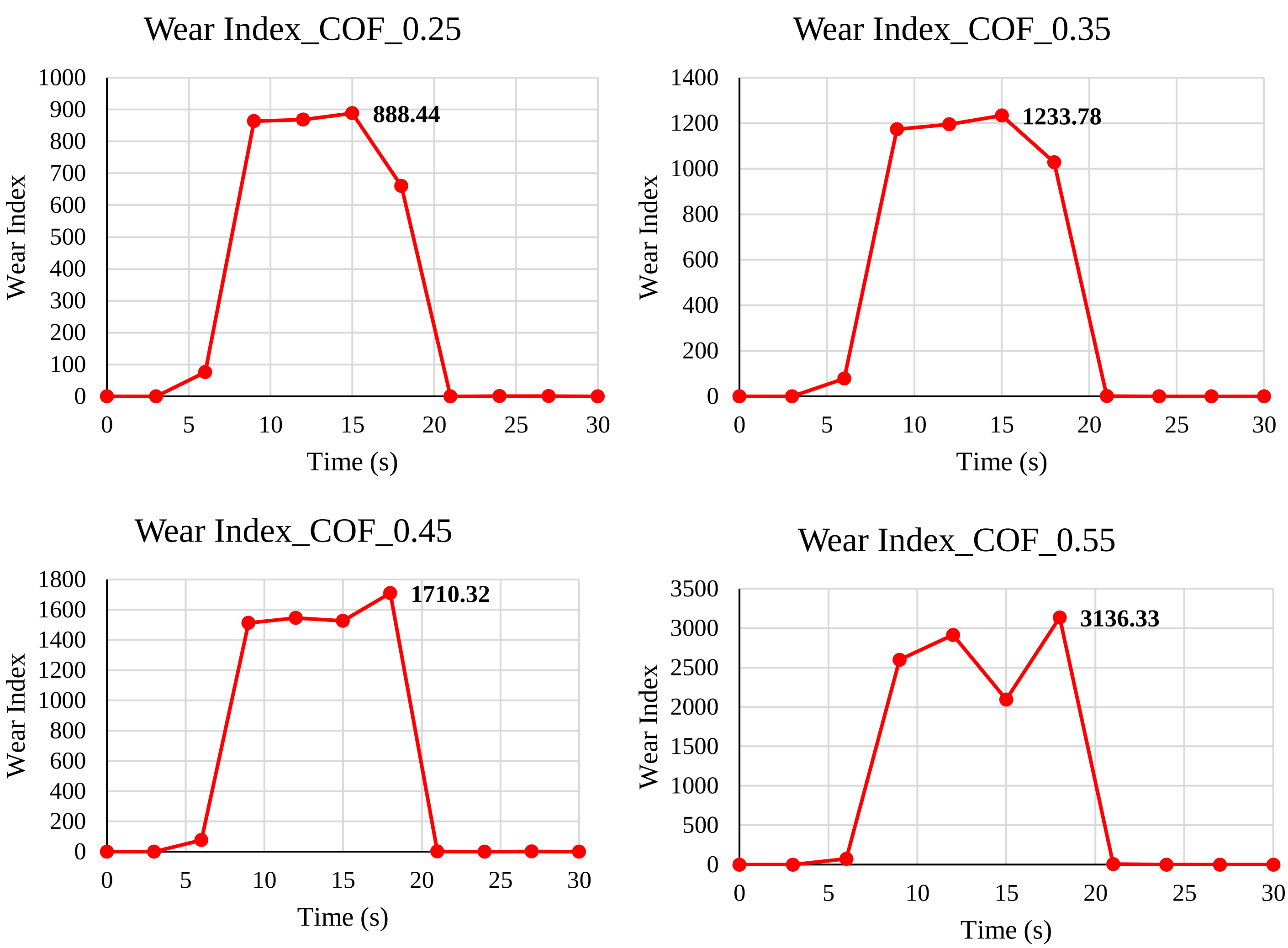

Figure 5.23: Wear index for different coefficient of friction (COF)

The wear index is calculated as shown in Table 5.4 for the different coefficient of frictions simulated in curving of 50 m track radius. The above figure 5.23 shows the wear index calculated for the different coefficient of frictions. The highest wear index of 3136.33 is resulted for coefficient of friction value of 0.55 and the lowest wear index of 888.44 is obtained at the lowest coefficient value of 0.25. It can be generalized that coefficient of friction is a very important factor in wheel/rail interaction and it is a critical factor in influencing wheel wear. Operation of AALRT vehicles is mostly of dry condition and this causes greater wear of the wheels.

5.5.4. Effect of load on wear

The effect of load is simulated by varying the load from empty to overload with operational speed of 20 km/hr while curving a 50m radius track. For each load, longitudinal creepage, lateral creepage, longitudinal creep force and lateral creep force are obtained from the SIMPACK simulation, as shown in Appendix E and then wear index is computed by exporting the results in Excel as shown in Table 5.5. As observed in figure 5.24, longitudinal and lateral creepages are higher with increase in load particularly during curving of the vehicle. In the same way, as observed in figure 5.25, significant increase in longitudinal and lateral creep forces as load of the vehicle increases; evidently when the vehicle is curving.

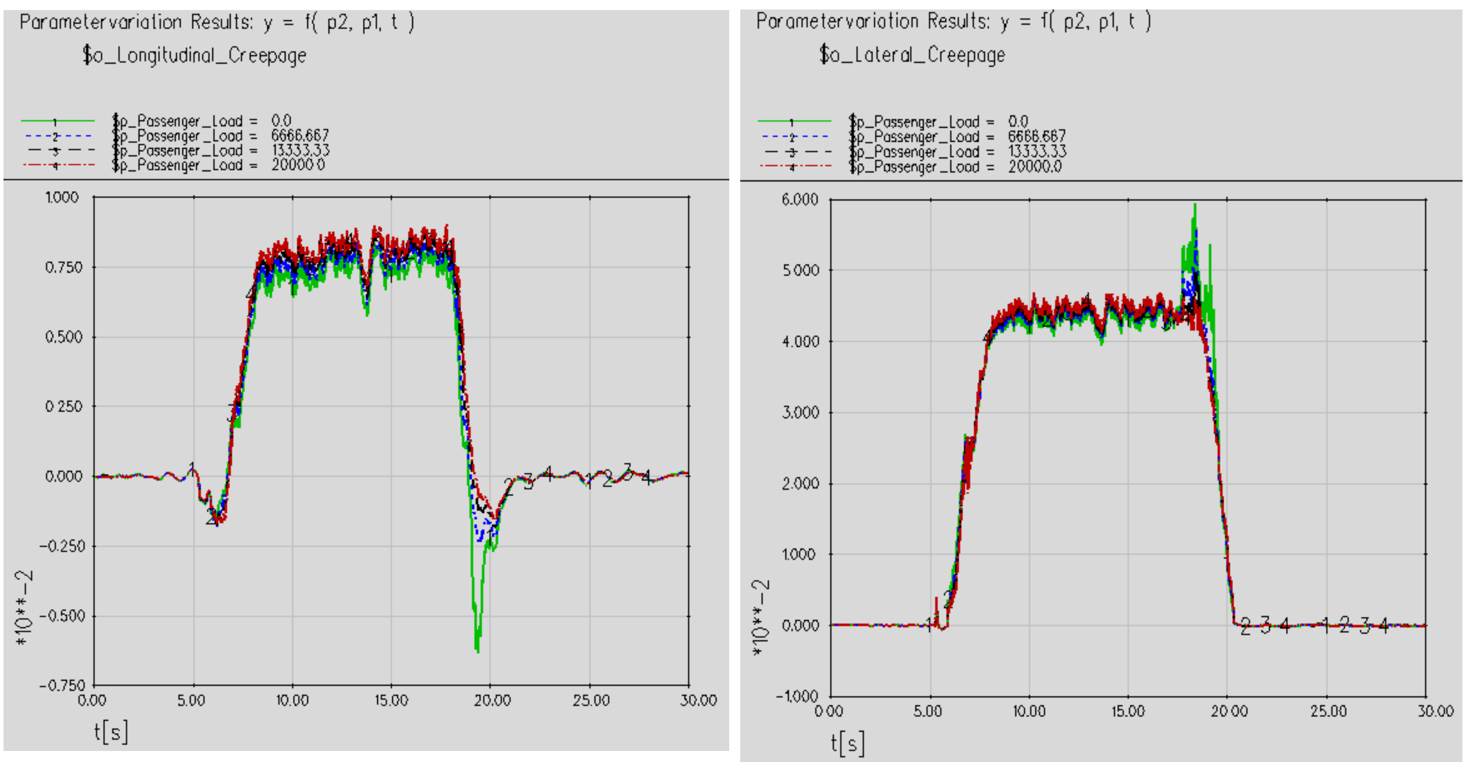

Figure 5.24: Longitudinal and lateral creepages for 4 different loads

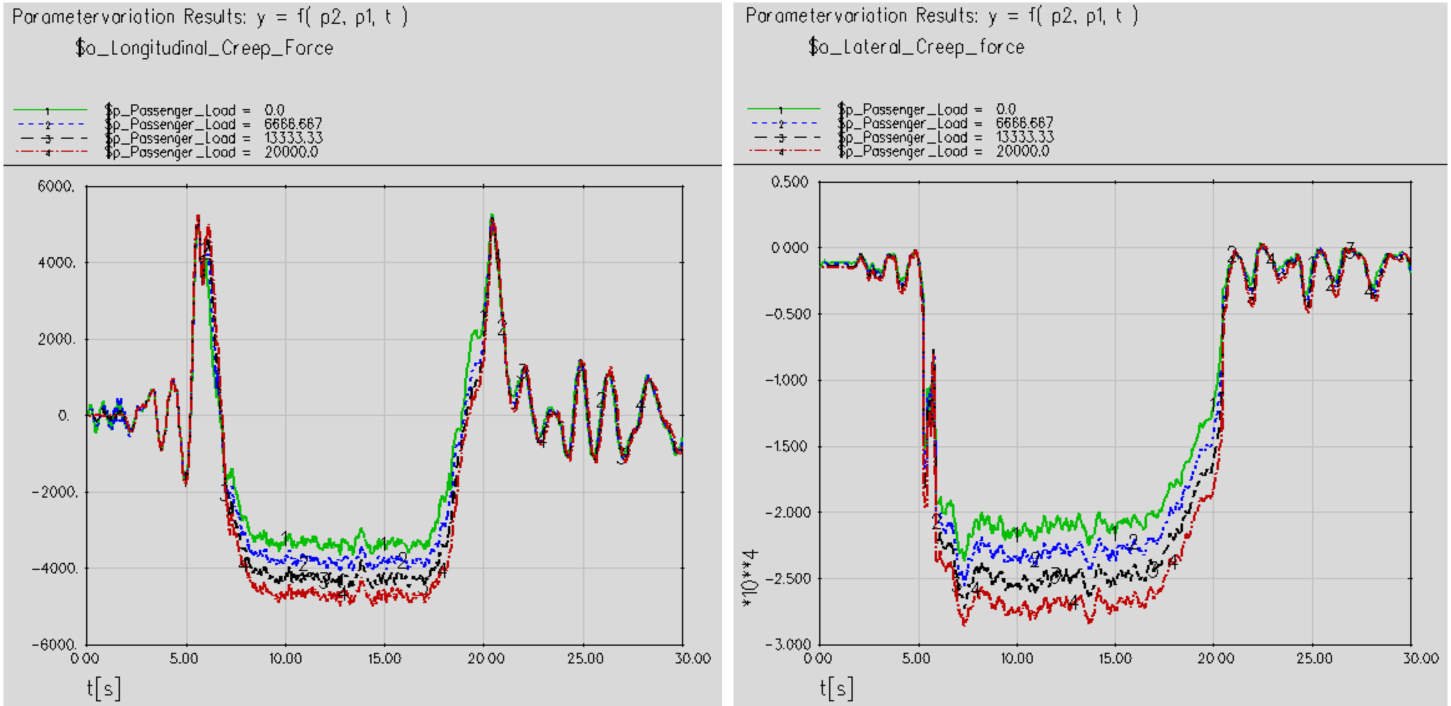

Figure 5.25: Longitudinal and lateral creep forces for 4 different loads

Table 5.5: Wear index of varying loads

Time (s)	Wear Index			
	For Load_0	*For Load_6.67 tons*	*For Load_13.3 tons*	*For Load_20 tons*
0.00	0.00	0.00	0.00	0.00
3.00	0.05	0.04	0.05	0.04
6.00	94.29	84.17	80.77	77.69
9.00	944.58	1019.81	1117.40	1220.32
12.00	919.63	1025.64	1128.36	1238.16
15.00	952.20	1070.39	1166.18	1278.63
18.00	977.07	997.65	1025.44	1075.75
21.00	0.97	0.87	0.83	0.78
24.00	0.16	0.15	0.12	0.20
27.00	0.21	0.20	0.16	0.15
30.00	0.25	0.21	0.13	0.09

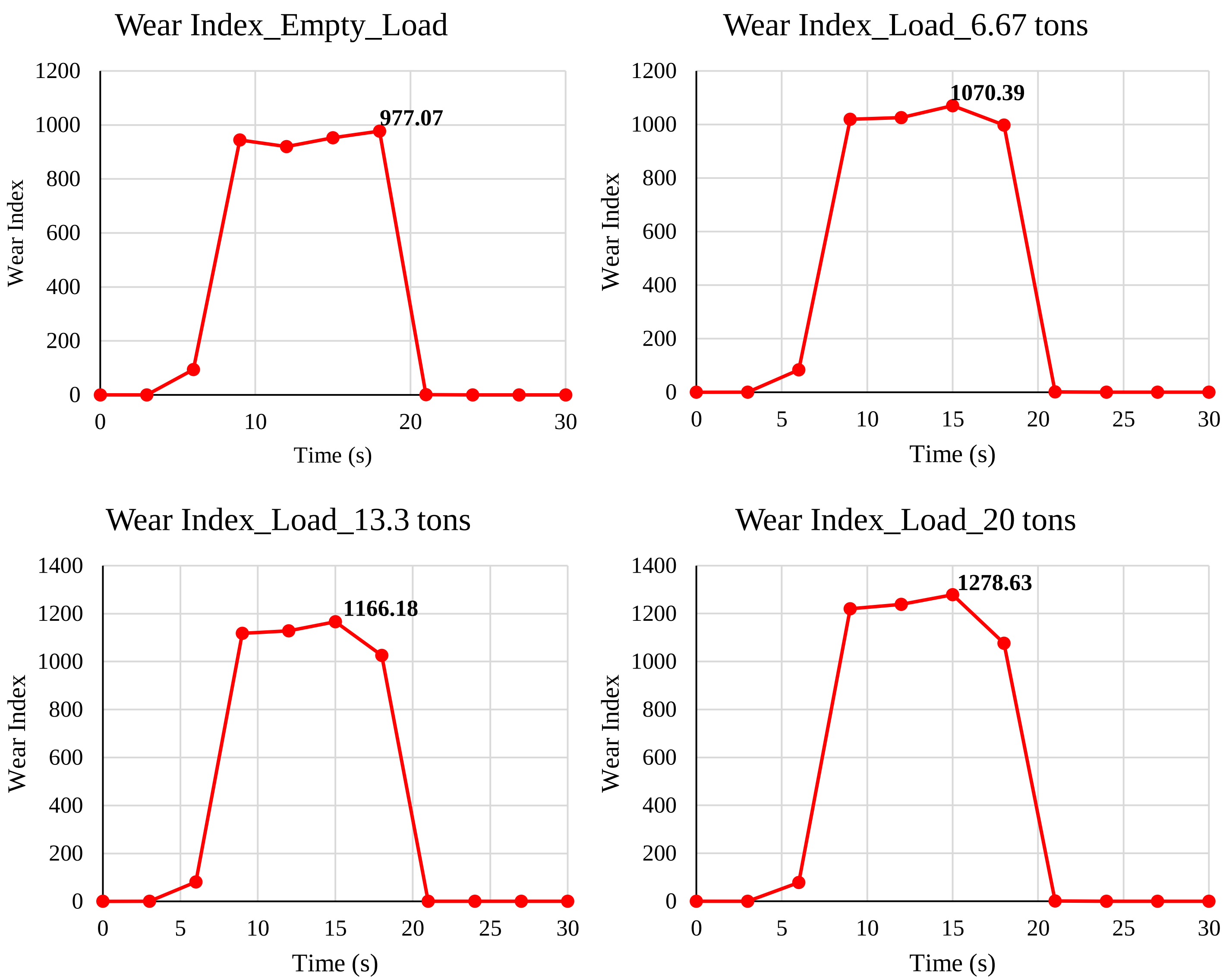

Figure 5.26: Wear index for varying loads

The wear index is calculated as shown in Table 5.5 for the loads simulated in curving of 50 m track radius. The above figure 5.26 shows the wear index calculated for the different loads. The highest wear index of 1278.63 is resulted for overload of 20 tons and the lowest wear index of 977.07 is obtained at empty load of the vehicle. It can be said that load can highly affect the wear particularly the effect is greater when the vehicle is curving sharper tracks.

5.9. Summary of results from simulation of AALRT vehicle using SIMPACK

a. Sharper curves showed that they cause higher lateral force and which in turn increase derailment of coefficient and decreased ride comfort.

b. Effect of critical speed on wear is studied and showed that increase in critical speed led to higher wear index. Increased speed at curves leads to derailment and increased risk of wear wheel based on existing track infrastructure of AALRT.

c. Effect of coefficient of friction is high in the wearing of wheels. Increasing coefficient of friction leads to higher lateral force and thus higher wear index. 4 stages of coefficient of frictions 0.25, 0.35, 0.45, and 0.55 are simulated and their effects on wear index are compared. The lowest coefficient of friction, 0.25, resulted in the lowest wear index of 888.44. The highest wear index of 3136.33 is attained for COF of 0.55. It should be noted that AALRT is operating in dry condition of COF 0.36 of which the wear index simulation result is 1240.14.

d. Effect of load is very much visible as shown in the results of the simulation. Based on existing infrastructure, overload conditions are risky for the wheel wear conditions. Overload conditions would increase wheel wear with adverse condition of the current infrastructure, which holds true for the case of sharp curves observed in the North-South line.

CHAPTER SIX

6. Conclusion, Recommendations and Future work

6.1. Conclusion

Over all, factors which led to wheel wear at AALRT are triangulated based on results from site inspections/experts, actual wheel data measurements and dynamic analysis of AALRT vehicle. Based on the inspections and wheel data analysis work undertaken for this investigation causes of the wheel wear of AALRT vehicles can be considered as the combination of issues related to inadequate friction management and poor track infrastructure. The tight curves at AALRT, mainly in the North-South line, contribute to high flange wear. Inadequate friction management at AALRT, in which lack of rolling stock solid lubricant and inadequate manual based track lubrication on the rail, have led to undesired wear due higher friction between wheel and rail. From simulation results, it is concluded that critical speed of vehicle has great influence on wheel wear. Higher critical speed leads to higher wear index on the existing track infrastructure. In addition, higher coefficient of friction between the wheel and rail causes higher wear index. It is also evident that based on existing track infrastructure, higher loading causes higher wear index.

6.2. Recommendations

The causes of wheel wear at AALRT are identified and the following options are recommended to reduce wheel (and rail) wear to prolong service time of AALRT vehicles' wheels. The recommendations given below are based on results of investigation in this research.

i. Friction Management

- The use of a suitable type of lubrication should be investigated and better method of application of lubrication should be taken into consideration.
- With improved conditions of wheel/rail contact, it can be observed that with the same curving speed of 20 km/hr of simulation with COF 0.36 and COF 0.25, the later resulted in lower wear index of 888.44 while the COF 0.36 resulted a wear index of 1240.14 for the case of AALRT. Therefore, the use of effective application and better lubricant is recommended.

- Method of improving wheel/rail contact should be considered i.e. rail grinding mechanisms and smoothening of the wheels to decrease roughness and thus, better contact between the components.

ii. Improved Wheel and Rail Material

The wear performance of wheel material that AALRT vehicles are using is not satisfactory as reflected by AALRT wheel measurement data examined in this investigation. Therefore, it must be pointed out that the use of material grades which provide better wear resistance should be investigated and applied with compliance of operational conditions of vehicles.

iii. Revise Track Alignment

The easing of sharp curves especially along the North-South route would reduce wear, even though such measures may come costly.

iv. Improved workshop facilities

Most of the maintenance activities carried out at AALRT are of preventive and corrective maintenances but lack of important vehicle testing is witnessed. Dynamic testing and simulation of vehicles should be considered in the future so that the interaction between wheel and rail can be well identified and corrective measures can be taken easily before risking severe wear. Of course, it may become costly as it needs trained human resources and huge facility area.

6.3. Future work

- The effect of bogie components such as primary, secondary suspension, longitudinal/lateral suspension dampers on wheel wear of AALRT vehicles should be investigated further with the use of multi-body simulation software such as SIMPACK.
- Further investigation into material composition and characteristics of AALRT vehicles' wheels and rails should be carried out and their compatibility with operational and environmental condition.
- The effect of track irregularities on wear should also be carried out further.
- The suitability of rail cant and track gauge standards that AART is using in compliance with current operation conditions of the environment, loading cycle, and vehicle speed.
- The suitability of wheel and rail profiles is not investigated in this work and therefore profile compatibility should also be looked at for further investigation.

References

[1] I. Dincer et al., *Clean Rail Transportation Options*, Green Energy and Technology, DOI 10.1007/978-3-319-21726-0_2, Springer International Publishing Switzerland 2016

[2] Carl D. Martland, *Railroad Transportation*, Massachusetts Institute of Technology, Cambridge, Massachusetts, USA, Transportation Engineering and Planning – Vol. I

[3] http://www.trainweb.org/oldtimetrains/industrial/steam/other/QNSP_86.jpg

[4] http://upload.wikimedia.org/wikipedia/commons/thumb/3/31/Shinkansen_500_Kyoto_2005-03-19.jpg/529px-Shinkansen_500_Kyoto_2005-03-19.jpg

[5] Dr. Richard Pankhurst, *The Franco-Ethiopian Railway and Its History*, August 31, 2005

[6] https://en.wikipedia.org/wiki/Rail_transport_in_Ethiopia

[7] http://semonegna.com/wp-content/uploads/2016/12/AALRT-Addis-Ababa.jpg

[8] "Ethiopia-Djibouti electric railway line opens". BBC News. 5 October 2016. Accessed 25 January 2017.

[9] http://www.erc.gov.et/index.php/projects/national-railway-network-of-ethiopianrne.html

[10] "Foundation stone laid for northern Ethiopia line". Railway Gazette. 25 February 2015. Accessed 26 January 2017.

[11] Muluken Yewondwossen (April 30, 2014), "Swiss bank approves $865 mln loan for Awash-Weldiya railway project". Accessed 26 January 2017.

[12] Molinari, Michele (June 3, 2015). "Ethiopia turns big plans into reality". International Railway Journal. Accessed on 21 January 2017. IAVSD in 2013. Available at: http://dx.doi.org/10.1080/00423114.2013.800215

[13] "Addis Ababa light rail opens". Railway Gazette International. 2015-09-21.

[14] http://www.railway-technology.com/features/featureimproved-access-for-ethiopia-opening-the-addis-ababa-djibouti-line-4836968/

[15] J.A. Williams, *Wear modelling, analytical, computing and mapping: a continuum mechanics approach.* Wear, 225–229 (1999) pp. 1–17.

[16] U. Olofsson, S. Andersson, and S. Björklund, *Simulation of mild wear in boundary lubricated spherical roller thrust bearings.* Wear 241 (200) pp. 180–185.

[17] J.L. Sullivan, *Boundary lubrication and oxidational wear.* Journal of Physics & Applied Physics. 19 (1986) pp. 1999–2011.

[18] U. Olofsson and G. Svedberg, *Low concentration level contaminant-related wear in sliding and rolling contacts*, 2nd World Tribology Congress Vienna Sept. 03-07 2001.

[19] Ulf Olofsson and Yi Zhu, Tribology of the wheel-rail contact – aspects of wear, particle emission and adhesion, Vehicle System Dynamics; Special Issue: State of Art Papers of the 23rd.

[20] A.Bevan, S.Iwnicki, Review of wheel turning data and identification of other wheel damage modes, T792 Report, RSSB, 2010.

[21] A.Innocenti, L.Marini, E.Meli*, G.Pallini, A.Rindi, *Development of a wear model for the analysis of complex railway networks*, November 2013.

[22] Pombo, J., Ambrosio, J., Pereira, M., Lewis, R., Dwyer-Joyce, R., Ariaudo, C., Kuka, N. (2010) *Study on the service conditions that influence the wear evolution on railway wheels*, http://eprints.whiterose.ac.uk/42643

[23] L. Mazzola†, S. Alfi and S. Bruni, *A Method to Optimize Stability and Wheel Wear in Railway Bogies*, IJR International Journal of Railway Vol. 3, No. 3 / September 2010, pp. 95-105.

[24] Na Wu andJing Zeng, *Parametric analysis of wheel wear in high-speed vehicles*, J. Mod. Transport. (2014) 22(2):76–83, DOI 10.1007/s40534-014-0053-z.

[25] Majid Elyasi *, Milad Hadinezhad, Mohammad Rajabi, Majid Abbasi**,** *Study on Influence of Effective Parameters on Wear Behavior of Wheel and Rails through ADAMS-RAIL Software*, Manufacturing Science and Technology 3(5): 308-315, 2015, DOI: 10.13189/mst.2015.030518, http://www.hrpub.org

[26] J. Nielsen, R. Lundén, A. Johansson and T. Vernersson, "Train-Track Interaction and Mechanisms of Irregular Wear on Wheel and Rail Sur-faces," *Vehicle System Dy-namics*, Vol. 40, No. 1, 2003, pp. 3-54. doi:10.1076/vesd.40.1.3.15874

[27] H. Hur, J. Park, W. You and T. Park, "A Study on the Critical Speed of Worn Wheel Profile Using a Scale Model," *Journal of Mechanical Science and Technology*, Vol. 23, No. 10, 2009, pp. 2790-2800. doi:10.1007/s12206-009-0732-6

[28] R. Fröhling, "Analysis of Asymmetric Wheel Profile Wear and Its Consequences," *Vehicle System Dynamics*, Vol. 44, No. 1, 2006, pp. 590-600. doi:10.1080/00423110600879296

[29] H. Wu, "Effects of Wheel and Rail Profiles on Vehicle Performance," *Vehicle System Dynamics*, Vol. 44, No. 1, 2006, pp. 541-550. doi:10.1080/00423110600875393

[30] S. Fergusson, R. Fröhling and H. Klopper, "Minimising Wheel Wear by Optimising the Primary Suspension Stiffness and Centre Plate Friction of Self-Steering Bogies," *Vehicle System Dynamics,* Vol. 46, No. 1, 2008, pp. 457-468. doi:10.1080/00423110801993094

[31] Christopher W. Jenks *"Center Truck Performance on Low-Floor Light Rail Vehicles*", 2006, http://nap.edu/14000, ISBN 978-0-309-09863-2 | DOI 10.17226/14000

[32] Osamu Kondu*, Yousuke Yamazaki "Simulation Technology of Railway vehicle dynamics" Nippon Steel and Sumitomo Metal Technical Report No. 105 December 2013

[33] Door Ivan Yevhenovich SHEVTSOV, mechanical engineer - researcher, Dnipropetrovsk State University "Wheel/Rail Interface Optimization", June 2008

APPENDICES

Appendix A: Interview Questions

Name:

Job Description:

1. How serious is the problem of wheel wear at AALRT?
2. What are the adverse conditions that may have led to wheel wear at AALRT?
3. Which type of wheel wear is serious for the case of AALRT vehicles?
4. What are the maintenances carried out on the wheels and rails at AALRT?
5. When are the wheels taken to lathe machining?
6. What facilities are available for testing performance of vehicles?
7. What are the types of maintenance carried out at AALRT workshops?
8. Are there problems related to friction management such as application of lubrication? If so, what are they?
9. What are the challenges faced due to wearing of the wheels?
10. What is the standard wear rate of the wheels?
11. How long were the wheels expected to service before they are worn completely?
12. What are the quality grades of wheel and rail that AALRT is using?
13. How suitable is the depot track infrastructure?
14. What are the existing problems related to the vehicles?

Appendix B: Wheel data measurements of AALRT vehicles

					pre-measurement					post-measurement						
No.	Date	mileage	vehicle No.	wheelset No.	diameter difference	diameter		flange thickness		diameter difference	diameter		flange thickness		total re-profiled wheelset	remark
						left	right	left	right		left	right	left	right		
1	3-9/2/2016	4888	104	1	0.08	660.66	660.58	23.25	23.26	-	-	-	-	-		burn on wheel thread
				2	0.1	660.54	660.64	23.18	23.3	-	-	-	-	-		
				3	0.67	659.87	660.55	22.4	22.97	1.77	**650.17**	**651.94**	19.75	19.96	1	
				4	0.21	660.45	660.66	22.95	22.51	0.06	**652.53**	**652.59**	20.6	21.03	2	
				5	0.15	660.48	660.63	23.07	23.19	-	-	-	-	-		
				6	0.06	660.47	660.53	23.53	23.36	-	-	-	-	-		
2	15-18/03/2016	6065	104	1	0.14	660.63	660.49	23.27	23.13	-	-	-	-	-		burn on wheel thread
				2	0.04	660.51	660.55	22.95	23.25	-	-	-	-	-		
				3	0.76	651.06	651.82	19.62	19.74	1.36	**649.92**	**651.28**	19.58	19.75	3	
				4	0.01	652.48	652.46	20.27	20.79	0.16	**651.36**	**651.2**	20.21	20.05	4	
				5	0.13	660.46	660.6	23.19	23.34	-	-	-	-	-		
				6	0.22	660.51	660.29	23.4	23.15	-	-	-	-	-		
3	25/03/2016 to 11/04/2016	30478	119	1	0.1	660	659.9	20.24	21	-	-	-	-	-		scratch on wheel thread
				2	0.15	659.94	660.1	20.82	20.81	-	-	-	-	-		
				3	0.01	660.36	660.37	19.77	20.4	0.3	**655.15**	**655.45**	22.28	22.3	5	
				4	0.49	660.79	660.29	20.18	19.45	0.39	**656.82**	**656.43**	19.65	19.71	6	
				5	0.08	660.13	660.05	20.75	20.62	-	-	-	-	-		
				6	0.09	660.13	660.03	21.08	20.83	-	-	-	-	-		
4	7-8/5/2016	no	213	1	0.53	659.07	659.6	16.74	17.04	0.01	**639.73**	**639.73**	19.88	19.86	7	wheel flange thickness
				2	0.84	659.34	658.5	17.5	14.61	0.16	**635.17**	**635.01**	19.41	19.57	8	
				3	-	-	-	-	-	-	-	-	-	-		
				4	-	-	-	-	-	-	-	-	-	-		
				5	0.1	659.69	659.79	15.7	17.56	-	-	-	-	-		
				6	0.35	659.54	659.19	17.77	15.49	-	-	-	-	-		
5	8-10/6/2016	26848	211	1	0.14	659.87	660.01	19.11	19.42	-	-	-	-	-		wheel flange thickness
				2	0.32	659.97	659.65	17.89	18.32	-	-	-	-	-		
				3	0.61	651.4	652.01	19.09	18.98	0.01	**640**	**639.99**	18.87	18.31	9	
				4	0.71	660.83	660.12	19.09	13.24	0.35	**634.84**	**635.18**	19.52	18.74	10	
				5	0.21	659.93	660.14	19.19	19.35	-	-	-	-	-		
				6	0.11	659.91	660.03	19.46	17.03	-	-	-	-	-		
6	11-12/6/2016	56447	209	1	0.2	659.18	659.38	15.34	17.24	0.41	**650.82**	**651.23**	17.3	17.3	11	scratch on wheel thread
				2	0.09	659.42	659.33	15.97	15.58	0.04	**650.91**	**650.95**	17.62	17.69	12	
				3	0.16	660.16	660	17.21	17.5	0.11	**648.69**	**648.58**	20.02	20.03		
				4	0.08	659.8	659.88	15.28	16.31	0.14	**648.47**	**648.61**	19.08	18.99		
				5	0.23	659.36	659.59	17.34	17.27	-	-	-	-	-		
				6	0.02	659.28	659.3	16.43	15.18	0.22	**654.08**	**654.3**	17.01	16.85	13	

7	12-14/06/2016	35955	216	1	0.18	659.61	659.79	16.81	17.78	0.4	**649.82**	**650.23**	19.17	19.16	14	
				2	0.07	659.74	659.8	15.25	14.45	0.12	**646.73**	**646.61**	17.94	17.87		
				3	0	660.32	660.32	18.13	17.95	-	-	-	-	-		wheel flange thickness
				4	0.07	660.35	660.29	18.5	18.46	-	-	-	-	-		
				5	0.23	659.78	660.01	17.49	16.6	0.17	**648.19**	**648.37**	20.21	19.9	15	
				6	0.02	659.76	659.74	18.28	14.84	0.6	**648.18**	**648.78**	18.58	18.35	16	
8	14-16/6/2016	44026	212	1	0.04	659.66	659.63	16.06	17.5	0.03	**641.17**	**641.14**	19.86	19.7	17	
				2	0.33	659.73	659.4	17.02	13.66	0.07	**638.31**	**638.38**	18.41	18.4	18	
				3	0.01	660.12	660.13	16.49	17.69	0.38	**653.41**	**653.03**	18.42	18.6	19	
				4	0.12	660.09	660.21	17.48	17.62	0.26	**653.65**	**653.39**	19.51	19.53	20	
				5	0.54	659.34	659.88	16.63	19.38	0.05	**653.52**	**653.58**	18.36	18.36	21	
				6	0.06	659.55	659.49	16.41	16.93	0	**653.14**	**653.15**	18.14	18.07	22	
9	17-18/6/2016	6518	107	1	0.25	659.56	659.32	19.92	20.31	-	-	-	-	-		
				2	0.04	659.46	659.51	19.75	19.65	-	-	-	-	-		
				3	0.3	660.1	660.39	18.2	16.09	0.31	**649.78**	**650.09**	18.68	18.87	23	wheel flange thickness
				4	0.32	660.09	660.41	17.95	14.81	0.32	**650.08**	**650.13**	18.03	17.86	24	
				5	0.36	659.73	659.37	19.28	19.51	-	-	-	-	-		
				6	0.07	659.51	659.44	20.08	20.31	-	-	-	-	-		
10	18-21/06/2016	35568	217	1	0.13	656.07	656.19	16.65	17.01	0.16	**652.04**	**652.2**	17.13	17.61	25	
				2	0.06	659.73	659.67	17.61	16.83	0.31	**655.46**	**655.77**	18.27	18.22	26	
				3	0.19	651.07	650.87	18.04	18.45	0.06	**641.08**	**641.14**	19.55	19.86	27	
				4	0.11	645.06	644.95	16.66	16.82	0.05	**640.98**	**641.03**	17.02	17.15	28	
				5	0.21	659.73	659.94	18.32	18.89	-	-	-	-	-		
				6	0.05	659.65	659.7	17.52	16.36	-	-	-	-	-		
11	4-24/06/2016	53109	206	1	0.39	659.05	659.44	16.25	17.22	0.16	**649.24**	**649.4**	18.97	19.38	29	
				2	0.06	659.3	659.24	16.87	15.14	0.16	**648.08**	**648.21**	18.04	18.57	30	
				3	0.29	660.31	660.02	14.01	15.07	0.16	**639.04**	**639.31**	18.56	18.8	31	wheel flange thickness
				4	0.23	660.21	659.98	12.45	14.48	0.16	**637.63**	**637.96**	17.68	17.94	32	
				5	0.21	659.35	659.55	17.35	16.63	0.16	**653.16**	**653.6**	17.9	18.01	33	
				6	0.02	659.44	659.46	15.92	15.36	0.16	**653.2**	**653.42**	17.61	17.91	34	
12	24-26/06/2016	45540	115	1	0.17	659.66	659.49	20.62	19.75	-	-	-	-	-		
				2	0.18	659.83	659.65	20.39	20.28	-	-	-	-	-		
				3	0.41	659.89	660.3	19.2	15.13	0.92	**635.37**	**636.3**	20	20.79	35	wheel flange thickness
				4	0.32	659.94	660.26	19.77	14.08	0.37	**635.29**	**635.66**	19.25	19.38	36	
				5	0.22	659.87	659.65	20.71	20.59	-	-	-	-	-		
				6	0.18	659.6	659.41	20.45	19.91	-	-	-	-	-		
13	27/6-1/7/2016	49030	205	1	0.11	659.42	659.53	16.71	16.54	0.44	**639.66**	**640.09**	20.31	20.09	37	
				2	0.02	659.62	659.64	17.48	13.48	0.47	**637.17**	**637.64**	17.56	17.56	38	
				3	0.04	660.15	660.19	17.38	18.24	-	-	-	-	-		wheel flange thickness
				4	0.08	659.96	660.04	16.38	17.37	-	-	-	-	-		
				5	0.04	659.55	659.59	16.48	16.59	-	-	-	-	-		
				6	0.08	659.61	659.69	17.59	18.51	-	-	-	-	-		

14	3-7/7/2016	54471	218	1	0.3	659.29	659.59	13.7	16.65	0.24	**642.86**	**643.11**	17.65	17.59	39	wheel flange thickness
				2	0.15	659.29	659.44	14.16	13.86	0.32	**643.27**	**642.96**	17.58	17.67	40	
				3	0.01	660.19	660.21	17.08	16.14	0.24	**636.55**	**636.79**	19.55	19.72	41	
				4	0.16	660.08	659.92	14.11	12.83	0.32	**637.96**	**638.28**	17.69	17.78	42	
				5	0.53	659.12	659.65	18.38	18.06	0.03	**647.98**	**647.95**	21.11	20.85	43	
				6	0.41	658.94	659.34	16.02	15.26	0.22	**648.16**	**647.94**	17.83	17.78	44	
15	08-11/07/2016	47312	215	1	0.44	659.56	660	17.07	17.93	0.31	**640.76**	**641.07**	20.97	21.08	45	wheel flange thickness
				2	0.06	659.79	659.73	15.46	13.46	0.1	**642.02**	**642.12**	17.44	17.55	46	
				3	0.09	660.33	660.41	18.05	16.75	0.3	**645.14**	**645.44**	19.71	19.94	47	
				4	0.18	660.1	660.28	17.09	15.45	0.21	**644.17**	**644.38**	18.82	18.81	48	
				5	0.02	659.79	659.81	16.54	16.65	-	-	-	-	-		
				6	0.17	659.79	659.62	16.17	16.03	-	-	-	-	-		
16	13-14/07/2016	22282	207	1	0.19	659.96	660.15	18.63	20.02	0.1	**655.17**	**655.27**	19.59	19.84	49	
				2	0.08	660	659.92	18.48	17.54	0.1	**654.87**	**654.76**	18.91	18.96	50	
				3	0.01	660.32	660.33	19.54	19.36	-	-	-	-	-		
				4	0.06	660.26	660.32	18.13	18.11	-	-	-	-	-		
				5	0.12	659.98	660.1	19.37	18.82	-	-	-	-	-		
				6	0.06	659.94	660	19.06	17.62	-	-	-	-	-		
17	15-27/07/2016	43452	208	1	0.07	659.43	659.5	16.34	17.53	0.29	**637.93**	**638.21**	20.11	20.24	51	wheel flange thickness
				2	0.22	659.56	659.78	13.45	18.34	0.19	**635.4**	**635.21**	17.41	17.75	52	
				3	0.15	660.14	660.29	17.05	15.44	0.1	**640.15**	**640.05**	18.58	18.78	53	
				4	0.06	660.19	660.12	17.28	14.47	0.23	**639.02**	**638.79**	18.3	18.3	54	
				5	0.12	659.67	659.56	18.68	16.96	0.19	**645.95**	**645.76**	19.68	19.82	55	
				6	0.2	659.36	659.55	17.09	15.99	0.07	**645.78**	**645.86**	18.86	18.9	56	
18	17-18/08/2016	45551	114	1	0.12	659.86	659.74	19.6	20.48	-	-	-	-	-		
				2	0.1	659.85	659.95	20.29	20.47	-	-	-	-	-		
				3	0.25	660.3	660.05	18.52	19.71	0.35	**655.78**	**655.43**	18.67	19.38	57	
				4	0.25	660.27	660.02	18.4	19.63	0.58	**655.16**	**655.75**	19.35	19.26	58	
				5	0.09	659.88	659.79	19.68	20.34	-	-	-	-	-		
				6	0.12	659.79	659.67	21.11	19.99	-	-	-	-	-		
19	9-22/08/2016	51662	210	1	0.32	659.02	659.34	16.12	16.36	0.29	**642.73**	**642.44**	18.99	18.99	59	wheel flange thickness
				2	0.24	659.44	659.2	16.3	14.39	0.61	**642.23**	**641.63**	17.75	18.09	60	
				3	0.23	660.06	660.3	15.52	14.21	0.39	**640.74**	**641.13**	17.39	17.46	61	
				4	0.21	650.68	650.89	17.51	17.45	0.05	**642.57**	**642.52**	18.1	18.44	62	
				5	0.2	659.25	659.45	16.4	16.93	0.15	**646.23**	**646.37**	18.02	18.11	63	
				6	0	659.15	659.16	16.38	14.98	0.41	**645.96**	**645.55**	17.27	17.58	64	
20	23-25/08/2016	40415	108	1	0.42	659.94	659.52	20.44	20.4	-	-	-	-	-		
				2	0.03	659.67	659.64	19.94	19.66	-	-	-	-	-		
				3	0.21	660.49	660.28	18.59	17.81	0.65	**654.65**	**655.3**	18.52	18.82	65	
				4	0.13	660.15	660.28	17.9	16.94	0.23	**654.01**	**654.54**	18.54	18.87	66	
				5	0.38	659.94	659.56	19.64	19.67	-	-	-	-	-		
				6	0.37	659.9	659.53	20.05	20.08	-	-	-	-	-		

21	25-30/08/2016	45551	111	1	0.44	659.16	658.73	18.52	18.79	-	-	-	-	-		wheel flange thickness
				2	0.19	**658.93**	**658.74**	18.05	18.59	-	-	-	-	-		
				3	0.53	659.83	660.36	17.14	13.11	0.31	**636.12**	**636.43**	17.94	17.76	67	
				4	0.56	659.73	660.29	17.26	13.04	0.51	**635.31**	**635.82**	17.23	16.99	68	
				5	0.09	659.88	659.79	19.68	20.34	-	-	-	-	-		
				6	0.12	659.79	659.67	21.11	19.99	-	-	-	-	-		
22	05-07/09/2016	54807	110	1	0.22	659.34	659.12	18.71	19.11	-	-	-	-	-		wheel flange thickness
				2	0.23	659.41	659.18	18.86	18.64	-	-	-	-	-		
				3	0.31	659.99	660.31	17.13	14.58	1.1	**637.47**	**636.36**	18.33	18.75	69	
				4	0.58	659.8	660.37	17.02	13.09	0.22	**636.5**	**636.28**	18.24	18.07	70	
				5	0.5	659.79	659.29	19.71	18.67	-	-	-	-	-		
				6	0.25	659.19	658.95	18.97	18.06	-	-	-	-	-		
23	09-16/09/2016	61474	219	1	0.42	658.83	659.26	13.78	15.73	0.22	**632.77**	**633**	18.46	18.34	71	wheel thread scratch & wheel flange thickness
				2	0.11	659.02	658.91	14.12	12.97	0.27	**631.54**	**631.8**	17.84	17.87	72	
				3	0.26	659.88	660.15	14.94	14.18	0.96	**630.83**	**630.91**	18.84	18.42	73	
				4	0.12	659.95	659.83	14.97	13.22	0.75	**631.27**	**631.42**	18.3	17.86	74	
				5	0.52	659.04	659.56	15.01	13.23	0.13	**634.26**	**634.4**	17.92	17.96	75	
				6	0.43	658.92	659.36	13.68	12.55	0.19	**633.38**	**633.19**	17.94	18.11	76	
24	14-15/11/2016	76430	109	1	0.11	658.81	658.7	18.71	18.59	-	-	-	-	-		wheel flange thickness
				2	0.05	658.86	658.81	19.16	18.28	-	-	-	-	-		
				3	0.49	660.35	659.86	12.45	17.42	0.65	**629.45**	**628.8**	17.88	18	77	
				4	0.31	660.17	659.86	13.68	16.42	0.27	**629.68**	**629.41**	19.6	19.49	78	
				5	0.19	659.16	658.97	18.65	18.27	-	-	-	-	-		
				6	0.09	658.89	658.8	19.18	18.24	-	-	-	-	-		
25	16-18/11/2016	78624	218	1	0.26	641.85	642.11	13.65	13.97	0.12	**618.12**	**618**	18.08	18.17	79	wheel flange thickness
				2	0.12	642.28	642.16	14.71	14.09	0.06	**616.53**	**616.59**	20.35	19.53	80	
				3	0.16	612.41	612.25	19.62	19.74	0.16	**612.41**	**612.25**	19.62	19.74	81	
				4	0.32	637.64	637.96	13.25	13.07	0.18	**609.91**	**609.73**	17.89	18.05	82	
				5	0.04	626.7	626.74	20.9	20.87	0.04	**626.7**	**626.74**	20.9	20.87	83	
				6	0.13	647.16	647.03	14.81	14.29	0.11	**626.16**	**626.05**	17.99	17.93	84	
26	19to21/11/2016	66522	216	1	0.15	648.92	649.07	16.52	16.1	0.3	**623.18**	**623.48**	20	20.09	85	wheel flange thickness
				2	0.07	645.61	645.54	15.96	15.02	0	**622.13**	**622.13**	18.46	18.4	86	
				3	0.07	660.03	659.96	17.86	16.84	-	-	-	-	-		
				4	0.15	659.99	659.84	18.15	17.53	-	-	-	-	-		
				5	0.08	647.3	647.22	18.47	16.75	0.05	**627.07**	**627.02**	19.69	19.12	87	
				6	0.06	647.24	647.3	16.6	14.75	0.01	**625**	**624.99**	18.38	18.36	88	
27	24/11/2016	26848	211	1	-	-	-	-	-	-	-	-	-	-	-	scratch on thread and abnormal wheel flange profile
				2	-	-	-	-	-	-	-	-	-	-	-	
				3	0.06	639.74	639.8	18.86	17.79	0.09	630.25	630.25	19.12	19.3	89	
				4	0.42	634.87	635.29	19.28	18.19	0.2	629.22	629.42	18.16	18.15	90	
				5	-	-	-	-	-	-	-	-	-	-	-	
				6	-	-	-	-	-	-	-	-	-	-	-	

28			217	1	0.06	651.32	651.26	15.26	15.04	0.11	625.02	625.13	19.14	19.36	91	wheel flange thickness
				2	0.01	654.81	654.82	17.26	16.56	0.07	625.34	625.41	20.76	20.74	92	
				3	0.37	640.7	641.07	17.08	16.19	0.02	616.36	616.34	19.46	19.61	93	
				4	0.2	640.46	640.66	14.77	13.67	0.33	614.21	614.54	18.18	18.31	94	
				5	0.36	659.25	659.61	18.39	18.23	0.22	642.37	642.59	20.91	20.84	95	
				6	0.03	659.23	659.26	17.59	15.38	0.14	641.21	641.36	18.53	18.44	96	
29	30/11/2016	69044	115	1	0.37	659.14	658.77	21.41	19.37	-	-	-	-	-		wheel flange thickness
				2	0.06	659.12	659.06	21.15	19.99	-	-	-	-	-		
				3	4.69	635.12	635.91	19.34	15.24	0.32	607.06	607.58	19.63	19.55	97	
				4	0.45	634.9	635.35	18.52	14.09	0.02	605.31	605.33	18.78	18.71	98	
				5	0.23	659.25	659.02	21.45	20.51	-	-	-	-	-		
				6	0.16	658.82	658.66	20.98	19.82	-	-	-	-	-		
30	12/5/2016	57012	220	1	0	659.3	659.3	18.42	17.65	-	-	-	-	-		wheel flange thickness
				2	0.03	659.72	659.3	17.82	16.97	-	-	-	-	-		
				3	0.22	659.89	660.11	17.64	15.57	0	636.33	636.33	19.69	19.83	99	
				4	0.1	659.82	659.92	18.55	18.69	0	636.29	636.29	18.55	18.69	100	
				5	0.33	658.98	659.31	18.23	17.66	-	-	-	-	-		
				6	0.02	659.12	659.1	18.34	16.64	-	-	-	-	-		
31	13-14/12/2016		219	1	0.22	632.52	632.74	20.21	19.32	-	-	-	-	-		scratch on wheel thread
				2	0.23	631.31	631.54	19.67	19.2	-	-	-	-	-		
				3	0.11	630.62	630.73	20.43	19.41	0.07	626.67	626.6	19.34	19.36	101	
				4	0.16	631.11	631.27	19.88	19.85	0.04	628.28	628.32	19.42	19.48	102	
				5	0.02	634.04	634.02	19.75	18.92	-	-	-	-	-		
				6	0.45	633.21	632.76	19.45	19.17	-	-	-	-	-		
32	15-20/12/2016	52732	108	1	0.43	659.65	659.23	21.29	20.63	0.01	653.12	653.13	21.54	21.61	103	scratch on wheel thread
				2	0.04	659.25	659.29	20.87	19.87	0.12	653.12	653.24	20.67	20.74	104	
				3	0.73	654.36	655.09	18.78	18.65	-	-	-	-	-		
				4	0.43	653.65	654.04	18.6	18.04	-	-	-	-	-		
				5	0.32	659.5	659.18	20.71	19.97	-	-	-	-	-		
				6	0.31	659.48	659.17	20.98	20.43	-	-	-	-	-		
33	22-28/12/2016	75028	206	1	0.07	648.45	648.52	17.08	16.77	0.02	625.49	625.48	20.46	20.34	105	wheel flange thickness
				2	0.06	647.39	647.45	16.57	15.74	0.05	623.99	623.93	19.81	19.69	106	
				3	0.15	638.77	638.92	15.41	15.38	0.23	615.7	615.47	19.21	19.21	107	
				4	0.23	637.33	637.56	14.6	14.34	0.02	615.31	615.29	18.44	18.28	108	
				5	0.14	652.58	652.72	16.52	16.09	0.0.15	625.91	626.06	20.72	20.44	109	
				6	0.23	652.36	652.59	16.07	15.47	0.33	625.06	624.73	19.94	19.91	110	
	>>> flange increase indicates the value added on list flange thickness															
	>>> diameter reduction indicates the total amount lathed from pre-measured diameter size															
	>>> factor of diameter reduction the amount of diameter reduction for unit increase or flange thickness															
	>>> pre-measurement refers the measurement before lathing															
	>>> post-measurement refers the measurement after lathing															
	>>> "-" refers wheels those not lathed															

Appendix C: Simpack simulation results of critical speed variation

Table C.1: Critical speed 10 km/hr

Time (s)	Longitudinal creepage	Lateral creepage	Longitudinal creep force (N)	Lateral creep force (N)
0	2.13144E-12	9.31649E-13	1.69459E-05	1469.41
3	2.78019E-06	5.40439E-06	21.6368	1644.63
6	2.83019E-05	5.78985E-05	204.455	2454.36
9	0.000115503	1.57784E-05	696.999	4323.07
12	0.00131582	0.00309985	4385.66	22299.8
15	0.00474674	0.0351521	3321.4	26250.7
18	0.00859239	0.04494	4632.25	25425.9
21	0.00824653	0.0455929	4501.15	26019.4
24	0.00831856	0.0452597	4719.51	26680.3
27	0.00914508	0.0454381	4.73E+03	2.48E+04
30	0.00845975	0.0461671	4557.86	25887.1

Table C.2: Critical Speed 20km/hr

Time (s)	Longitudinal creepage	Lateral creepage	Longitudinal Creep force (N)	Lateral creep force (N)
0	2.13144E-12	9.31649E-13	1.69459E-05	1469.41
3	5.00269E-05	4.41856E-06	377.48	2149.13
6	0.00132971	0.00355769	4424.13	23599.9
9	0.00805958	0.0455515	4401.52	26446.3
12	0.00854727	0.0454929	4639.31	26260.3
15	0.00795917	0.0440784	4650.3	27126.8
18	0.0079921	0.0433977	3880.88	23445.2
21	0.000326719	0.000165004	2346.85	229.724
24	0.000208608	6.94079E-05	1597.83	1672.71
27	5.43883E-05	3.57684E-06	349.892	2634.48
30	0.000149116	1.99415E-06	1232.01	981.905

Table C.3: Critical speed 30 km/hr

Time (s)	Longitudinal creepage	Lateral creepage	Longitudinal creep force (N)	Lateral creep force (N)
0	2.13165E-12	9.31649E-13	1.69476E-05	1469.41
3	0.0001981	1.36891E-05	1150.2	3919.46
6	0.00724619	0.0437391	4354.54	28250.6
9	0.00639956	0.0415346	4399.01	30171.8
12	0.00479069	0.0448856	2152.65	22528.1
15	0.000445541	7.34143E-05	2860.82	2820.18
18	0.00004614	3.55234E-06	328.792	2548.77
21	4.52885E-05	9.60194E-05	382.365	148.711
24	0.000199955	4.48944E-05	1512.81	112.141
27	0.000119573	6.37118E-05	754.732	3352.98
30	3.28497E-05	3.64593E-05	263.664	1186.82

Table C.4: Critical speed 40 km/hr

Time (s)	Longitudinal creepage	Lateral creepage	Longitudinal creep force (N)	Lateral creep force (N)
0	2.13144E-12	9.31649E-13	1.69459E-05	1469.41
3	0.00124004	0.00335478	4330.07	24779.3
6	0.00574272	0.0414488	3943.52	30908.9
9	0.00251136	0.0336751	1664.92	24841.3
12	0.000128602	8.68292E-06	944.363	273.494
15	0.000336686	9.56556E-05	1953.96	4939.14
18	8.02942E-05	2.32949E-05	588.107	149.023
21	0.000226531	0.000200343	1394.18	1734.99
24	2.91694E-05	5.24232E-05	229.582	876.995
27	5.65296E-05	0.000236972	362.016	3428.59
30	5.48094E-05	4.65881E-08	388.491	333.759

Appendix D: Simpack simulation results of coefficient of friction variation

Table D.1: Coefficient of friction, 0.25

Time (s)	Longitudinal creepage	Lateral creepage	Longitudinal creep force (N)	Lateral creep force (N)
0	1.6619E-11	9.31649E-13	0.000123922	1460.61
3	5.22571E-05	7.63535E-06	358.244	2329.35
6	0.00154151	0.0041419	4016.74	16774.2
9	0.00833518	0.0459311	3255.21	18221
12	0.00945376	0.0466045	3586.16	17907.7
15	0.00931952	0.0467291	3614.26	18291.7
18	0.00847672	0.0407469	3077.53	15562.7
21	8.27512E-06	0.000124035	58.7595	775.477
24	0.000239688	0.00013987	1325.41	4276.32
27	5.29093E-05	7.08818E-05	330.148	3509.16
30	5.14141E-05	2.31974E-06	399.055	1073.09

Table D.2: Coefficient of friction, 0.35

Time (s)	Longitudinal creepage	Lateral creepage	Longitudinal creep force (N)	Lateral creep force (N)
0	1.6619E-11	9.31649E-13	0.00013175	1468.83
3	4.83681E-05	1.10762E-05	357.257	2316.44
6	0.00132789	0.00314404	4574.69	22878.6
9	0.00766818	0.0439553	4272.33	25955.1
12	0.00853541	0.045087	4571.93	25650.7
15	0.00814309	0.04541	4508.27	26361.4
18	0.00836569	0.0435892	3987.94	22832.8
21	0.00029065	0.000099901	2193.08	364.944
24	0.000083073	9.96991E-05	737.522	1396.18
27	0.000153463	6.55809E-05	1214.22	87.2642
30	9.51175E-05	5.59773E-05	715.216	2045.32

Table D.3: Coefficient of friction, 0.45

Time (s)	Longitudinal creepage	Lateral creepage	Longitudinal creep force (N)	Lateral creep force (N)
0	1.6619E-11	9.31649E-13	0.000136051	1473.4
3	4.80502E-05	1.26045E-05	367.737	2311.05
6	0.00119516	0.00251348	4734.61	28528.5
9	0.00722306	0.0441941	4900.42	33426.9
12	0.00778303	0.0451801	5127.08	33333.8
15	0.00760851	0.0442692	5262.79	33570.7
18	0.00705777	0.0576904	3096.25	29267.7
21	0.000542344	1.98752E-05	3654.76	1767.55
24	4.36605E-05	3.86017E-05	334.841	2271.81
27	0.000159241	2.28951E-05	1047.64	2953.85
30	3.44234E-05	6.22081E-06	291.577	767.369

Table D.4: Coefficient of friction, 0.55

Time (s)	Longitudinal creepage	Lateral creepage	Longitudinal creep force (N)	Lateral creep force (N)
0	1.6619E-11	9.31649E-13	0.00013985	1475.35
3	4.62094E-05	1.36223E-05	365.282	2306.68
6	0.00112551	0.00201412	4871.85	33640.5
9	0.00835328	0.0638614	4505.9	40116.3
12	0.00921306	0.0712737	4459.97	40320.8
15	0.00766123	0.0514199	5193.36	39953
18	0.00739987	0.0838473	2859.93	37152.8
21	0.000934158	6.38479E-05	5459.58	4258.76
24	6.08374E-05	9.70826E-07	461.56	1501.2
27	8.37028E-05	3.92013E-05	684.359	173.394
30	0.000037305	8.21917E-05	252.857	3699.94

Appendix E: Simpack simulation results of loading variation

Table E.1: Empty load

Time (s)	Longitudinal creepage	Lateral creepage	Longitudinal creep force (N)	Lateral creep force (N)
0	2.69772E-11	9.31649E-13	0.000214484	1469.44
3	6.23757E-05	1.57329E-05	382.214	1736.39
6	0.00149429	0.00460395	3800.81	19247.6
9	0.00702512	0.0431407	3222.58	21370.6
12	0.00784863	0.0433903	3430.27	20573.8
15	0.00715611	0.0429754	3361.78	21597.1
18	0.0074715	0.0532035	2217.94	18053.3
21	0.000417065	0.000111757	2207.13	405.368
24	0.000101373	8.27539E-05	750.257	1017
27	0.000182772	5.56778E-06	1140.1	309.475
30	9.29109E-05	0.000105099	562.958	1890.06

Table E.2: Passenger load, 6.67 tons

Time (s)	Longitudinal creepage	Lateral creepage	Longitudinal creep force (N)	Lateral creep force (N)
0	2.69772E-11	9.31649E-13	0.000214484	1469.44
3	5.38731E-05	1.28425E-05	354.981	1940.33
6	0.00143971	0.00377753	4246.58	20663.2
9	0.00719983	0.0431132	3594.03	23054.1
12	0.00798582	0.0438377	3837.58	22697.2
15	0.00752868	0.0442191	3777.89	23563.4
18	0.00786476	0.0486585	2862.93	20040.4
21	0.000368769	9.76942E-05	2251.92	431.958
24	8.55831E-05	8.52607E-05	674.552	1120.75
27	0.000168748	3.48793E-05	1160.95	210.122
30	0.000101683	7.94128E-05	680.238	1811.41

Table E.3: Passenger load, 13.33 tons

Time (s)	Longitudinal creepage	Lateral creepage	Longitudinal creep force (N)	Lateral creep force (N)
0	2.69772E-11	9.31649E-13	0.000214484	1469.44
3	5.33716E-05	1.23648E-05	375.545	2131.26
6	0.00137365	0.00336992	4463.48	22148.4
9	0.00743028	0.0435205	3994.88	24993.2
12	0.00827113	0.0442455	4302.86	24697.9
15	0.00778443	0.0446372	4191.92	25394.6
18	0.00799782	0.0455709	3436.91	21899
21	0.000340373	9.61754E-05	2321	447.011
24	7.25033E-05	7.07667E-05	604.044	1118.38
27	0.000143346	3.86981E-05	1078.97	242.583
30	0.000114879	2.33521E-05	850.043	1412.31

Table E.4: Passenger load, 20 tons

Time (s)	Longitudinal creepage	Lateral creepage	Longitudinal creep force (N)	Lateral creep force (N)
0	2.69772E-11	9.31649E-13	0.000214484	1469.44
3	4.76458E-05	1.02834E-05	355.844	2332.63
6	0.00129516	0.00303358	4588.97	23649.7
9	0.00783481	0.044108	4487.41	26869.6
12	0.00846522	0.0449807	4701.04	26641.8
15	0.00802059	0.0452983	4613.23	27410
18	0.00825384	0.0439358	4030.89	23727.4
21	0.000314462	6.97573E-05	2347.27	631.059
24	5.53209E-05	0.000113548	485.119	1556.53
27	0.000132055	4.70057E-05	1054.54	228.991
30	0.000102717	3.23245E-07	824.411	1278.64